Staggered Discontinuous Galerkin Method for the Curl-curl Operator and Convection-diffusion Equation

LEE, Chak Shing

A Thesis Submitted in Partial Fulfilment
of the Requirements for the Degree of
Master of Philosophy
in
Mathematics

The Chinese University of Hong Kong
August 2011

Thesis/Assessment Committee

Professor CHAN Hon Fu Raymond (Chair)

Professor CHUNG Tsz Shun Eric (Thesis Supervisor)

Professor LUI Lok Ming Ronald (Committee Member)

Professor YALCHIN Efendiev (External Examiner)

Abstract

The discontinuous Galerkin(DG) methods have been extensively studied and applied to numerically solve partial differential equations since 1970s, see [1, 2] for a detailed account of the historical development of the methods. Because of various reasons, DG methods are getting popular. For instance, they are flexible in the sense that different polynomial degrees can be used for approximation in different regions of the computational domain. Besides, they can be applied on non-conforming meshes, and their local property makes them well-suited for parallel computing. Among them, for example, the interior penalty(IP) method and the local discontinuous Galerkin(LDG) method were used to deal with the curl-curl operator [18, 23, 27]. These methods produce spurious-free approximation of highly singular functions, but the drawbacks are the additional degrees of freedom and the bulky penalty terms, which greatly increase the computational cost.

Recently, Chung and Engquist [11, 12] have developed a new DG method for wave propagation, which is explicit, energy conservative and optimal in the order of convergence. In this thesis, we will investigate a staggered DG method for the curl-curl operator in $\mathbb{R}^2$ using a similar discretization technique. Such discretization imposes extra continuity conditions carefully on functions in the approximation space such that no extra penalty terms are needed in the resulting bilinear forms and the number of degrees of freedom is much reduced. In this regard, the proposed method is superior to the conventional DG methods. Another purpose of this thesis is to apply a similar scheme to solve the convection-diffusion equation, which is rarely seen in the literature. Both the static and time-dependent problems will be studied. The stability and the convergence of the methods are analyzed and the results of numerical experiments are given to support the theoretical analysis.

摘要

自20世紀70年代，間斷伽遼金(discontinuous Galerkin)方法已被廣泛研究並應用於PDE的數值求解，可看[1, 2]詳細地了解這方法的歷史發展。 基於各種原因，間斷伽遼金方法越來越受歡迎。例如，在計算域的不同地區它們可靈活地使用不同次數的多項式。此外，它們可以應用在非協調網格上，其局部特性更使其非常適用於並行計算。其中，內部處罰(interior penalty)方法和局部間斷伽遼金(local discontinuous Galerkin)方法就被用來處理捲曲-捲曲算子的問題[18, 23, 27]。這些方法能準確地計算出高度奇異的函數，但缺點是額外的自由度和笨重的處罰項大大提高了計算成本。

最近Chung及Enquist[11, 12]研發出一種新的間斷伽遼金方法用作解決波的傳播問題。這方法直截，能量守衡並且擁有最佳的收斂速度。在這篇論文中，我們將使用類似的離散技巧去處理二維空間的捲曲-捲曲算子。這種離散方法對間斷有限元空間內的函數施加額外的連續性條件使得產生的雙線性式不需要額外的處罰項，而且自由度的數量也大大減少。在這方面，該方法較傳統的間斷伽遼金方法優勝。這論文的另一個目的是應用類似的方法去求對流-擴散問題的數值解，這在文獻中是罕見的。不論是靜態的或是隨時間變化的問題都會被探討。這個新方法的穩定性和收斂性會在論文中深入地分析。為了支持分析的結論，我們會給予數值實驗的結果。

ACKNOWLEDGMENTS

My sincere gratitude goes to Prof. Eric T. Chung for his invaluable guidance throughout my M.Phil. studies. He is always supportive and willing to explain patiently the problems and ideas for me. His suggestions are key ingredients in the accomplishment of this thesis.

I am grateful to Prof. Ralf Hiptmair (ETH Zürich, Switzerland) who introduced me to computational electromagnetism and gave me a first practical experience of the Lagrangian finite element methods and the IP-DG methods.

I want to thank Prof. Raymond H. Chan who aroused my interest in computational and applied mathematics when I was taking his tutorial seminar. I would not consider further study without his encouragement.

I would also like to thank Dr. Kwai Wong, Dr. Ed D'Azevedo and Dr. Nicky Lam (Oak Ridge National Laboratory, USA) for providing me a valuable research experience on computer programming and parallel computing in the summer of my second year undergraduate studies.

Moreover, I want to thank my colleagues in the Department of Mathematics of CUHK, especially to Healy Lee Ho Fung, Yu Tang Fei, Hester Chan Hiu Ning and Leung Wing Tat, for having substantial discussions with me, both on academic and daily life issues. I learned a lot from those discussions and I would not have such a joyful postgraduate journey without them.

Lastly, I want to show my gratitude to my parents and my sister for giving me such a warm family, letting me continue to study without much pressure and taking care of me every single day. I deeply thank their selfless contribution, their tolerance to my bad temper and their smiles in every morning.

Contents

Chapter 1

Model Problems

1.1 Introduction

The discontinuous Galerkin(DG) methods have been extensively studied and applied to numerically solve partial differential equations since 1970s, see [1, 2] for a detailed account of the historical development of the methods. Because of various reasons, DG methods are getting popular. For instance, they are flexible in the sense that different polynomial degrees can be used for approximation in different regions of the computational domain. As a result, adaptive hp-finite element method is easy to carry out with DG methods. Besides, they can be applied on non-conforming meshes, and their local property makes them well-suited for parallel computing. With the rapid advance in high performance computers, DG method is surely a favorite choice in scientific computing.

In the context of computational electromagnetism, one often encounters the curl-curl operator which result from eliminating either the electric field or the magnetic field. If continuous finite elements is applied to discretize the resulting equations, the numerical solution may converge to a wrong answer(spurious solution) in the case of non-convex domain. To overcome the problem, the interior penalty(IP) method and the local discontinuous Galerkin(LDG) method were used to deal with the curl-curl operator [18, 23, 27]. These methods produce spurious-free approximation of highly singular functions, but the drawbacks are the additional degrees of freedom and the bulky penalty terms, which greatly increase the computational cost.

Recently, Chung and Engquist [11, 12] have developed a new DG method for wave propagation, which is explicit, energy conservative and optimal in the order of convergence of both L^2 norm and the energy norm. In this thesis, we will investigate a staggered DG method for the curl-curl operator in $\mathbb{R}^2$ using a similar discretization technique. Such discretization imposes extra continuity conditions carefully on functions in the approximation space such that no extra penalty terms are needed in the resulting bilinear forms and the number of degrees of freedom is much reduced. In this regard, the proposed method is superior to the conventional DG methods. Another purpose of this thesis is to apply a similar scheme to solve the convection-diffusion equation, which is rarely seen in the literature. Both the static and time-dependent problems will be studied in detail. The equation will be further discretized in time using the Crank Nicolson scheme, which give rise to a unconditionally stable scheme. The stability and the convergence of the methods are analyzed and the results of numerical experiments are given to support the theoretical analysis.

1.2 The curl-curl operator

The first model problem being considered is the following:

$$\begin{aligned} \mathbf{curl}\,\mathrm{curl}\,\boldsymbol{u} - \omega^2 \boldsymbol{u} = \boldsymbol{f} \quad &\text{in} \quad \Omega \\ \boldsymbol{u}\cdot\boldsymbol{t} = g \quad &\text{on} \quad \partial\Omega, \end{aligned} \tag{1.1}$$

where Ω is a bounded domain in $\mathbb{R}^2$ and $\boldsymbol{t}$ is the anti-clockwisely oriented unit tangent on $\partial\Omega$. For a vector field $\boldsymbol{u} = (u_1, u_2)$, curl $\boldsymbol{u} = \dfrac{\partial u_2}{\partial x} - \dfrac{\partial u_1}{\partial y}$, while for a scalar field ϕ, we have $\mathbf{curl}\ \phi = (\dfrac{\partial \phi}{\partial y}, -\dfrac{\partial \phi}{\partial x})$. We assume the source function $\boldsymbol{f} \in \boldsymbol{L}^2(\Omega)$ satisfies $\mathrm{div}\boldsymbol{f} = 0$ in Ω, this implies that $\mathrm{div}\,\boldsymbol{u} = 0$ in Ω. That is $\boldsymbol{u}$ satisfies a natural divergence-free condition. Besides, the Dirichlet boundary datum g is assumed to belong to $L^2(\partial\Omega)$. This boundary value problem normally arises from the time harmonic Maxwell's equations, here $\omega > 0$ is the given pulsation. Throughout the paper, symbols with bold face are vector quantities.

Variational form We define the following function spaces:

$$
\begin{aligned}
H(\mathrm{div};\Omega) &= \{\boldsymbol{v} \in \boldsymbol{L}^2(\Omega) : \mathrm{div}\, \boldsymbol{v} \in L^2(\Omega)\},\\
H(\mathrm{curl};\Omega) &= \{\boldsymbol{v} \in \boldsymbol{L}^2(\Omega) : \mathrm{curl}\, \boldsymbol{v} \in L^2(\Omega)\},\\
H_0(\mathrm{curl};\Omega) &= \{\boldsymbol{v} \in H(\mathrm{curl};\Omega) : \boldsymbol{v}\cdot\boldsymbol{t} = 0 \text{ on } \partial\Omega\},\\
H_0(\mathrm{curl}^0;\Omega) &= \{\boldsymbol{v} \in H_0(\mathrm{curl};\Omega) : \mathrm{curl}\, \boldsymbol{v} = 0 \text{ in } \Omega\},\\
V &= \{\boldsymbol{v} \in H(\mathrm{curl};\Omega) : \boldsymbol{v}\cdot\boldsymbol{t} = g \text{ on } \partial\Omega\},
\end{aligned}
$$

where $L^2(\Omega)$ denotes the set of square integrable functions over the domain Ω and $\boldsymbol{L}^2(\Omega)$ is the set of vector functions having each of its components in $L^2(\Omega)$. The properties of these space can be found in [24, 16].

An equivalent variational formulation is obtained simply by multiplying the first equation of (1.1) with test functions and integrating by parts, to reach

$$
\begin{aligned}
&\text{find } \boldsymbol{u} \in V \text{ such that}\\
&(\mathrm{curl}\, \boldsymbol{u}, \mathrm{curl}\, \boldsymbol{v})_{L^2(\Omega)} - \omega^2 (\boldsymbol{u}, \boldsymbol{v})_{\boldsymbol{L}^2(\Omega)} = (\boldsymbol{f}, \boldsymbol{v})_{\boldsymbol{L}^2(\Omega)} \quad \forall \boldsymbol{v} \in H_0(\mathrm{curl};\Omega).
\end{aligned}
\tag{1.2}
$$

By introducing an additional unknown, namely $q := \mathrm{curl}\, \boldsymbol{u}$, we can recast equivalently this problem, and obtain a suitable framework for our new discontinuous Galerkin discretization, the so-called mixed formulation.

$$
\begin{aligned}
&\text{find } (\boldsymbol{u}, q) \in V \times L^2(\Omega) \text{ such that}\\
&(q,\psi)_{L^2(\Omega)} - (\mathrm{curl}\, \boldsymbol{u}, \psi)_{L^2(\Omega)} = 0 && \forall \psi \in L^2(\Omega),\\
&(q, \mathrm{curl}\, \boldsymbol{v})_{L^2(\Omega)} - \omega^2 (\boldsymbol{u}, \boldsymbol{v})_{\boldsymbol{L}^2(\Omega)} = (\boldsymbol{f}, \boldsymbol{v})_{\boldsymbol{L}^2(\Omega)} && \forall \boldsymbol{v} \in H_0(\mathrm{curl};\Omega).
\end{aligned}
\tag{1.3}
$$

If the domain is non-convex, the solution has singularities at the re-entrant corners. It is well-known that using conforming finite element methods will produce spurious solutions for the singularities due to the fact that the standard H^1-conforming nodal element space is not dense in $V \cap H(\mathrm{div};\Omega)$, see [13, ?, 20]. Rather, it is a subspace of $V \cap H(\mathrm{div};\Omega)$ and the inclusion is strict. For example, consider the exact solution given by the function $\nabla\left[r^{2/3}\sin(\frac{2\theta}{3})\right]$ on a L-shaped domain with re-entrant corner at the origin, Figure 1.1 shows the graph of this function. In order to illustrate the inability of conforming finite element method, we consider the conforming finite element method

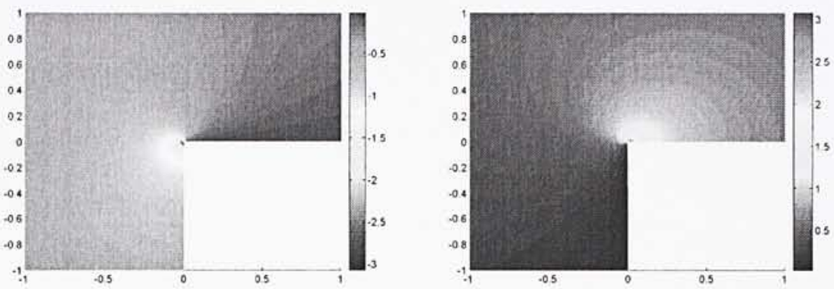

(a) x component (b) y component

Figure 1.1: Graph of $\nabla\left[r^{2/3}\sin(\frac{2\theta}{3})\right]$

based on the following weak formulation:

$$\begin{aligned} &\text{find } \boldsymbol{u} \in V \cap H(\text{div};\Omega) \text{ such that } \quad \forall \boldsymbol{v} \in H_0(\text{curl};\Omega) \\ &(\text{curl } \boldsymbol{u}, \text{curl } \boldsymbol{v})_{L^2(\Omega)} + (\text{div } \boldsymbol{u}, \text{div } \boldsymbol{v})_{L^2(\Omega)} - \omega^2 (\boldsymbol{u}, \boldsymbol{v})_{\boldsymbol{L}^2(\Omega)} = (\boldsymbol{f}, \boldsymbol{v})_{\boldsymbol{L}^2(\Omega)}. \end{aligned} \tag{1.4}$$

Note that since div $\boldsymbol{u} = 0$, the exact solution of (1.1) still satisfies this variational form (1.4). The numerical solution obtained by using conforming piecewise linear nodal elements is shown in Figure 1.2. This approximation, which is completely different from the exact solution, is the so-called spurious solution. To obtain numerical solutions without spurious modes, methods using Nédélec's first

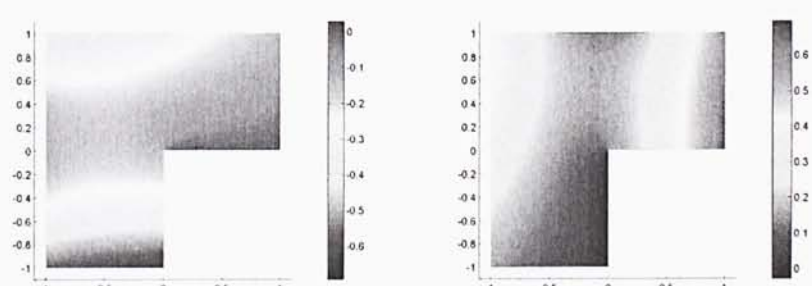

(a) x component (b) y component

Figure 1.2: Numerical approximation of $\nabla\left[r^{2/3}\sin(\frac{2\theta}{3})\right]$ using conforming finite element method with piecewise linear elements and $h = 0.0625$

family finite elements are developed for the mixed form of the Maxwell's equations; see, e.g., [20] and [24]. In these methods, the divergence free condition are automatically satisfied. However, the order of convergence of these elements is one order lesser than nodal elements for approximation of regular functions. One can also use the Nédélec's second family finite elements to achieve optimal rate of convergence, but they generally do not produce weak divergence free numerical solutions. Hence, a scheme that can produce good approximation for the singularities and possesses optimal convergence rate is desirable. There are many successful works in the area of solving the Helmholtz and the Maxwell's equations by the discontinuous Galerkin (DG) method. For instances, in [17], a DG method using plane waves is developed and analyzed for the Helmholtz equation, while in [4], a stabilized DG method is analyzed for the first order hyperbolic system. Regarding the time-harmonic Maxwell's equations, DG methods based on a mixed formulation are proposed and analyzed for the low frequency model in [21] and [26]. In these works, the divergence free condition is handled by a suitable Lagrange multiplier. In [22], the first optimal error estimates in both energy and L^2-norm are proved for the interior penalty DG method for the $3D$ time harmonic Maxwell's equations in the second order form. Moreover, in [23], the same type of method is applied to the time harmonic Maxwell's equations in the mixed form. In addition to optimal error estimates, the numerical solution is shown to automatically satisfy a weak form of the divergence free condition. There is also an interior penalty DG method for the $2D$ curl-curl problem that gives pointwise divergence free condition by using divergence free basis functions, see [3], where optimal convergence estimates are also proved. For the Maxwell eigenvalue problem, [5] and [6] prove estimates for the convergence rate of the eigenvalues. In [19], the computation of Maxwell eigenvalue problem in three space dimensions is considered. For the time-dependent Maxwell's equations, [18] developed an interior penalty DG method and analyzed its optimal convergence.

In this thesis, we investigate a new discontinuous Galerkin method aiming to achieve the aforementioned two properties. In fact, our new finite element space can be seen as a local $H(\text{curl};\Omega)$-conforming edge element space. Similar techniques have also been applied to time-dependent Maxwell's equations and the Helmholtz equation, see [10], [8] and [9]. There are some distinctive advantages in using our new discretization. First, the discrete versions of the two curl operators are adjoint operators to each other, which hold for the differential operators. Thus, our discretization preserves some conservation properties arising naturally from the differential equation. In fact, if the same method is applied to the time-dependent Maxwell's equation, the resulting method will have block-diagonal mass matrix and conserve the electromagnetic energy. Another advantage is that the numerical solution of our new method will satisfy automatically a discrete divergence-free condition. Thus, there is no need to enforce, either weakly or strongly, this divergence-free condition in our method. We emphasize that this condition is important for elimination of spurious mode in the numerical solution.

1.3 The convection-diffusion equation

The other model problem that will be investigated in this thesis is the following convection-diffusion equation

$$\frac{\partial u}{\partial t} = \Delta u - \nabla \cdot (\mathbf{b} u) + f, \qquad (x,t) \in \Omega \times (0,T), \tag{1.5}$$

where Ω is a polyhedral domain in $\mathbb{R}^d$, $d = 2, 3$, and $T > 0$ is a fixed time. In (1.5), u is the unknown function to be approximated and f is a given source term. We supplement (1.5) with initial condition $u(x,0) = u_0(x)$ for $x \in \Omega$ and the homogeneous Dirichlet boundary condition $u(x,t) = 0$ for $x \in \partial\Omega$. The extension to the cases with inhomogeneous Dirichlet boundary condition and other types of boundary conditions are straightforward. We assume that the velocity field $\mathbf{b}(x,t)$ is divergence free, namely $\nabla \cdot \mathbf{b} = 0$ for $(x,t) \in \Omega \times (0,T)$. We will also derive and analyze our new method for solving the corresponding static problem

$$-\Delta u + \nabla \cdot (\mathbf{b} u) = f \tag{1.6}$$

supplemented with a suitable boundary condition.

Over the past few decades, staggered type methods have been applied successfully to many problems, such as wave propagation and fluid flow problems [7, 8, 9, 11, 12, 25, 28]. A distinctive feature of these methods is that the physical laws arising from the corresponding partial differential equations are automatically preserved. Nevertheless, staggered methods for convection-diffusion equations are rarely seen in literature. It is thus the second main goal of this thesis to develop and analyze a class of staggered numerical schemes for the approximation of convection-diffusion equations such that the underlying physical laws are preserved by the numerical scheme automatically. One key step in the development of the new approach is a new mixed formulation of the convection-diffusion equation, which will be defined in the following. The construction of our new method is then based on the techniques developed in [11, 12], in which a new class of staggered DG methods for the wave equations are presented and analyzed. Moreover, stability and convergence of the new method are rigorously analyzed.

To be precise, we will develop the new staggered DG scheme that preserves the following conservative structures arising from the convection-diffusion equation (1.5). The first one is the conservation of density, namely

$$\frac{d}{dt}\int_{\Omega'} u\,dx = \int_{\partial\Omega'} (\frac{\partial u}{\partial n} - u\,\mathbf{b}\cdot n)\,d\sigma + \int_{\Omega'} f\,dx \tag{1.7}$$

where $\Omega' \subset \Omega$ is any subdomain. The second one is a relation about the rate of change of energy and flux:

$$\frac{1}{2}\frac{d}{dt}\int_{\Omega} u^2\,dx = -\int_{\Omega} |\nabla u|^2\,dx + \int_{\Omega} fu\,dx \tag{1.8}$$

and for any subdomain $\Omega' \subset \Omega$:

$$\frac{1}{2}\frac{d}{dt}\int_{\Omega'} u^2\,dx = -\int_{\Omega'} |\nabla u|^2\,dx + \int_{\partial\Omega'} (\nabla u - \frac{1}{2}\mathbf{b}\,u)u\cdot n\,d\sigma + \int_{\Omega'} fu\,dx.$$

The key step in the construction of the new staggered DG method is the following new mixed form for the convection-diffusion equation (1.5). To derive the new formulation, we introduce the new variables

$$\mathbf{w} = \mathbf{b}\,u, \quad \mathbf{p} = \nabla u - \frac{1}{2}\,\mathbf{b}\,u.$$

Then we have

$$\Delta u - \nabla\cdot(\mathbf{b}u) = \nabla\cdot(\nabla u) - \frac{1}{2}\nabla\cdot(\mathbf{b}u) - \frac{1}{2}\nabla\cdot(\mathbf{b}u) = \nabla\cdot\mathbf{p} - \frac{1}{2}\mathbf{b}\cdot\nabla u. \tag{1.9}$$

By the definition of $\mathbf{p}$, we have

$$\mathbf{b}\cdot\nabla u = \mathbf{b}\cdot(\mathbf{p} + \frac{1}{2}\,\mathbf{b}\,u) = \mathbf{b}\cdot(\mathbf{p} + \frac{1}{2}\,\mathbf{w}).$$

Using this relation in (1.9), we have the following new mixed form

$$\mathbf{p} = \nabla u - \frac{1}{2}\,\mathbf{b}\,u, \tag{1.10}$$

$$\mathbf{w} = \mathbf{b}\,u, \tag{1.11}$$

$$\frac{\partial u}{\partial t} = \nabla\cdot\mathbf{p} - \frac{1}{2}\mathbf{b}\cdot\mathbf{p} - \frac{1}{4}\mathbf{b}\cdot\mathbf{w} + f. \tag{1.12}$$

The new staggered DG method derived and analyzed in Chapter 3 is based on this formulation.

Chapter 2

Staggered DG method for the Curl-Curl operator

2.1 Introduction

This chapter is devoted to the boundary value problem:

$$\begin{aligned} \mathbf{curl}\ \mathrm{curl}\ \boldsymbol{u} - \omega^2 \boldsymbol{u} = \boldsymbol{f} \quad &\text{in} \quad \Omega \\ \boldsymbol{u} \cdot \boldsymbol{t} = g \quad &\text{on} \quad \partial\Omega, \end{aligned} \tag{2.1}$$

where Ω is a bounded domain in $\mathbb{R}^2$ and $\boldsymbol{t}$ is the anti-clockwisely oriented unit tangent on $\partial\Omega$.

This chapter is organized as follows. In Section 2.2, the optimal discontinuous Galerkin discretization will be defined. The stability and optimal convergence of the new method are analyzed in Section 2.3 and Section 2.4. Numerical results for testing rate of convergence and eigenvalue computations will be given in Section 2.5. Section 2.6 concludes the chapter.

2.2 Discontinuous Galerkin discretization

Following Chung and Engquist [11, 12], we first define the initial triangulation $\mathcal{T}_q$. Suppose the domain Ω is triangulated by a set of triangles. We use the notation $\mathcal{F}_q$ to denote the set of all edges in this triangulation and use the notation $\mathcal{F}_q^0$ to denote the subset of all interior edges – that is edges that are not embedded in $\partial\Omega$ – in $\mathcal{F}_q$. For each triangle, we take an interior point ν and call this triangle

$\mathcal{S}(\nu)$. In practice, ν is chosen as the center of the triangle to enhance mesh regularity. Using the point ν, we can further subdivide each triangle into 3 sub-triangle by connecting the point ν to the 3 vertices of the triangle. We denote by $\mathcal{T}$ the triangulation made up of all sub-triangles. We use the notation $\mathcal{F}_u$ to denote all new faces obtained by the subdivision of triangle, and we let $\mathcal{F} = \mathcal{F}_q \cup \mathcal{F}_u$, respectively $\mathcal{F}^0 = \mathcal{F}_q^0 \cup \mathcal{F}_u$. Figure 3.1 illustrates these ideas, where the solid lines belong to $\mathcal{F}_q$ and the dotted lines belong to $\mathcal{F}_u$. For each edge $\kappa \in \mathcal{F}_q$, we let $\mathcal{R}(\kappa)$ be the union of the two sub-triangles sharing the edge κ. If κ is a boundary edge, we let $\mathcal{R}(\kappa)$ be the only triangle having the edge κ. For an illustration, see again Figure 3.1.

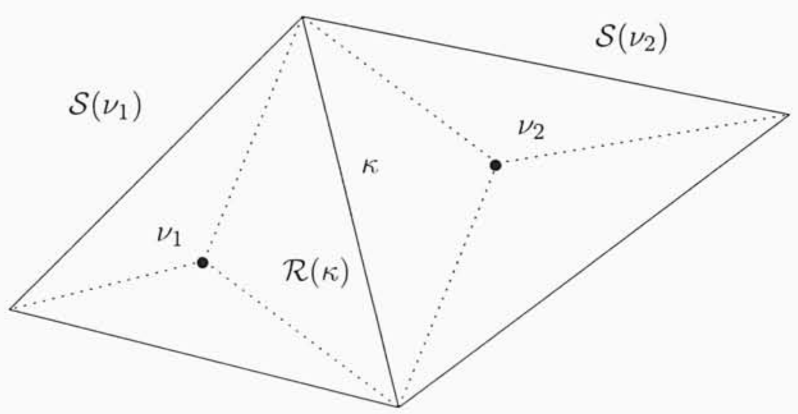

Figure 2.1: Triangulation in 2D.

We will also define a unit tangent vector $\boldsymbol{t}_\kappa$ on each edge κ in $\mathcal{F}$ by the following way. If $\kappa \in \mathcal{F} \backslash \mathcal{F}^0$, then we define $\boldsymbol{t}_\kappa$ as the anti-clockwisely oriented unit tangent on $\partial\Omega$. If $\kappa \in \mathcal{F}^0$ is an interior face, then we fix $\boldsymbol{t}_\kappa$ as one of the two possible unit tangent vectors on κ. When it is clear which edge we are considering, we will use $\boldsymbol{t}$ instead of $\boldsymbol{t}_\kappa$ to simplify the notations.

Now, we will discuss the finite element spaces. Let $k \geq 0$ be a non-negative integer. Let $\tau \in \mathcal{T}$. We define $P^k(\tau)$ as the space of polynomials of degree less than or equal to k on τ. Then we introduce the following discrete space for scalar fields.

Locally $H^1(\Omega)$-conforming finite element space for scalar fields

$$S_h = \{\psi \mid \psi_{|\tau} \in P^k(\tau),\ \forall \tau \in \mathcal{T};\ \psi \text{ is continuous on } \kappa \in \mathcal{F}_q^0\}. \tag{2.2}$$

In the space $\mathcal{S}_h$ we define the following norms

$$\|\psi\|_X^2 = \int_\Omega \psi^2 \, dx + \sum_{\kappa \in \mathcal{F}_q} h_\kappa \int_\kappa \psi^2 \, d\sigma, \tag{2.3}$$

$$\|\psi\|_Z^2 = \int_\Omega |\mathbf{curl}\, \psi|^2 \, dx + \sum_{\kappa \in \mathcal{F}_u} h_\kappa^{-1} \int_\kappa [\psi]^2 \, d\sigma \tag{2.4}$$

where we remark that the integral of $\mathbf{curl}\, \psi$ in (3.4) is defined elementwisely:

$$\int_\Omega |\mathbf{curl}\, \psi|^2 \, dx = \sum_{\tau \in \mathcal{T}} \int_\tau |\mathbf{curl}\, \psi_{|\tau}|^2 \, dx.$$

Here we recall that, by definition, $\psi \in \mathcal{S}_h$ is always continuous on each edge κ in the set $\mathcal{F}_q^0$, whereas it can be discontinuous on each edge κ in the set $\mathcal{F}_u$. We say $\|\psi\|_X$ is the discrete L^2-norm of ψ and $\|\psi\|_Z$ is the discrete H^1-norm of ψ. In the above definition, the jump $[\psi]$ is defined in the following way. For each $\kappa \in \mathcal{F}_u$, there exist two (sub-)triangles τ_1 and τ_2 such that κ is a common edge of them. Moreover, each τ_i, $i = 1, 2$, has a edge κ_i that belongs to $\mathcal{F}_q$. Thus, $\kappa \subset \partial\mathcal{R}(\kappa_i)$ for $i = 1, 2$. Then for such $\kappa \in \mathcal{F}_u$, we write $\boldsymbol{m}_i$ as the anti-clockwisely oriented unit tangent of $\partial\mathcal{R}(\kappa_i)$ for $i = 1, 2$, and define

$$\delta_\kappa^{(i)} = \begin{cases} 1 & \text{if } \boldsymbol{m}_i = \boldsymbol{t} \text{ on } \kappa \\ -1 & \text{if } \boldsymbol{m}_i = -\boldsymbol{t} \text{ on } \kappa \end{cases}$$

where $\boldsymbol{t}$ is the unit tangent vector of the face κ. Then the jump $[\psi]$ on the face κ is defined as

$$[\psi] = \delta_\kappa^{(1)} \psi_1 + \delta_\kappa^{(2)} \psi_2$$

where $\psi_i = \psi_{|\tau_i}$.

Note that one can prove, by the argument used in the proof of Theorem 3.1 of Ref [12], that there exists a constant $\alpha > 0$, independent of h, such that

$$\|\psi\|_{L^2(\Omega)}^2 \leq \|\psi\|_X^2 \leq \alpha \|\psi\|_{L^2(\Omega)}^2 \quad \forall \psi \in \mathcal{S}_h.$$

Locally $H(\text{curl};\Omega)$-conforming finite element space for vector fields

Now, we introduce the following discrete space for vector fields.

$$\mathcal{V}_h = \{\boldsymbol{v} \mid \boldsymbol{v}_{|\tau} \in P^k(\tau)^2,\ \forall \tau \in \mathcal{T};\ \boldsymbol{v} \cdot \boldsymbol{t} \text{ is continuous on } \kappa \in \mathcal{F}_u\}. \tag{2.5}$$

In the space $\mathcal{V}_h$, we define the following norms

$$\|\boldsymbol{v}\|_{\boldsymbol{X}'}^2 = \int_\Omega |\boldsymbol{v}|^2 \, dx + \sum_{\kappa \in \mathcal{F}_u} h_\kappa \int_\kappa (\boldsymbol{v} \cdot \boldsymbol{t})^2 \, d\sigma, \tag{2.6}$$

$$\|\boldsymbol{v}\|_{\boldsymbol{Z}'}^2 = \int_\Omega (\text{curl } \boldsymbol{v})^2 \, dx + \sum_{\kappa \in \mathcal{F}_q^0} h_\kappa^{-1} \int_\kappa [\boldsymbol{v} \cdot \boldsymbol{t}]^2 \, d\sigma + \sum_{\kappa \in \partial\Omega} h_\kappa^{-1} \int_\kappa (\boldsymbol{v} \cdot \boldsymbol{t})^2 \, d\sigma \tag{2.7}$$

where we remark again that the integral of curl $\boldsymbol{v}$ in (3.7) is defined elementwisely. Here we recall that, by definition, $\boldsymbol{v} \in \mathcal{V}_h$ has continuous tangential component on each edge $\kappa \in \mathcal{F}_u$. We say $\|\boldsymbol{v}\|_{\boldsymbol{X}'}$ is the discrete $\boldsymbol{L}^2$-norm of $\boldsymbol{v}$ and $\|\boldsymbol{v}\|_{\boldsymbol{Z}'}$ is the discrete $H(\text{curl};\Omega)$-norm of $\boldsymbol{v}$. In the above definition, the jump $[\boldsymbol{v} \cdot \boldsymbol{t}]$ is defined in the following way. Let $\kappa \subset \mathcal{F}_q^0$. Then there are exactly two triangles τ_1 and τ_2 such that κ is a common edge of them. Let ν_i be an interior node of τ_i. Then we have $\kappa \in \partial\mathcal{S}(\nu_i)$ for $i = 1, 2$. Let $\boldsymbol{m}_i$ be the anti-clockwisely oriented unit tangent of $\partial\mathcal{S}(\nu_i)$. We define

$$\delta_\kappa^{(i)} = \begin{cases} 1 & \text{if } \boldsymbol{m}_i = \boldsymbol{t} \text{ on } \kappa \\ -1 & \text{if } \boldsymbol{m}_i = -\boldsymbol{t} \text{ on } \kappa \end{cases}$$

where $\boldsymbol{t}$ is the unit tangent vector of the edge κ. Then the jump $[\boldsymbol{v} \cdot \boldsymbol{t}]$ on the edge κ is defined as

$$[\boldsymbol{v} \cdot \boldsymbol{t}] = \delta_\kappa^{(1)} \boldsymbol{v}_1 \cdot \boldsymbol{t} + \delta_\kappa^{(2)} \boldsymbol{v}_2 \cdot \boldsymbol{t},$$

where $\boldsymbol{v}_i = \boldsymbol{v}_{|\tau_i}$.

One can prove, by the argument used in the proof of Theorem 3.2 of Ref [12], that there exists a constant $\beta > 0$, independent of h, such that

$$\|\boldsymbol{v}\|_{\boldsymbol{L}^2(\Omega)}^2 \le \|\boldsymbol{v}\|_{\boldsymbol{X}'}^2 \le \beta \, \|\boldsymbol{v}\|_{\boldsymbol{L}^2(\Omega)}^2 \quad \forall \boldsymbol{v} \in \mathcal{V}_h. \tag{2.8}$$

We define for $\psi, q \in \mathcal{S}_h, \boldsymbol{v}, \boldsymbol{u} \in \mathcal{V}_h$,

$$B_h(q, \boldsymbol{v}) = \int_\Omega q \,\text{curl}\, \boldsymbol{v} \, dx - \sum_{\kappa \in \mathcal{F}_q^0} \int_\kappa q \, [\boldsymbol{v} \cdot \boldsymbol{t}] \, d\sigma - \sum_{\kappa \in \partial\Omega} \int_\kappa q \, \boldsymbol{v} \cdot \boldsymbol{t} \, d\sigma, \tag{2.9}$$

$$B_h^*(\boldsymbol{u}, \psi) = \int_\Omega \boldsymbol{u} \cdot \textbf{curl}\, \psi \, dx + \sum_{\kappa \in \mathcal{F}_u} \int_\kappa \boldsymbol{u} \cdot \boldsymbol{t} \, [\psi] \, d\sigma. \tag{2.10}$$

Using the same technique in proving Lemma 2.4 of Chung and Engquist [12], we have

$$B_h(\psi, \boldsymbol{v}) = B_h^*(\boldsymbol{v}, \psi), \quad \forall (\psi, \boldsymbol{u}) \in \mathcal{S}_h \times \mathcal{V}_h. \tag{2.11}$$

Moreover, the following holds

$$B_h(\boldsymbol{v},\psi) \leq \|\psi\|_X \, \|\boldsymbol{v}\|_{\boldsymbol{Z}'}, \quad \forall(\psi,\boldsymbol{v}) \in \mathcal{S}_h \times \mathcal{V}_h. \tag{2.12}$$

The discrete variational formulation, or numerical method, is

$$\begin{aligned} &\text{find } (q_h,\boldsymbol{u}_h) \in \mathcal{S}_h \times \mathcal{V}_h \text{ such that} \\ &(q_h,\psi)_{\boldsymbol{L}^2(\Omega)} - B_h^*(\boldsymbol{u}_h,\psi) = (g,\psi)_{L^2(\partial\Omega)}, \qquad \forall\, \psi \in \mathcal{S}_h \\ &B_h(q_h,\boldsymbol{v}) - \omega^2\,(\boldsymbol{u}_h,\boldsymbol{v})_{\boldsymbol{L}^2(\Omega)} = (\boldsymbol{f},\boldsymbol{v})_{\boldsymbol{L}^2(\Omega)}, \qquad \forall\, \boldsymbol{v} \in \mathcal{V}_h. \end{aligned} \tag{2.13}$$

Note that (1.3) is the continuous variational form and (2.13) is the discontinuous Galerkin formulation.

Using a proof similar to the proof of Theorem 3.2 of [12], we know that there is a uniform constant $K > 0$ such that the global inf-sup condition below holds:

$$\inf_{\boldsymbol{v}\in\mathcal{V}_h} \sup_{\psi\in\mathcal{S}_h} \frac{B_h(\psi,\boldsymbol{v})}{\|\psi\|_X \, \|\boldsymbol{v}\|_{\boldsymbol{Z}'}} \geq K. \tag{2.14}$$

Let $\mathcal{V}(h) := \mathcal{V}_h + H_0(\text{curl};\Omega)$, then we have the following norm compatibility: If $\boldsymbol{v} \in \mathcal{V}(h)$ satisfies $\|\boldsymbol{v}\|_{\boldsymbol{Z}'} = 0$, then $\boldsymbol{v} \in H_0(\text{curl}^0;\Omega)$. Furthermore, if $\boldsymbol{v} \in H_0(\text{curl};\Omega)$, then $\|\boldsymbol{v}\|_{\boldsymbol{Z}'} = \|\text{curl } \boldsymbol{v}\|_{L^2(\Omega)}$. We define some more discrete function spaces below:

$$\begin{aligned} Q_h &= \{q \in L^2(\Omega) : q_{|\tau} \in P^{k+1}(\tau),\ \forall \tau \in \mathcal{T}\}, \\ \mathcal{V}_h^c &= \mathcal{V}_h \cap H_0(\text{curl};\Omega), \\ Q_h^c &= Q_h \cap H_0^1(\Omega), \\ K_h &= \mathcal{V}_h^c \cap H_0(\text{curl}^0;\Omega), \\ K_h^{\perp} &= \{\boldsymbol{v} \in \mathcal{V}_h : (\boldsymbol{v},\boldsymbol{w}) = 0 \quad \forall \boldsymbol{w} \in K_h\}. \end{aligned}$$

Note that we have $K_h = \nabla Q_h^c$, c.f. [6], so we have

$$K_h^{\perp} = \{\boldsymbol{v} \in \mathcal{V}_h : (\boldsymbol{v},\nabla p) = 0 \quad \forall p \in Q_h^c\}.$$

Moreover, one can show, in the spirit of [6], that the following discrete Poincaré inequality and the discrete compactness property hold in our setting. More precisely, there exists a constant C_p independent of h such that

$$\|\boldsymbol{v}\|_{\boldsymbol{L}^2(\Omega)} \leq C_p \|\boldsymbol{v}\|_{\boldsymbol{Z}'} \quad \forall \boldsymbol{v} \in K_h^{\perp}. \tag{2.15}$$

And for any sequence $(\boldsymbol{w}_h)_h$ in $K_h^\perp$ with $(\|\boldsymbol{w}_h\|^2_{\boldsymbol{L}^2(\Omega)} + \|\boldsymbol{w}_h\|^2_{\boldsymbol{Z}'})^{\frac{1}{2}} \leq C$ for some C independent of h, there exists a subsequence, still denoted by $(\boldsymbol{w}_h)_h$, and an element $\boldsymbol{v} \in \boldsymbol{L}^2(\Omega)$ such that

$$\lim_{h\to 0} \|\boldsymbol{w}_h - \boldsymbol{v}\|_{\boldsymbol{L}^2(\Omega)} = 0. \tag{2.16}$$

Lemma 2.2.1 *The discrete solution $\boldsymbol{u}_h$ of (2.13) belongs to $K_h^\perp$.*

Proof Since $(q_h, \boldsymbol{u}_h)$ solves (2.13) and $\nabla Q_h^c = K_h \subset \mathcal{V}_h$, the following holds:

$$B_h(q_h, \nabla p) - \omega^2 (\boldsymbol{u}_h, \nabla p)_{\boldsymbol{L}^2(\Omega)} = (\boldsymbol{f}, \nabla p)_{\boldsymbol{L}^2(\Omega)}, \qquad \forall\, p \in Q_h^c.$$

Since for any $p \in Q_h^c$, $\nabla p \in K_h \subset H_0(\mathrm{curl}^0;\Omega)$, $B_h(q_h, \nabla p) = 0$. Also, as $\mathrm{div}\boldsymbol{f} = 0$, we have $(\boldsymbol{f}, \nabla p)_{\boldsymbol{L}^2(\Omega)} = 0$. Hence, together with $\omega \neq 0$, we conclude $(\boldsymbol{u}_h, \nabla p)_{\boldsymbol{L}^2(\Omega)} = 0 \quad \forall\, p \in Q_h^c$. So $\boldsymbol{u}_h \in K_h^\perp$. □

From now on, we say the discrete fields $(q_h, \boldsymbol{u}_h) \in \mathcal{S}_h \times K_h^\perp$ are *aligned* if

$$(q_h, \psi)_{L^2(\Omega)} = B_h^*(\boldsymbol{u}_h, \psi), \qquad \forall\, \psi \in \mathcal{S}_h, \tag{2.17}$$

and let A_h be the set of aligned fields, i.e.

$$A_h = \{(\psi, \boldsymbol{v}) \in \mathcal{S}_h \times K_h^\perp \text{ such that (2.17) are satisfied }\}. \tag{2.18}$$

Note that by the norm equivalence of $\|\cdot\|_{L^2(\Omega)}$ and $\|\cdot\|_X$, and the global inf-sup condition (3.11), for $(\psi, \boldsymbol{v}) \in A_h$, we have

$$\begin{aligned}
\|\psi\|_{L^2(\Omega)} &= \sup_{\phi\in\mathcal{S}_h} \frac{(\psi,\phi)_{L^2(\Omega)}}{\|\phi\|_{L^2(\Omega)}} \\
&\geq \sup_{\phi\in\mathcal{S}_h} \frac{(\psi,\phi)_{L^2(\Omega)}}{\|\phi\|_X} \\
&= \sup_{\phi\in\mathcal{S}_h} \frac{B_h^*(\boldsymbol{v},\phi)}{\|\phi\|_X} \\
&= \sup_{\phi\in\mathcal{S}_h} \frac{B_h(\phi,\boldsymbol{v})}{\|\phi\|_X} \\
&\geq K\|\boldsymbol{v}\|_{Z'}.
\end{aligned} \tag{2.19}$$

Also, we introduce the following bilinear forms which will be used in the convergence and error analysis:

$$\begin{aligned} b_h\Big((q,\boldsymbol{u}),(\psi,\boldsymbol{v})\Big) &= B_h(q,\boldsymbol{v}) + (q,\psi)_{L^2(\Omega)} - B_h^*(\boldsymbol{u},\psi) \\ a_h\Big((q,\boldsymbol{u}),(\psi,\boldsymbol{v})\Big) &= b_h\Big((q,\boldsymbol{u}),(\psi,\boldsymbol{v})\Big) - \omega^2(\boldsymbol{u},\boldsymbol{v})_{\boldsymbol{L}^2(\Omega)} \end{aligned}$$

2.3 Stability for aligned fields

In this section, we will prove the uniform stability of the form $(a_h)_h$ for aligned fields. More precisely, we will prove the following theorem.

Theorem 2.3.1 *There exists $\sigma > 0, h_0 > 0$ such that $\forall\, 0 < h < h_0, \forall(\psi_h, \boldsymbol{v}_h) \in A_h$,*

$$\sup_{(\phi_h,\boldsymbol{w}_h)\in\mathcal{S}_h\times K_h^{\perp}} \frac{\Big|a_h\Big((\psi_h,\boldsymbol{v}_h),(\phi_h,\boldsymbol{w}_h)\Big)\Big|}{\|(\phi_h,\boldsymbol{w}_h)\|_h} \geq \sigma\|(\psi_h,\boldsymbol{v}_h)\|_h, \tag{2.20}$$

where the norm $\|\cdot\|_h$ is defined on $L^2 \times (\mathcal{V}_h + H(curl;\Omega))$ by

$$\|(\psi_h,\boldsymbol{v}_h)\|_h = \Big(\|\psi_h\|^2_{L^2(\Omega)} + \|\boldsymbol{v}_h\|^2_{\boldsymbol{Z}'}\Big)^{\frac{1}{2}}. \tag{2.21}$$

Proof We will need the uniform coercivity of $(b_h)_h$ for aligned fields to prove (2.20). This can be obtained by using (2.11) and (2.19) that for all $(\psi_h, \boldsymbol{v}_h) \in A_h$,

$$\begin{aligned} b_h\Big((\psi_h,\boldsymbol{v}_h),(\psi_h,\boldsymbol{v}_h)\Big) &= B_h(\psi_h,\boldsymbol{v}_h) + (\psi_h,\psi_h)_{L^2(\Omega)} - B_h^*(\boldsymbol{v}_h,\psi_h) \\ &= \|\psi_h\|^2_{L^2(\Omega)} \\ &\geq \gamma\|(\psi_h,\boldsymbol{v}_h)\|_h, \end{aligned} \tag{2.22}$$

where $\gamma = \frac{1}{2}\min\{1, K\}$.

Let us now prove (2.20) by contradiction. Suppose (2.20) is not true, then there exists $(\mu_h)_h > 0, \lim_{h\to 0}\mu_h = 0$, such that $\forall\, h_0 > 0$, there exists h with $0 < h < h_0$, and $(\psi_h, \boldsymbol{v}_h) \in A_h, \|(\psi_h, \boldsymbol{v}_h)\|_h = 1$ such that

$$\sup_{(\phi_h,\boldsymbol{w}_h)\in\mathcal{S}_h\times K_h^{\perp}} \frac{\Big|a_h\Big((\psi_h,\boldsymbol{v}_h),(\phi_h,\boldsymbol{w}_h)\Big)\Big|}{\|(\phi_h,\boldsymbol{w}_h)\|_h} \leq \mu_h. \tag{2.23}$$

Note that $\|\psi_h\|_{L^2(\Omega)} \leq 1$ and $\|\boldsymbol{v}_h\|_{\boldsymbol{Z}'} \leq 1$, for all h. By the discrete Poincaré inequality (2.15), we have $(\|\boldsymbol{v}_h\|^2_{\boldsymbol{L}^2(\Omega)} + \|\boldsymbol{v}_h\|^2_{\boldsymbol{Z}'})^{\frac{1}{2}} \leq (1 + C_p^2)^{\frac{1}{2}}$, where C_p is the constant in the discrete Poincaré inequality. Hence, by the discrete compactness property (2.16), there exists a subsequence of $(\boldsymbol{v}_h)_h$ that converges strongly in $\boldsymbol{L}^2(\Omega)$. Thus, if we still denote this subsequence by $(\boldsymbol{v}_h)_h$, then there exists $\boldsymbol{u}^* \in \boldsymbol{L}^2(\Omega)$ such that

$$\lim_{h\to 0} \|\boldsymbol{v}_h - \boldsymbol{u}^*\|_{\boldsymbol{L}^2(\Omega)} = 0. \tag{2.24}$$

We claim that $\boldsymbol{u}^* = 0$, so that $\lim_{h\to 0} \|\boldsymbol{v}_h\|_{\boldsymbol{L}^2(\Omega)} = 0$. Then, it follows from the uniform coercivity of $(b_h)_h$ for aligned fields (2.22) and our assumption on the lack of stability of $(a_h)_h$ (2.23) that for all $h > 0$,

$$\gamma \leq a_h\Big((\psi_h, \boldsymbol{v}_h), (\psi_h, \boldsymbol{v}_h)\Big) + \omega^2(\boldsymbol{v}_h, \boldsymbol{v}_h)_{\boldsymbol{L}^2(\Omega)} \leq \mu_h + \omega^2\|\boldsymbol{v}_h\|^2_{\boldsymbol{L}^2(\Omega)}. \tag{2.25}$$

Since both $\lim_{h\to 0} \mu_h = 0$ and $\lim_{h\to 0} \|\boldsymbol{v}_h\|_{\boldsymbol{L}^2(\Omega)} = 0$, we have found a contradiction. So we conclude that the forms $(a_h)_h$ are uniformly stable for aligned fields in the sense of (2.20).

Now we go back to prove our claim, i.e. $\boldsymbol{u}^* = 0$.

Note that the sequence $(\psi_h)_h$ is bounded in $L^2(\Omega)$, so one can extract a subsequence, which we still denote it by $(\psi_h)_h$, such that $(\psi_h)_h$ converges *weakly* to some q^* in $L^2(\Omega)$, where $q^* \in L^2(\Omega)$:

$$\psi_h \rightharpoonup q^* \text{ weakly in } L^2(\Omega). \tag{2.26}$$

In the following, we want to prove that $(q^*, \boldsymbol{u}^*)$ solves the two-unknown problem (1.3) with $\boldsymbol{f} = \boldsymbol{0}$ and $g = 0$. First, we have to prove that curl $\boldsymbol{u}^* \in L^2(\Omega)$ and $\boldsymbol{u}^* \cdot \boldsymbol{t} = 0$ on $\partial\Omega$. By the definition of differentiation in the sense of distributions, for any $\phi \in \mathcal{D}(\Omega)$, we have

$$\begin{aligned} \langle \text{curl } \boldsymbol{u}^*, \phi \rangle &= \langle \boldsymbol{u}^*, \textbf{curl } \phi \rangle = \textstyle\int_\Omega \boldsymbol{u}^* \textbf{ curl } \phi \, dx \\ &= \lim_{h\to 0} \int_\Omega \boldsymbol{v}_h \textbf{ curl } \phi \, dx = \lim_{h\to 0} B_h(\phi, \boldsymbol{v}_h). \end{aligned}$$

Using a similar argument in proving (3.15) and (3.22) of [12], one can show that given $\phi \in H^{k+1}(\Omega)$, there exists $\phi_h \in \mathcal{S}_h$ such that

$$\begin{aligned} &B_h(\phi_h - \phi, \boldsymbol{w}) = 0 \quad \forall \boldsymbol{w} \in \mathcal{V}_h \\ &\|\phi_h - \phi\|_{L^2(\Omega)} \leq C h^{k+1} |\phi|_{H^{k+1}(\Omega)} \end{aligned}$$

where C is independent of $\boldsymbol{w}$ and h. As $(\psi_h, \boldsymbol{v}_h) \in A_h$, we have by (2.11) and (2.17),

$$\begin{aligned} B_h(\phi, \boldsymbol{v}_h) &= B_h(\phi_h, \boldsymbol{v}_h) \\ &= B_h^*(\boldsymbol{v}_h, \phi_h) = \int_\Omega \psi_h \, \phi_h \, dx. \end{aligned}$$

Since $(\phi_h)_h$ converge strongly in $L^2(\Omega)$ and $(\psi_h)_h$ converge weakly in $L^2(\Omega)$, we conclude that

$$\langle \text{curl } \boldsymbol{u}^*, \phi \rangle = \int_\Omega q^* \, \phi \, dx. \quad \forall \phi \in \mathcal{D}(\Omega).$$

In other words, $\boldsymbol{u}^* \in H(\text{curl}; \Omega)$ and moreover curl $\boldsymbol{u}^* = q^*$. Second, one has $\boldsymbol{u}^* \in H_0(\text{curl}; \Omega)$ if and only if, there holds

$$\int_\Omega \boldsymbol{u}^* \, \mathbf{curl} \, \phi \, dx = \int_\Omega \text{curl } \boldsymbol{u}^*, \phi \, dx. \quad \forall \phi \in C^\infty(\Omega).$$

This time, we find

$$\begin{aligned} \int_\Omega \boldsymbol{u}^* \, \mathbf{curl} \, \phi \, dx &= \lim_{h\to 0} \int_\Omega \boldsymbol{v}_h \, \mathbf{curl} \, \phi \, dx = \lim_{h\to 0} B_h(\phi, \boldsymbol{v}_h) \\ &= \lim_{h\to 0} B_h(\phi_h, \boldsymbol{v}_h) = \lim_{h\to 0} B_h^*(\boldsymbol{v}_h, \phi_h,) = \lim_{h\to 0} (\psi_h, \phi_h)_{L^2(\Omega)} \\ &= \int_\Omega q^* \, \phi \, dx = \int_\Omega \text{curl } \boldsymbol{u}^*, \phi \, dx, \end{aligned}$$

which proves $\boldsymbol{u}^* \in H_0(\text{curl}; \Omega)$. Third, let us check that $(q^*, \boldsymbol{u}^*) \in L^2(\Omega) \times H_0(\text{curl}; \Omega)$ solves the original two unknown problem (1.3), with $\boldsymbol{f} = \mathbf{0}$ and $g = 0$. As $q^* =$ curl $\boldsymbol{u}^*$, we obviously have that

$$\langle \text{curl } \boldsymbol{u}^*, \phi \rangle - \langle q^*, \phi \rangle = 0 \quad \forall \phi \in L^2(\Omega).$$

Consider next $\boldsymbol{w} \in (\mathcal{D}(\Omega))^2$:

$$(q*, \text{curl } \boldsymbol{w})_{L^2(\Omega)} - \omega^2 (\boldsymbol{u}^*, \boldsymbol{w})_{\boldsymbol{L}^2(\Omega)} = \lim_{h\to 0} \{ (\psi_h, \text{curl } \boldsymbol{w})_{L^2(\Omega)} - \omega^2 (\boldsymbol{v}_h, \boldsymbol{w})_{\boldsymbol{L}^2(\Omega)} \}.$$

Again, let us integrate the first term by parts, element by element:

$$\begin{aligned} (\psi_h, \text{curl } \boldsymbol{w})_{L^2(\Omega)} &= \sum_{\tau \in \mathcal{T}} \int_\tau \psi_h \text{ curl } \boldsymbol{w} \, dx \\ &= \sum_{\tau \in \mathcal{T}} \left\{ \int_\tau \mathbf{curl} \, \psi_h \, \boldsymbol{w} \, dx + \int_{\partial \tau} \psi_h (\boldsymbol{w} \cdot \boldsymbol{t}|_{\partial \tau}) \, d\sigma \right\} \\ &= \int_\Omega \mathbf{curl} \, \psi_h \, \boldsymbol{w} \, dx + \sum_{\kappa \in \mathcal{F}_u} \int_\kappa [\psi_h] \boldsymbol{w} \cdot \boldsymbol{t} \, d\sigma \\ &= B_h^*(\boldsymbol{w}, \psi_h). \end{aligned} \tag{2.27}$$

Above, we used the fact that $\boldsymbol{w}|_{\partial\Omega} = \boldsymbol{0}$, ψ_h is continuous across edges of $\mathcal{F}_q$ and $\boldsymbol{w}\cdot\boldsymbol{t} = 0$ on $\mathcal{F}\backslash\mathcal{F}_q$. Also, to compute the contribution on the remaining edges(i.e. those of $\mathcal{F}_u$), we used the definition of the jumps of the scalar field on those edges(See section 2.2).

Using again a similar argument in proving (3.13) and (3.19) of [12], one can show that given $\boldsymbol{w} \in \boldsymbol{H}^{k+1}(\Omega)$, there exists $\boldsymbol{w}_h \in \mathcal{V}_h$ such that

$$B_h^*(\boldsymbol{w}_h - \boldsymbol{w}, \phi) = 0 \quad \forall \phi \in \mathcal{S}_h$$
$$\|\boldsymbol{w}_h - \boldsymbol{w}\|_{\boldsymbol{L}^2(\Omega)} \leq Ch^{k+1}|\boldsymbol{w}|_{\boldsymbol{H}^{k+1}(\Omega)}$$

where C is independent of ϕ and h. Therefore, we reach

$$\begin{aligned}
& (\psi_h, \text{curl } \boldsymbol{w})_{L^2(\Omega)} - \omega^2(\boldsymbol{v}_h, \boldsymbol{w})_{\boldsymbol{L}^2(\Omega)} \\
= \; & B_h^*(\boldsymbol{w}_h, \psi_h) - \omega^2(\boldsymbol{v}_h, \boldsymbol{w})_{\boldsymbol{L}^2(\Omega)} \\
= \; & B_h(\psi_h, \boldsymbol{w}_h) - \omega^2(\boldsymbol{v}_h, \boldsymbol{w})_{\boldsymbol{L}^2(\Omega)} \\
= \; & B_h(\psi_h, \boldsymbol{w}_h) - \omega^2(\boldsymbol{v}_h, \boldsymbol{w}_h)_{\boldsymbol{L}^2(\Omega)} + \omega^2(\boldsymbol{v}_h, \boldsymbol{w}_h - \boldsymbol{w})_{\boldsymbol{L}^2(\Omega)} \\
= \; & a_h\Big((\psi_h, \boldsymbol{v}_h), (0, \boldsymbol{w}_h)\Big) + \omega^2(\boldsymbol{v}_h, \boldsymbol{w}_h - \boldsymbol{w})_{\boldsymbol{L}^2(\Omega)}.
\end{aligned}$$

Let us consider each term of the right-hand side separately, when h goes to zero:

$$\Big|a_h\Big((\psi_h, \boldsymbol{v}_h), (0, \boldsymbol{w}_h)\Big)\Big| \leq \mu_h \|(0, \boldsymbol{w}_h)\|_h = \mu_h \|\boldsymbol{w}_h\|_{\boldsymbol{Z}'} \to 0.$$

For the other term, by the Cauchy-Schwarz inequality:

$$|(\boldsymbol{v}_h, \boldsymbol{w}_h - \boldsymbol{w})_{\boldsymbol{L}^2(\Omega)}| \leq \|\boldsymbol{v}_h\|_{\boldsymbol{L}^2(\Omega)} \|\boldsymbol{w}_h - \boldsymbol{w}\|_{\boldsymbol{L}^2(\Omega)} \to 0.$$

We thus conclude that

$$(q*, \text{curl } \boldsymbol{w})_{L^2(\Omega)} - \omega^2(\boldsymbol{u}^*, \boldsymbol{w})_{\boldsymbol{L}^2(\Omega)} = 0, \quad \forall \boldsymbol{w} \in \mathcal{D}(\Omega)^2.$$

By density, this is also true for all $\boldsymbol{w} \in H_0(\text{curl}; \Omega)$. In other words, $(q^*, \boldsymbol{u}^*)$ solves (1.3), with $\boldsymbol{f} = \boldsymbol{0}$ and $g = 0$. As a consequence, under the well-posedness of the continuous problem (1.3), we find that $(q^*, \boldsymbol{u}^*) = (0, \boldsymbol{0})$. □

2.4 Error estimates

We use the notation $\|(\psi, \boldsymbol{v})\|_0 = \Big(\|\psi\|^2_{L^2(\Omega)} + \|\boldsymbol{v}\|_{\boldsymbol{L}^2(\Omega)}\Big)^{\frac{1}{2}}$ to represent the $L^2(\Omega)$ norm on $L^2(\Omega) \times (\mathcal{V}_h + V)$.

We recall that $(q, \boldsymbol{u})$(resp. $(q_h, \boldsymbol{u}_h)$) denotes the solution to the exact two-unknown problem (1.3)(resp. discrete two-known problem (2.13)). Let $\boldsymbol{v}$ be arbitrary element in $K_h^{\perp}$. The we define ψ by

$$(\psi, \phi)_{L^2(\Omega)} = B_h^*(\boldsymbol{v}, \phi) + (g, \phi)_{L^2(\partial\Omega)}, \quad \forall\, \phi \in \mathcal{S}_h. \tag{2.28}$$

Thus, $(\psi - q_h, \boldsymbol{v} - u_h)$ are aligned fields. Let us now use the uniform stability of the form $(a_h)_h$, i.e. condition (2.20), to establish error estimates. Accordingly, we have

$$\begin{aligned}
\|(\psi - q_h, \boldsymbol{v} - \boldsymbol{u}_h)\|_h &\le \frac{1}{\sigma} \sup_{(\phi,\boldsymbol{w})\in\mathcal{S}_h\times K_h^{\perp}} \frac{a_h\Big((\psi - q_h, \boldsymbol{v} - \boldsymbol{u}_h), (\phi, \boldsymbol{w})\Big)}{\|(\phi, \boldsymbol{w})\|_h} \\
&\le \frac{1}{\sigma} \sup_{(\phi,\boldsymbol{w})\in\mathcal{S}_h\times K_h^{\perp}} \frac{a_h\Big((q - q_h, \boldsymbol{u} - \boldsymbol{u}_h), (\phi, \boldsymbol{w})\Big)}{\|(\phi, \boldsymbol{w})\|_h} \\
&\quad + \frac{1}{\sigma} \sup_{(\phi,\boldsymbol{w})\in\mathcal{S}_h\times K_h^{\perp}} \frac{a_h\Big((\psi - q, \boldsymbol{v} - \boldsymbol{u}), (\phi, \boldsymbol{w})\Big)}{\|(\phi, \boldsymbol{w})\|_h} \\
&= \frac{1}{\sigma} \sup_{(\phi,\boldsymbol{w})\in\mathcal{S}_h\times K_h^{\perp}} \frac{a_h\Big((q, \boldsymbol{u}), (\phi, \boldsymbol{w})\Big) - (\boldsymbol{f}, \boldsymbol{w})_{\boldsymbol{L}^2(\Omega)} - (g, \phi)_{L^2(\partial\Omega)}}{\|(\phi, \boldsymbol{w})\|_h} \\
&\quad + \frac{1}{\sigma} \sup_{(\phi,\boldsymbol{w})\in\mathcal{S}_h\times K_h^{\perp}} \frac{a_h\Big((\psi - q, \boldsymbol{v} - \boldsymbol{u}), (\phi, \boldsymbol{w})\Big)}{\|(\phi, \boldsymbol{w})\|_h}
\end{aligned} \tag{2.29}$$

The first term on the right hand side of (2.29) represents the consistency error while the second term on the right side of (2.29) represents the approximation error.

Approximation error By the definition of a_h, we have

$$\begin{aligned}
a_h\Big((\psi - q, \boldsymbol{v} - \boldsymbol{u}), (\phi, \boldsymbol{w})\Big) &= B_h(\psi - q, \boldsymbol{w}) + (\psi - q, \phi)_{L^2(\Omega)} \\
&\quad - B_h^*(\boldsymbol{v} - \boldsymbol{u}, \phi) - \omega^2(\boldsymbol{v} - \boldsymbol{u}, \boldsymbol{w})_{\boldsymbol{L}^2(\Omega)}.
\end{aligned} \tag{2.30}$$

By a similar argument in proving (3.13) and (3.15) of [12], we know that there exists elements $\pi_h q \in \mathcal{S}_h$ and $\boldsymbol{\pi}_h \boldsymbol{u} \in K_h^{\perp}$ such that

$$\begin{aligned}
B_h(\pi_h q - q, \boldsymbol{w}) = 0 \qquad &\forall \boldsymbol{w} \in \mathcal{V}_h \\
B_h^*(\boldsymbol{\pi}_h \boldsymbol{u} - \boldsymbol{u}, \phi) = 0 \qquad &\forall \phi \in \mathcal{S}_h
\end{aligned}$$

Now we choose $\boldsymbol{v} = \boldsymbol{\pi}_h \boldsymbol{u}$ and note that the corresponding ψ is defined such that they satisfy (2.28).

Then, for all $\phi \in \mathcal{S}_h$, we have

$$(\psi, \phi)_{L^2(\Omega)} = B_h^*(\boldsymbol{\pi}_h \boldsymbol{u}, \phi) + (g, \phi)_{L^2(\partial\Omega)} = B_h^*(\boldsymbol{u}, \phi) + (g, \phi)_{L^2(\partial\Omega)} = (q, \phi)_{L^2(\Omega)}$$

Thus, ψ is merely the L^2-projection of q. Therefore, (2.30) becomes

$$a_h\Big((\psi - q, \boldsymbol{\pi}_h \boldsymbol{u} - \boldsymbol{u}), (\phi, \boldsymbol{w})\Big) = \quad B_h(\psi - q, \boldsymbol{w}) - \omega^2(\boldsymbol{\pi}_h \boldsymbol{u} - \boldsymbol{u}, \boldsymbol{w})_{\boldsymbol{L}^2(\Omega)}.$$

Using the definition of $\pi_h q$,

$$a_h\Big((\psi - q, \boldsymbol{\pi}_h \boldsymbol{u} - \boldsymbol{u}), (\phi, \boldsymbol{w})\Big) = \quad B_h(\psi - \pi_h q, \boldsymbol{w}) - \omega^2(\boldsymbol{\pi}_h \boldsymbol{u} - \boldsymbol{u}, \boldsymbol{w})_{\boldsymbol{L}^2(\Omega)}.$$

By the continuity of B_h (2.12) and the equivalence of the norms $\|\cdot\|_X$ and $\|\cdot\|_{L^2(\Omega)}$,

$$\begin{aligned}
& a_h\Big((\psi - q, \boldsymbol{\pi}_h \boldsymbol{u} - \boldsymbol{u}), (\phi, \boldsymbol{w})\Big) \\
\leq \quad & \|\psi - \pi_h q\|_X \|\boldsymbol{w}\|_{\boldsymbol{Z}'} + \omega^2 \|\boldsymbol{\pi}_h \boldsymbol{u} - \boldsymbol{u}\|_{\boldsymbol{L}^2(\Omega)} \|\boldsymbol{w}\|_{\boldsymbol{L}^2(\Omega)} \\
\leq \quad & \alpha \|\psi - \pi_h q\|_{L^2(\Omega)} \|\boldsymbol{w}\|_{\boldsymbol{Z}'} + \omega^2 \|\boldsymbol{\pi}_h \boldsymbol{u} - \boldsymbol{u}\|_{\boldsymbol{L}^2(\Omega)} \|\boldsymbol{w}\|_{\boldsymbol{L}^2(\Omega)}.
\end{aligned}$$

We observe that by the triangle inequality

$$\|\psi - \pi_h q\|_{L^2(\Omega)} \leq \|\psi - q\|_{L^2(\Omega)} + \|q - \pi_h q\|_{L^2(\Omega)},$$

and then since ψ is the L^2-projection of q, the following holds:

$$\|\psi - \pi_h q\|_{L^2(\Omega)} \leq \|q - \pi_h q\|_{L^2(\Omega)}.$$

And with the help of the discrete version of Poincaré inequality in $K_h^\perp$ (2.15), we obtain

$$a_h\Big((\psi - q, \boldsymbol{\pi}_h \boldsymbol{u} - \boldsymbol{u}), (\phi, \boldsymbol{w})\Big) \leq C \left\|(q - \pi_h q, \boldsymbol{\pi}_h \boldsymbol{u} - \boldsymbol{u})\right\|_0 \left\|(\phi, \boldsymbol{w})\right\|_h,$$

where $C = C(\omega, C_p, \alpha)$. Hence,

$$\sup_{(\phi, \boldsymbol{w}) \in \mathcal{S}_h \times K_h^\perp} \frac{a_h\Big((\psi - q, \boldsymbol{\pi}_h \boldsymbol{u} - \boldsymbol{u}), (\phi, \boldsymbol{w})\Big)}{\|(\phi, \boldsymbol{w})\|_h} \leq \left\|(q - \pi_h q, \boldsymbol{\pi}_h \boldsymbol{u} - \boldsymbol{u})\right\|_0.$$

With that, we can obtain error estimates: by using a proof similar to the proof of theorem 3.4 and theorem 3.5 of [12], we have respectively

$$\|\pi_h q - q\|_{L^2(\Omega)} \leq Ch^{\min\{k+1,S+1\}}|q|_{H^{S+1}(\Omega)} \quad \text{if } q \in H^{S+1}(\Omega),$$
$$\|\boldsymbol{\pi}_h \boldsymbol{u} - \boldsymbol{u}\|_{\boldsymbol{L}^2(\Omega)} \leq Ch^{\min\{k+1,s+1\}}|\boldsymbol{u}|_{\boldsymbol{H}^{s+1}(\Omega)} \quad \text{if } \boldsymbol{u} \in \boldsymbol{H}^{s+1}(\Omega),$$

where k is the maximal degree of the polynomials that define the discrete fields, and C is independent of $q, \boldsymbol{u}$ and h. It is possible to obtain more precise results. Note that since $q = \text{curl } \boldsymbol{u}$, we have automatically $S = s - 1$, and s can be non-integer values. So we find that for $\boldsymbol{u} \in \boldsymbol{H}^{s+1}(\Omega)$, we have

$$\|\pi_h q - q\|_{L^2(\Omega)} \leq Ch^{\min\{k+1,s\}}, \|\boldsymbol{\pi}_h \boldsymbol{u} - \boldsymbol{u}\|_{\boldsymbol{L}^2(\Omega)} \leq Ch^{\min\{k+1,s+1\}}, \tag{2.31}$$

where C is independent of h.

Thus, we conclude that for the term representing the approximation error, we have

$$\sup_{(\phi,\boldsymbol{w})\in S_h\times K_h^\perp} \frac{a_h\Big((\psi - q, \boldsymbol{\pi}_h \boldsymbol{u} - \boldsymbol{u}), (\phi, \boldsymbol{w})\Big)}{\|(\phi, \boldsymbol{w})\|_h} \leq Ch^{\min\{k+1,s\}}.$$

Consistency error by the definition of a_h, we have

$$\begin{aligned} & a_h\Big((q, \boldsymbol{u}), (\phi, \boldsymbol{w})\Big) - (\boldsymbol{f}, \boldsymbol{w})_{\boldsymbol{L}^2(\Omega)} - (g, \phi)_{L^2(\partial\Omega)} \\ = \;& B_h(q, \boldsymbol{w}) + (q, \phi)_{L^2(\Omega)} - B_h^*(\boldsymbol{u}, \phi) - \omega^2(\boldsymbol{u}, \boldsymbol{w})_{\boldsymbol{L}^2(\Omega)} - (\boldsymbol{f}, \boldsymbol{w})_{\boldsymbol{L}^2(\Omega)} - (g, \phi)_{L^2(\partial\Omega)}. \end{aligned}$$

Integrating by parts, we find that $B_h^*(\boldsymbol{u}, \phi) + (g, \phi)_{L^2(\partial\Omega)} = (q, \phi)_{L^2(\Omega)}$. Using the other definition of $B_h(q, \boldsymbol{w})$, we have

$$\begin{aligned} & a_h\Big((q, \boldsymbol{u}), (\phi, \boldsymbol{w})\Big) - (\boldsymbol{f}, \boldsymbol{w})_{\boldsymbol{L}^2(\Omega)} - (g, \phi)_{L^2(\partial\Omega)} \\ = \;& (q - \text{curl } \boldsymbol{u}, \phi)_{L^2(\Omega)} + (\textbf{curl } q - \omega^2 \boldsymbol{u} - \boldsymbol{f}, \boldsymbol{w})_{\boldsymbol{L}^2(\Omega)}. \end{aligned}$$

Therefore, as $q = \text{curl } \boldsymbol{u}$ in $L^2(\Omega)$, and $\textbf{curl } q - \omega^2 \boldsymbol{u} = \boldsymbol{f}$ in $\boldsymbol{L}^2(\Omega)$, we conclude that the consistency term is zero.

Error estimate We obtain finally the following estimates.

Theorem 2.4.1 *Let $\boldsymbol{u} \in \boldsymbol{H}^s(\Omega)$ and $q \in H^s(\Omega)$ with $s > \frac{1}{2}$. Moreover let k be the maximal degree of the polynomials that define the discrete fields. Then one has*

$$\begin{aligned} \|q - q_h\|_{L^2(\Omega)} &\leq Ch^{\min\{k+1,s\}}, \\ \|\boldsymbol{u} - \boldsymbol{u}_h\|_{Z'} &\leq Ch^{\min\{k,s\}}, \\ \|\boldsymbol{u} - \boldsymbol{u}_h\|_{\boldsymbol{L}^2(\Omega)} &\leq Ch^{\min\{k+1,s\}}, \end{aligned} \tag{2.32}$$

where $0 < h < h_0$ *and* h_0 *is defined in Theorem 2.3.1.*

Proof Starting from (2.29) and combining all the previous results, we know that

$$\|(\psi - q_h, \boldsymbol{\pi}_h \boldsymbol{u} - \boldsymbol{u}_h)\|_h \leq Ch^{\min\{k+1,s\}}, \tag{2.33}$$

where ψ is the $L^2(\Omega)$-projection of q.

Then, by triangle inequality, we find

$$\|q - q_h\|_{L^2(\Omega)} \leq \|q - \psi\|_{L^2(\Omega)} + \|\psi - q_h\|_{L^2(\Omega)} \leq Ch^{\min\{k+1,s\}}.$$

Next, using a proof similar to the proof of theorem 3.4 of [12], we know that $\|\boldsymbol{u} - \boldsymbol{\pi}_h \boldsymbol{u}\|_{\boldsymbol{Z}'} \leq Ch^{\min\{k,s\}}$, so we get

$$\|\boldsymbol{u} - \boldsymbol{u}_h\|_{\boldsymbol{Z}'} \leq \|\boldsymbol{u} - \boldsymbol{\pi}_h \boldsymbol{u}\|_{\boldsymbol{Z}'} + \|\boldsymbol{\pi}_h \boldsymbol{u} - \boldsymbol{u}_h\|_{\boldsymbol{Z}'} \leq Ch^{\min\{k,s\}}.$$

Moreover, by the discrete Poincaré inequality on the space $K_h^{\perp}$ (2.15),

$$\|\boldsymbol{\pi}_h \boldsymbol{u} - \boldsymbol{u}_h\|_{\boldsymbol{L}^2(\Omega)} \leq C_p \|\boldsymbol{\pi}_h \boldsymbol{u} - \boldsymbol{u}_h\|_{\boldsymbol{Z}'} \leq Ch^{\min\{k+1,s\}}.$$

Using again theorem 3.4 of [12] to reach $\|\boldsymbol{u} - \boldsymbol{\pi}_h \boldsymbol{u}\|_{\boldsymbol{L}^2(\Omega)} \leq Ch^{\min\{k+1,s\}}$, we conclude that

$$\|\boldsymbol{u} - \boldsymbol{u}_h\|_{\boldsymbol{L}^2(\Omega)} \leq \|\boldsymbol{u} - \boldsymbol{\pi}_h \boldsymbol{u}\|_{\boldsymbol{L}^2(\Omega)} + \|\boldsymbol{\pi}_h \boldsymbol{u} - \boldsymbol{u}_h\|_{\boldsymbol{L}^2(\Omega)} \leq Ch^{\min\{k+1,s\}}.$$

□

2.5 Numerical experiments

Numerical results which verify the error estimates in the previous section will be shown in this section. We will test our method on the square domain $\Omega_1 = (0,1)^2$ and the L-shaped domain $\Omega_2 = (-1,1)^2 \backslash ([0,1] \times [0,-1])$. Experiments have been conducted with the theoretical solution given by the following functions:

$$\begin{aligned}
S_1(x,y) &= \begin{pmatrix} -e^x(y\cos y + \sin y) \\ e^x y \sin y \end{pmatrix} \\
S_2(x,y) &= \nabla \left[r^{4/3} \sin(\frac{4\theta}{3}) \right] \\
S_3(x,y) &= \nabla \left[r^{2/3} \sin(\frac{2\theta}{3}) \right],
\end{aligned}$$

where $r = \sqrt{x^2+y^2}$ and $\theta = \tan^{-1}(y/x)$. Note that S_1 is smooth, $S_2 \in H^{\frac{4}{3}}(\Omega_2)$ and $S_3 \in H^{\frac{2}{3}}(\Omega_2)$. The data function $\boldsymbol{f}$ and g are obtained according to (1.1) with $\omega = 1$. Note that the L-shaped domain is non-convex, so the Lagrangian finite elements fail to recover S_3 in the L-shaped domain. For each function we will test our DG method with piecewise constant elements and piecewise linear elements.

In order to make it more clear, we give explicitly the basis functions that we have used for both elements. Firstly, in the piecewise constant case, since we require the tangential component of the vector functions in $\mathcal{V}_h$ to be continuous across each edge $\kappa \in \mathcal{F}_u$, the degrees of freedom for the vector function $\boldsymbol{v}$ in each $\mathcal{S}(\nu)$ is 3. So there will be 3 basis functions associated with each $\mathcal{S}(\nu)$. Before defining the basis functions, we have to fix some notations. We first fix one $\mathcal{S}(\nu)$. Note that $\mathcal{S}(\nu)$ itself is a triangle, let v_i, i = 1,2,3, be its vertices, ordered in the anti-clockwise direction. $\mathcal{S}(\nu)$ such that v_i is not one of its vertices. Moreover, let $\boldsymbol{t}_i = (t_i^1, t_i^2)$ be the unit vector pointing from v_i to ν. Lastly, let τ_i be the sub-triangle in $\mathcal{S}(\nu)$ such that v_i is not one of its vertices. See Figure 2.2 for an example of such $\mathcal{S}(\nu)$.

Now we define the basis functions, associated with each $\mathcal{S}(\nu)$, as follows:

$$\boldsymbol{v}_1 = \begin{cases} \frac{1}{\boldsymbol{t}_3\times\boldsymbol{t}_1}(-t_3^2, t_3^1) & \text{if } (x,y)\in\tau_2 \\ \frac{1}{\boldsymbol{t}_2\times\boldsymbol{t}_1}(-t_2^2, t_2^1) & \text{if } (x,y)\in\tau_3 \\ 0 & \text{otherwise} \end{cases}$$

$$\boldsymbol{v}_2 = \begin{cases} \frac{1}{\boldsymbol{t}_3\times\boldsymbol{t}_2}(-t_3^2, t_3^1) & \text{if } (x,y)\in\tau_1 \\ \frac{1}{\boldsymbol{t}_1\times\boldsymbol{t}_2}(-t_1^2, t_1^1) & \text{if } (x,y)\in\tau_3 \\ 0 & \text{otherwise} \end{cases}$$

$$\boldsymbol{v}_3 = \begin{cases} \frac{1}{\boldsymbol{t}_2\times\boldsymbol{t}_3}(-t_2^2, t_2^1) & \text{if } (x,y)\in\tau_1 \\ \frac{1}{\boldsymbol{t}_1\times\boldsymbol{t}_3}(-t_1^2, t_1^1) & \text{if } (x,y)\in\tau_2 \\ 0 & \text{otherwise} \end{cases}$$

As for the scalar functions in $\mathcal{S}_h$, it must be constant in each $\mathcal{R}(\kappa)$, where $\kappa \in \mathcal{F}_q$, so the basis functions can be defined to be 1 on one $\mathcal{R}(\kappa)$ and 0 elsewhere. The numerical results for this piecewise constant approximation are summarized in Tables 2.1-2.4. Next, we consider the piecewise linear

h	$\|\boldsymbol{u}-\boldsymbol{u}_h\|_{\boldsymbol{L}^2(\Omega)}$	Order	$\|\boldsymbol{u}-\boldsymbol{u}_h\|_{Z'}$	order	$\|q-q_h\|_{L^2(\Omega)}$	Order
0.7071	5.9611e-001	-	3.4472e+000	-	2.7736e-001	-
0.3536	2.9944e-001	0.99332	3.4463e+000	0.00035	1.3837e-001	1.00324
0.1768	1.4990e-001	0.99821	3.4461e+000	0.00011	6.9132e-002	1.00107
0.0884	7.4975e-002	0.99954	3.4460e+000	0.00002	3.4559e-002	1.00029
0.0442	3.7491e-002	0.99989	3.4460e+000	-0.00000	1.7279e-002	1.00007

Table 2.1: Piecewise constant approximation of S_1 in the square domain

h	$\|\boldsymbol{u}-\boldsymbol{u}_h\|_{\boldsymbol{L}^2(\Omega)}$	Order	$\|\boldsymbol{u}-\boldsymbol{u}_h\|_{Z'}$	order	$\|q-q_h\|_{L^2(\Omega)}$	Order
1.0000	1.0371e+000	-	3.9884e+000	-	7.3379e-001	-
0.5000	4.2708e-001	1.27997	3.9167e+000	0.02618	2.4136e-001	1.60416
0.2500	2.0785e-001	1.03892	3.8976e+000	0.00705	1.1173e-001	1.11122
0.1250	1.0338e-001	1.00758	3.8904e+000	0.00268	5.4978e-002	1.02307
0.0625	5.1630e-002	1.00172	3.8873e+000	0.00115	2.7388e-002	1.00532

Table 2.2: Piecewise constant approximation of S_1 in the L-shaped domain

h	$\|\boldsymbol{u}-\boldsymbol{u}_h\|_{\boldsymbol{L}^2(\Omega)}$	Order	$\|\boldsymbol{u}-\boldsymbol{u}_h\|_{Z'}$	order	$\|q-q_h\|_{L^2(\Omega)}$	Order
1.0000	3.8985e-001	-	2.0449e-001	-	6.6573e-002	-
0.5000	1.9968e-001	0.96525	1.4271e-001	0.51900	1.6129e-002	2.04524
0.2500	1.0220e-001	0.96632	1.0072e-001	0.50267	4.0192e-003	2.00471
0.1250	5.1928e-002	0.97675	7.1203e-002	0.50037	1.0071e-003	1.99663
0.0625	2.6235e-002	0.98505	5.0346e-002	0.50005	2.5242e-004	1.99639

Table 2.3: Piecewise constant approximation of S_2 in the L-shaped domain

h	$\|\boldsymbol{u}-\boldsymbol{u}_h\|_{\boldsymbol{L}^2(\Omega)}$	Order	$\|\boldsymbol{u}-\boldsymbol{u}_h\|_{Z'}$	order	$\|q-q_h\|_{L^2(\Omega)}$	Order
1.0000	7.9598e-001	-	3.2337e-001	-	6.4408e-001	-
0.5000	3.1653e-001	1.33038	1.1442e-001	1.49885	1.8848e-001	1.77280
0.2500	1.6912e-001	0.90429	5.7055e-002	1.00393	6.7538e-002	1.48068
0.1250	1.0068e-001	0.74835	3.4706e-002	0.71716	2.5803e-002	1.38816
0.0625	6.2316e-002	0.69203	2.3239e-002	0.57864	1.0090e-002	1.35466

Table 2.4: Piecewise constant approximation of S_3 in the L-shaped domain

case. Again, we fix one $\mathcal{S}(\nu)$. Let λ_i, λ_ν be the scalar linear function such that $\lambda_i = 1$ at v_i and $\lambda_i = 0$ at the other three vertices, $\lambda_\nu = 1$ at ν and $\lambda_\nu = 0$ at the other three vertices, respectively. The degrees of freedom for the vector function $\boldsymbol{v}$ in each $\mathcal{S}(\nu)$ is 12. We define the basis functions, associated with each $\mathcal{S}(\nu)$, as follows:

$$\boldsymbol{v}_1 = \begin{cases} \frac{\lambda_\nu}{1-(\boldsymbol{t}_1\cdot\boldsymbol{t}_3)^2}\boldsymbol{t}_1 - \frac{\boldsymbol{t}_1\cdot\boldsymbol{t}_3\lambda_\nu}{1-(\boldsymbol{t}_1\cdot\boldsymbol{t}_3)^2}\boldsymbol{t}_3 & \text{if } (x,y)\in\tau_2 \\ \frac{\lambda_\nu}{1-(\boldsymbol{t}_1\cdot\boldsymbol{t}_2)^2}\boldsymbol{t}_1 - \frac{\boldsymbol{t}_1\cdot\boldsymbol{t}_2\lambda_\nu}{1-(\boldsymbol{t}_1\cdot\boldsymbol{t}_2)^2}\boldsymbol{t}_2 & \text{if } (x,y)\in\tau_3 \\ 0 & \text{otherwise} \end{cases}$$

$$\boldsymbol{v}_2 = \begin{cases} \frac{\lambda_1}{1-(\boldsymbol{t}_1\cdot\boldsymbol{t}_3)^2}\boldsymbol{t}_1 - \frac{\boldsymbol{t}_1\cdot\boldsymbol{t}_3\lambda_1}{1-(\boldsymbol{t}_1\cdot\boldsymbol{t}_3)^2}\boldsymbol{t}_3 & \text{if } (x,y)\in\tau_2 \\ \frac{\lambda_1}{1-(\boldsymbol{t}_1\cdot\boldsymbol{t}_2)^2}\boldsymbol{t}_1 - \frac{\boldsymbol{t}_1\cdot\boldsymbol{t}_2\lambda_1}{1-(\boldsymbol{t}_1\cdot\boldsymbol{t}_2)^2}\boldsymbol{t}_2 & \text{if } (x,y)\in\tau_3 \\ 0 & \text{otherwise} \end{cases}$$

$$\boldsymbol{v}_3 = \begin{cases} \frac{\lambda_3}{1-(\boldsymbol{t}_1\cdot\boldsymbol{t}_3)^2}\boldsymbol{t}_1 - \frac{\boldsymbol{t}_1\cdot\boldsymbol{t}_3\lambda_3}{1-(\boldsymbol{t}_1\cdot\boldsymbol{t}_3)^2}\boldsymbol{t}_3 & \text{if } (x,y)\in\tau_2 \\ 0 & \text{otherwise} \end{cases}$$

$$\boldsymbol{v}_4 = \begin{cases} \frac{\lambda_2}{1-(\boldsymbol{t}_1\cdot\boldsymbol{t}_3)^2}\boldsymbol{t}_1 - \frac{\boldsymbol{t}_1\cdot\boldsymbol{t}_3\lambda_2}{1-(\boldsymbol{t}_1\cdot\boldsymbol{t}_3)^2}\boldsymbol{t}_3 & \text{if } (x,y)\in\tau_3 \\ 0 & \text{otherwise} \end{cases}$$

$$\boldsymbol{v}_5 = \begin{cases} \frac{\lambda_\nu}{1-(\boldsymbol{t}_2\cdot\boldsymbol{t}_3)^2}\boldsymbol{t}_2 - \frac{\boldsymbol{t}_2\cdot\boldsymbol{t}_3\lambda_\nu}{1-(\boldsymbol{t}_2\cdot\boldsymbol{t}_3)^2}\boldsymbol{t}_3 & \text{if } (x,y)\in\tau_1 \\ \frac{\lambda_\nu}{1-(\boldsymbol{t}_1\cdot\boldsymbol{t}_2)^2}\boldsymbol{t}_2 - \frac{\boldsymbol{t}_1\cdot\boldsymbol{t}_2\lambda_\nu}{1-(\boldsymbol{t}_1\cdot\boldsymbol{t}_2)^2}\boldsymbol{t}_2 & \text{if } (x,y)\in\tau_3 \\ 0 & \text{otherwise} \end{cases}$$

$$\boldsymbol{v}_6 = \begin{cases} \frac{\lambda_2}{1-(\boldsymbol{t}_2\cdot\boldsymbol{t}_3)^2}\boldsymbol{t}_2 - \frac{\boldsymbol{t}_2\cdot\boldsymbol{t}_3\lambda_2}{1-(\boldsymbol{t}_2\cdot\boldsymbol{t}_3)^2}\boldsymbol{t}_3 & \text{if } (x,y)\in\tau_1 \\ \frac{\lambda_2}{1-(\boldsymbol{t}_1\cdot\boldsymbol{t}_2)^2}\boldsymbol{t}_2 - \frac{\boldsymbol{t}_1\cdot\boldsymbol{t}_2\lambda_2}{1-(\boldsymbol{t}_1\cdot\boldsymbol{t}_2)^2}\boldsymbol{t}_2 & \text{if } (x,y)\in\tau_3 \\ 0 & \text{otherwise} \end{cases}$$

$$\boldsymbol{v}_7 = \begin{cases} \frac{\lambda_3}{1-(\boldsymbol{t}_2\cdot\boldsymbol{t}_3)^2}\boldsymbol{t}_2 - \frac{\boldsymbol{t}_2\cdot\boldsymbol{t}_3\lambda_3}{1-(\boldsymbol{t}_2\cdot\boldsymbol{t}_3)^2}\boldsymbol{t}_3 & \text{if } (x,y)\in\tau_1 \\ 0 & \text{otherwise} \end{cases}$$

$$\boldsymbol{v}_8 = \begin{cases} \frac{\lambda_1}{1-(\boldsymbol{t}_1\cdot\boldsymbol{t}_2)^2}\boldsymbol{t}_2 - \frac{\boldsymbol{t}_1\cdot\boldsymbol{t}_2\lambda_1}{1-(\boldsymbol{t}_1\cdot\boldsymbol{t}_2)^2}\boldsymbol{t}_2 & \text{if } (x,y)\in\tau_3 \\ 0 & \text{otherwise} \end{cases}$$

$$\boldsymbol{v}_9 = \begin{cases} \frac{\lambda_\nu}{1-(\boldsymbol{t}_1\cdot\boldsymbol{t}_3)^2}\boldsymbol{t}_1 - \frac{\boldsymbol{t}_1\cdot\boldsymbol{t}_3\lambda_\nu}{1-(\boldsymbol{t}_1\cdot\boldsymbol{t}_3)^2}\boldsymbol{t}_3 & \text{if } (x,y)\in\tau_2 \\ \frac{\lambda_\nu}{1-(\boldsymbol{t}_1\cdot\boldsymbol{t}_2)^2}\boldsymbol{t}_1 - \frac{\boldsymbol{t}_1\cdot\boldsymbol{t}_2\lambda_\nu}{1-(\boldsymbol{t}_1\cdot\boldsymbol{t}_2)^2}\boldsymbol{t}_2 & \text{if } (x,y)\in\tau_3 \\ 0 & \text{otherwise} \end{cases}$$

$$\boldsymbol{v}_{10} = \begin{cases} \frac{\lambda_3}{1-(\boldsymbol{t}_2\cdot\boldsymbol{t}_3)^2}\boldsymbol{t}_3 - \frac{\boldsymbol{t}_2\cdot\boldsymbol{t}_3\lambda_3}{1-(\boldsymbol{t}_2\cdot\boldsymbol{t}_3)^2}\boldsymbol{t}_2 & \text{if } (x,y)\in\tau_1 \\ \frac{\lambda_3}{1-(\boldsymbol{t}_1\cdot\boldsymbol{t}_3)^2}\boldsymbol{t}_3 - \frac{\boldsymbol{t}_1\cdot\boldsymbol{t}_3\lambda_3}{1-(\boldsymbol{t}_1\cdot\boldsymbol{t}_3)^2}\boldsymbol{t}_1 & \text{if } (x,y)\in\tau_2 \\ 0 & \text{otherwise} \end{cases}$$

$$\boldsymbol{v}_{11} = \begin{cases} \frac{\lambda_2}{1-(\boldsymbol{t}_2\cdot\boldsymbol{t}_3)^2}\boldsymbol{t}_3 - \frac{\boldsymbol{t}_2\cdot\boldsymbol{t}_3\lambda_2}{1-(\boldsymbol{t}_2\cdot\boldsymbol{t}_3)^2}\boldsymbol{t}_2 & \text{if } (x,y)\in\tau_1 \\ 0 & \text{otherwise} \end{cases}$$

$$\boldsymbol{v}_{12} = \begin{cases} \frac{\lambda_1}{1-(\boldsymbol{t}_1\cdot\boldsymbol{t}_3)^2}\boldsymbol{t}_3 - \frac{\boldsymbol{t}_1\cdot\boldsymbol{t}_3\lambda_1}{1-(\boldsymbol{t}_1\cdot\boldsymbol{t}_3)^2}\boldsymbol{t}_1 & \text{if } (x,y)\in\tau_2 \\ 0 & \text{otherwise} \end{cases}$$

For the basis functions for the scalar field, there will be 4 such basis on each $\mathcal{R}(\kappa)$, each of them is a linear function such that it is continuous within $\mathcal{R}(\kappa)$, and it equals to 1 at one of the 4 nodes and 0 at the other three nodes. The numerical results for piecewise linear approximation are summarized in Tables 2.5-2.8. As you can see from Tables 2.1-2.8, the numerical solutions $\boldsymbol{u}_h$ converge to the theoretical solution in the $\boldsymbol{L}^2$-norm with the expected order of convergence in all cases. More importantly, the method recovers S_3, the highly singular function, in a non-convex domain, so our DG method is spurious free. See Figure 2.3 for the graph of the approximation of S_3 by our method. For S_1, the smooth function, the order of convergence of $\boldsymbol{u}_h$ in the discrete $H(\text{curl};\Omega)$-norm and q_h in the L^2-norm again agree with Theorem 2.4.1. Surprisingly, the order of convergence of $\boldsymbol{u}_h$ in the discrete $H(\text{curl};\Omega)$-norm for S_2 and S_3 are higher than predicted. The same happens to the convergence of q_h in the L^2-norm.

Eigenvalue problem Beside using our new DG method to solve the equations (1.1), we also tried to use the discrete system to approximate the eigenvalues of the **curl** curl operator. More precisely, we want to approximate the value $\lambda \in \mathbb{C}$ such that there exists $\mathbf{0} \neq \boldsymbol{u} \in H_0(\text{curl};\Omega)$,

$$(\text{curl } \boldsymbol{u}, \text{curl } \boldsymbol{v})_{L^2(\Omega)} = \lambda(\boldsymbol{u}, \boldsymbol{v})_{\boldsymbol{L}^2(\Omega)} \qquad \forall \boldsymbol{v} \in H_0(\text{curl};\Omega) \tag{2.34}$$

h	$\|\boldsymbol{u}-\boldsymbol{u}_h\|_{\boldsymbol{L}^2(\Omega)}$	Order	$\|\boldsymbol{u}-\boldsymbol{u}_h\|_{\boldsymbol{Z}'}$	order	$\|q-q_h\|_{L^2(\Omega)}$	Order
0.7071	4.2730e-02	-	2.7207e-01	-	2.1238e-02	-
0.3536	1.1081e-02	1.94715	1.3755e-01	0.98404	5.3234e-03	1.99622
0.1768	2.8005e-03	1.98435	6.8812e-02	0.99922	1.3313e-03	1.99950
0.0884	7.0223e-04	1.99566	3.4373e-02	1.00138	3.3284e-04	1.99997
0.0442	1.7570e-04	1.99885	1.7173e-02	1.00113	8.3209e-05	2.00000

Table 2.5: Piecewise linear approximation of S_1 in the square domain

h	$\|\boldsymbol{u}-\boldsymbol{u}_h\|_{\boldsymbol{L}^2(\Omega)}$	Order	$\|\boldsymbol{u}-\boldsymbol{u}_h\|_{\boldsymbol{Z}'}$	order	$\|q-q_h\|_{L^2(\Omega)}$	Order
1.0000	8.5857e-02	-	4.2364e-01	-	3.7549e-02	-
0.5000	2.1898e-02	1.97114	2.1642e-01	0.96902	9.6156e-03	1.96534
0.2500	5.5377e-03	1.98345	1.0840e-01	0.99744	2.4182e-03	1.99147
0.1250	1.3927e-03	1.99136	5.4117e-02	1.00223	6.0538e-04	1.99801
0.0625	3.4924e-04	1.99563	2.7021e-02	1.00201	1.5139e-04	1.99953

Table 2.6: Piecewise linear approximation of S_1 in the L-shaped domain

h	$\|\boldsymbol{u}-\boldsymbol{u}_h\|_{\boldsymbol{L}^2(\Omega)}$	Order	$\|\boldsymbol{u}-\boldsymbol{u}_h\|_{\boldsymbol{Z}'}$	order	$\|q-q_h\|_{L^2(\Omega)}$	Order
1.0000	4.6391e-02	-	1.2824e-02	-	2.8166e-03	-
0.5000	1.8939e-02	1.29251	4.4299e-03	1.53350	5.5840e-04	2.33457
0.2500	7.6035e-03	1.31659	1.5688e-03	1.49764	1.1202e-04	2.31755
0.1250	3.0317e-03	1.32656	5.5484e-04	1.49950	2.2355e-05	2.32507
0.0625	1.2054e-03	1.33062	1.9617e-04	1.49996	4.4467e-06	2.32980

Table 2.7: Piecewise linear approximation of S_2 in the L-shaped domain

h	$\|\boldsymbol{u}-\boldsymbol{u}_h\|_{\boldsymbol{L}^2(\Omega)}$	Order	$\|\boldsymbol{u}-\boldsymbol{u}_h\|_{\boldsymbol{Z}'}$	order	$\|q-q_h\|_{L^2(\Omega)}$	Order
1.0000	1.4936e-01	-	8.4435e-02	-	8.4590e-02	-
0.5000	8.3248e-02	0.84332	3.2631e-02	1.37158	3.2541e-02	1.37824
0.2500	4.9699e-02	0.74420	1.2831e-02	1.34660	1.2778e-02	1.34855
0.1250	3.0613e-02	0.69906	5.0715e-03	1.33918	5.0509e-03	1.33908
0.0625	1.9110e-02	0.67980	2.0086e-03	1.33625	2.0013e-03	1.33558

Table 2.8: Piecewise linear approximation of S_3 in the L-shaped domain

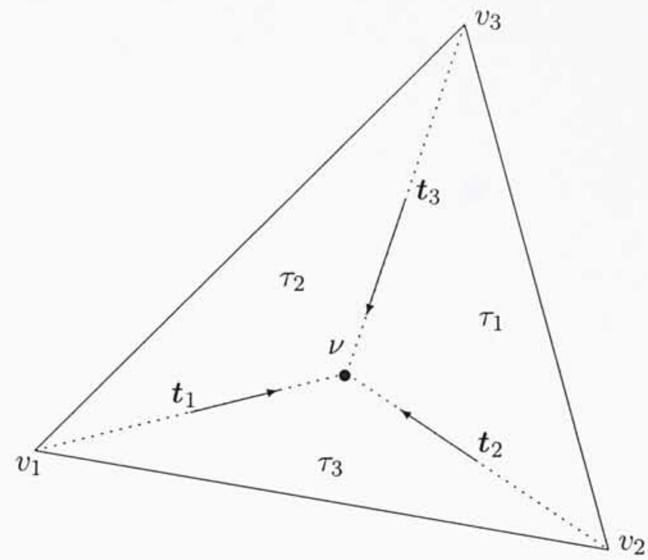

Figure 2.2: Notations on a specific $\mathcal{S}(\nu)$.

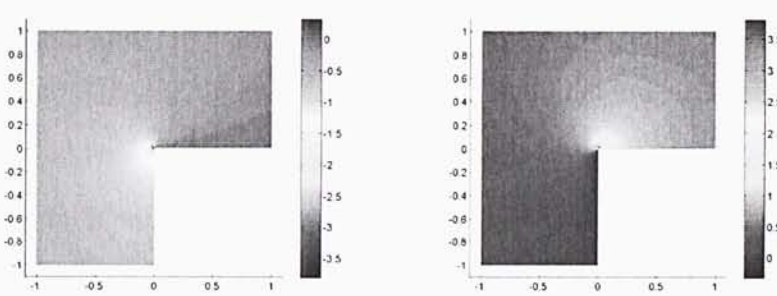

(a) x component (b) y component

Figure 2.3: Numerical solution of the new DG method with piecewise linear elements and $h = 0.0625$

Note that our discrete eigen problem are in the following form:

$$\begin{aligned} M_q \boldsymbol{q} - B^* \boldsymbol{u} &= \mathbf{0} \\ B\boldsymbol{q} - \lambda_h M_u \boldsymbol{u} &= \mathbf{0} \end{aligned} \tag{2.35}$$

So one needs to find the generalized eigenvalues λ_h such that for some $\mathbf{0} \neq \boldsymbol{u}$,

$$B(M_q)^{-1} B^* \boldsymbol{u} = \lambda_h M_u \boldsymbol{u} \tag{2.36}$$

We give the approximations of the first 40 eigenvalues in the square domain and also the first 5 eigenvalues of the L-shaped domain. The theoretical eigenvalues for the square domain are $(n^2+m^2)\pi^2$

where n and m are nonnegative integers and they are not equal to zero at the same time. The numerical results with piecewise linear elements approximation are shown in Figures 2.4-2.6, we denote λ_i the i-th eigenvalue for the continuous problem and $\lambda_{i,h}$ the approximation for i-th eigenvalue. The y-axis shows the magnitudes of the eigenvalues while the x-axis corresponds to the eigenvalue number, i.e. the n-th eigenvalue. We remark that we have discarded all the zero eigenvalues in the approximation in Figures 2.4-2.6. As the mesh is getting finer, the approximation are better. We can observe from Figure 2.6 that the method does not produce spurious eigenvalues and also the multiplicity of the dimension of the eigenspace is correct at least for the first 40 eigenvalues.

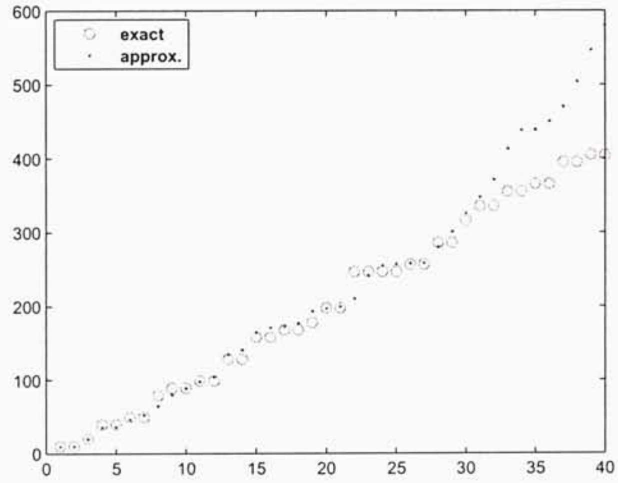

Figure 2.4: λ_i and $\lambda_{i,h}$, $i = 1, 2, ..., 40$, for the square domain with $h = 0.7071$

For the L-shaped domain, the first 5 eigenvalues are 1.47562182408, 3.53403136678, π^2, π^2 and 11.3894793979, c.f. [5, 15]. This time we give the numerical results regarding the convergence of the first 5 approximations in Figure 2.7-2.11, the y-axis shows the absolute error $|\lambda_i - \lambda_{i,h}|$ and the x-axis is the corresponding mesh width h. The convergence analysis of the eigen problem will be our further work.

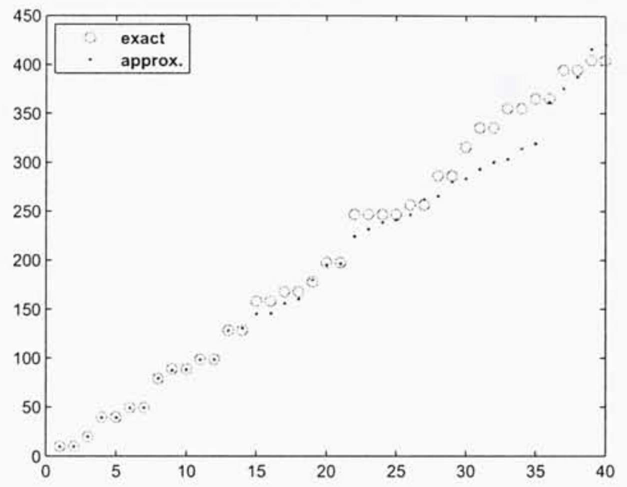

Figure 2.5: λ_i and $\lambda_{i,h}$, $i = 1, 2, ..., 40$, for the square domain with $h = 0.3536$

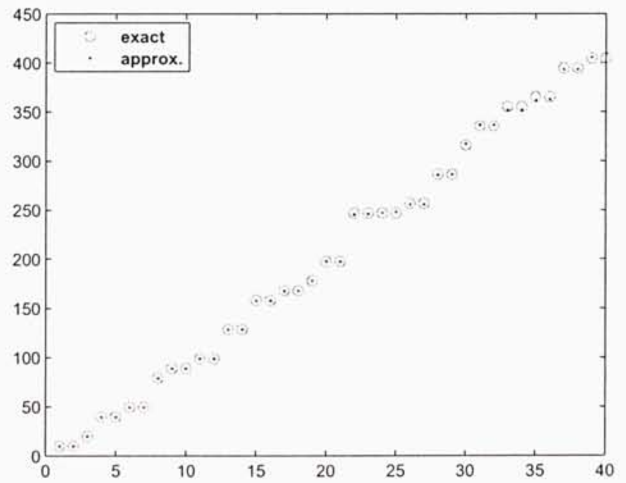

Figure 2.6: λ_i and $\lambda_{i,h}$, $i = 1, 2, ..., 40$, for the square domain with $h = 0.1768$

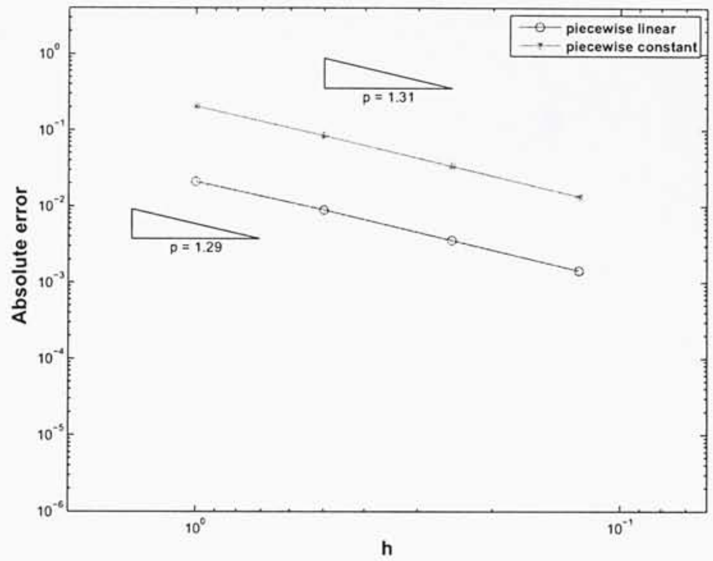

Figure 2.7: convergence of λ_1 for the L-shaped domain

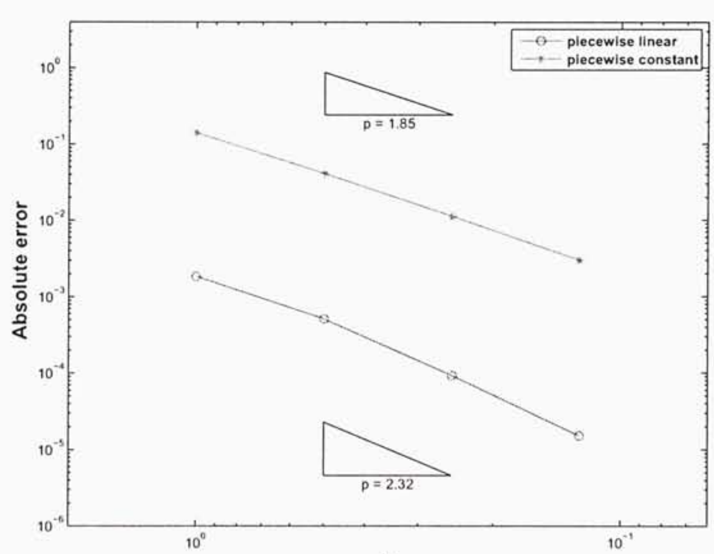

Figure 2.8: convergence of λ_2 for the L-shaped domain

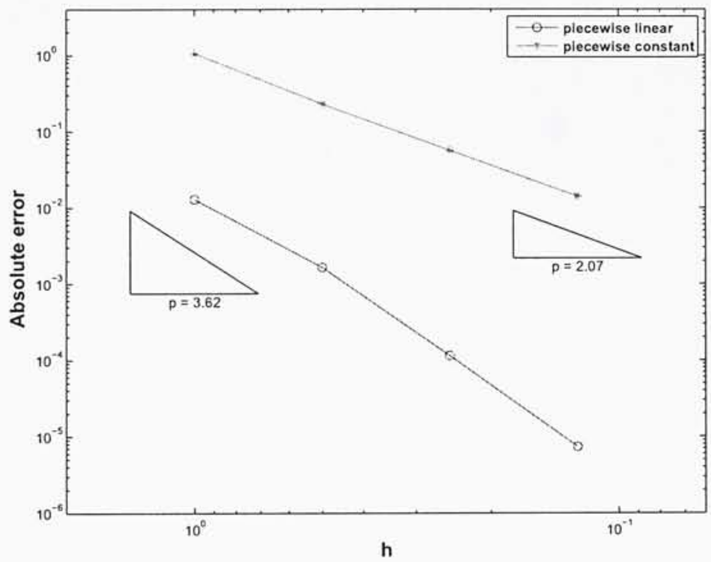

Figure 2.9: convergence of λ_3 for the L-shaped domain

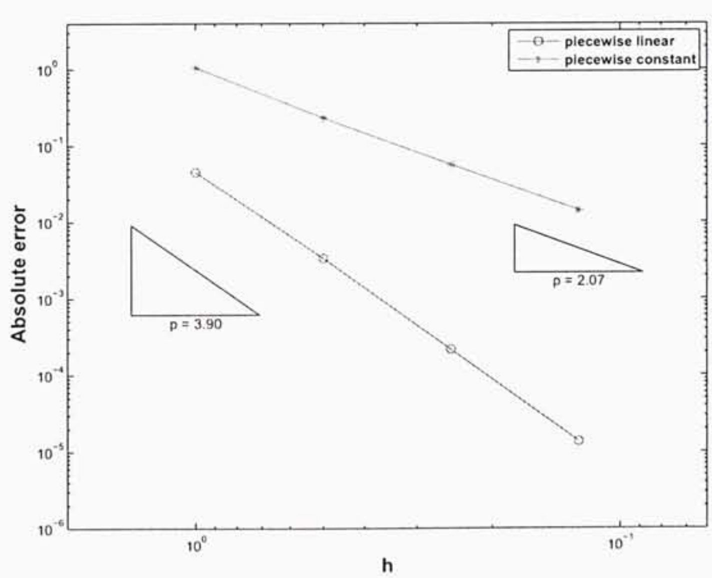

Figure 2.10: convergence of λ_4 for the L-shaped domain

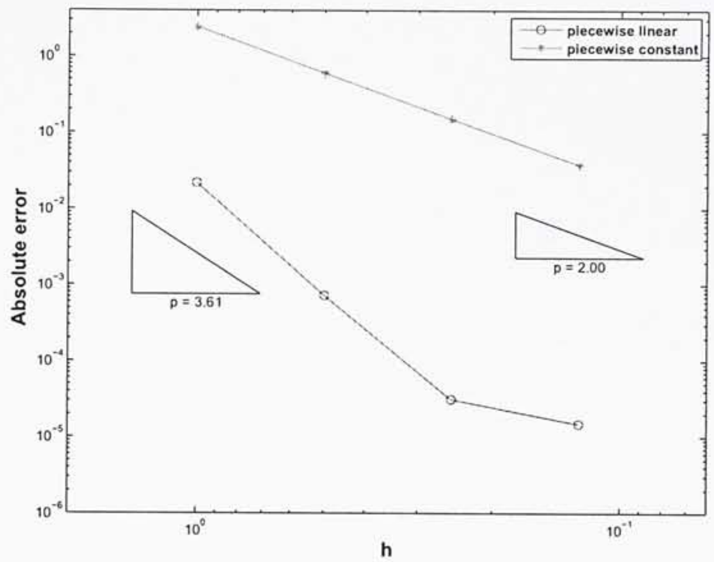

Figure 2.11: convergence of λ_5 for the L-shaped domain

2.6 Concluding Remarks

In this chapter, we propose a new discontinuous Galerkin method for the **curl** curl operator in two dimension space. The method is stable with respect to both the L^2 norm and the energy norm. We have shown that the order of convergence of the proposed method is optimal in the above norms, and this is verified in the numerical experiments. Numerical examples also show that our proposed method is able to recover highly singular functions in a non-convex domain, and it does not produce spurious eigenvalues in the approximation of the spectrum of the **curl** curl operator.

Chapter 3

Staggered DG method for the convection-diffusion equation

3.1 Introduction

Recall the convection-diffusion equation, which is the subject of the current chapter:

$$\frac{\partial u}{\partial t} = \Delta u - \nabla \cdot (\mathbf{b}u) + f, \qquad (x,t) \in \Omega \times (0,T), \tag{3.1}$$

where Ω is a polyhedral domain in $\mathbb{R}^d$, $d = 2, 3$, and $T > 0$ is a fixed time.

This chapter is organized as follows. In Section 3.2, the new staggered DG method will be derived. Then, in Section 3.3, we will show that the numerical scheme preserves the physical laws (1.7)-(1.3) arising from the convection-diffusion equation. The stability and convergence are then analyzed in Section 3.4 for the semi-discrete scheme and in Section 3.5 for the fully discrete scheme. In Section 3.6, numerical results for both the static and time-dependent problems are presented to verify our theoretical estimates. Finally, a conclusion is given.

3.2 Method description

In this Section, we will derive our new staggered DG method for the convection-diffusion equation (1.5). Following Chung and Engquist [11, 12], we first define the triangulation. Suppose the domain Ω is triangulated by a set of tetrahedra. We use the notation $\mathcal{F}_u$ to denote the set of all faces in this triangulation and use the notation $\mathcal{F}_u^0$ to denote the subset of all interior faces in $\mathcal{F}_u$. For each tetrahedron, we take an interior point ν and call the this tetrahedron $\mathcal{S}(\nu)$. Using the point ν, we can subdivide each tetrahedron into 4 sub-tetrahedra by connecting the point ν to the 4 vertices of the tetrahedron. We use the notation $\mathcal{F}_p$ to denote all new faces obtained by the subdivision of tetrahedra. For an example in 2D, see Figure 3.1. For each face κ, we let $\mathcal{R}(\kappa)$ be the union of the two tetrahedra sharing the face κ. If κ is a boundary face, we let $\mathcal{R}(\kappa)$ the only tetrahedron having the face κ. For an example in 2D, see Figure 3.1.

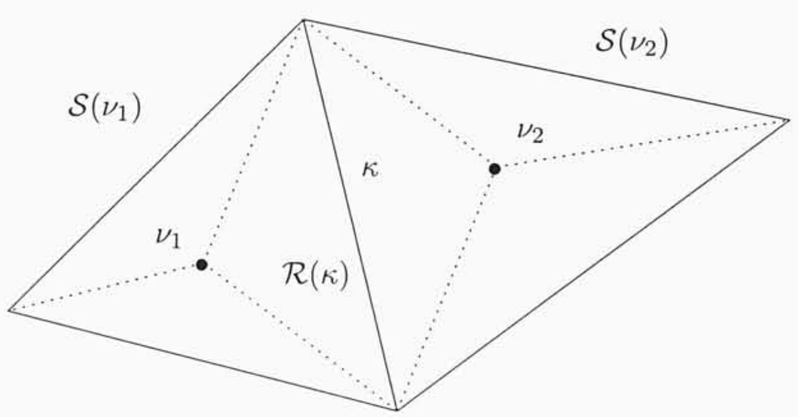

Figure 3.1: Triangulation in 2D.

We will also define a unit normal vector n_κ on each face κ in $\mathcal{F}$ by the following way. If $\kappa \in \mathcal{F}\backslash\mathcal{F}^0$ is a boundary face, then we define n_κ as the unit normal vector of κ pointing outside of Ω. If $\kappa \in \mathcal{F}^0$ is an interior face, then we fix n_κ as one of the two possible unit normal vectors on κ. When it is clear that which face we are considering, we will use n instead of n_κ to simplify the notations.

Now, we will discuss the finite element spaces. Let $k \geq 0$ be a non-negative integer. Let $\tau \in \mathcal{T}$ and $\kappa \in \mathcal{F}$. We define $P^k(\tau)$ and $P^k(\kappa)$ as the spaces of polynomials of degree less than or equal to k on τ and κ respectively. Then we define the following:

Local $H^1(\Omega)$-conforming finite element space

$$U_h = \{v \mid v|_\tau \in P^k(\tau);\ v \text{ is continuous on } \kappa \in \mathcal{F}_u^0;\ v|_{\partial\Omega} = 0\}. \tag{3.2}$$

Notice that, if $v \in U_h$, then $v|_{\mathcal{R}(\kappa)} \in H^1(\mathcal{R}(\kappa))$ for each face $\kappa \in \mathcal{F}_u$. Furthermore, the condition $v|_{\partial\Omega} = 0$ is equivalent to $v|_\kappa = 0$ for all $\kappa \in \mathcal{F}_u \backslash \mathcal{F}_u^0$ since $\mathcal{F}_u$ contains all boundary faces. We also define the following degrees of freedom.

(UD1). For each face $\kappa \in \mathcal{F}_u^0$, we have

$$\phi_\kappa(v) := \int_\kappa v p_k \, d\sigma$$

for all $p_k \in P^k(\kappa)$.

(UD2). For each $\tau \in \mathcal{T}$, we have

$$\phi_\tau(v) := \int_\tau v p_{k-1} \, dx$$

for all $p_{k-1} \in P^{k-1}(\tau)$.

In this paper, we use the notation $|\mathcal{S}|$ to represent the number of elements in the set $\mathcal{S}$. By Chung and Engquist [12], any function v in the local $H^1(\Omega)$-conforming finite element space U_h is uniquely determined by the degrees of freedom (UD1)-(UD2).

In the space U_h we define the following norms

$$\|u\|_X^2 = \int_\Omega u^2 \, dx + \sum_{\kappa \in \mathcal{F}_u^0} h_\kappa \int_\kappa u^2 \, d\sigma, \tag{3.3}$$

$$\|u\|_Z^2 = \int_\Omega |\nabla u|^2 \, dx + \sum_{\kappa \in \mathcal{F}_p} h_\kappa^{-1} \int_\kappa [u]^2 \, d\sigma \tag{3.4}$$

where we remark that the integral of ∇u in (3.4) is defined element by element. Here we recall that, by definition, $u \in U_h$ is continuous on each face κ in the set $\mathcal{F}_u^0$ and is discontinuous on each face κ in the set $\mathcal{F}_p$. We say $\|u\|_X$ is the discrete L^2-norm of u and $\|u\|_Z$ is the discrete H^1-norm of u. In the above definition, the jump $[u]$ is defined in the following way. For each $\kappa \in \mathcal{F}_p$, there exist two tetrahedra τ_1 and τ_2 such that κ is a common face of them. Moreover, each τ_i, $i = 1, 2$, has a face κ_i that belongs to $\mathcal{F}_u$. Thus, $\kappa \subset \partial\mathcal{R}(\kappa_i)$ for $i = 1, 2$. Then for such $\kappa \in \mathcal{F}_p$, we write m_i as the outward unit normal vector of $\partial\mathcal{R}(\kappa_i)$ for $i = 1, 2$, and define

$$\delta_\kappa^{(i)} = \begin{cases} 1 & \text{if } m_i = n \text{ on } \kappa \\ -1 & \text{if } m_i = -n \text{ on } \kappa \end{cases}$$

where n is the unit normal vector of the face κ. Then the jump $[u]$ on the face κ is defined as

$$[u] = \delta_\kappa^{(1)} u_1 + \delta_\kappa^{(2)} u_2$$

where $u_i = u|_{\tau_i}$.

Now, we define the following:

Local $H(\mathbf{div};\Omega)$-conforming finite element space

$$W_h = \{\mathbf{q} \mid \mathbf{q}|_\tau \in P^k(\tau)^3 \text{ and } \mathbf{q}\cdot n \text{ is continuous on } \kappa \in \mathcal{F}_p\}. \tag{3.5}$$

Notice that, if $\mathbf{q} \in W_h$, then $\mathbf{q}|_{\mathcal{S}(\nu)} \in H(\text{div};\mathcal{S}(\nu))$ for each $\nu \in \mathcal{N}_1$. We also define the following degrees of freedom.

(WD1). For each $\kappa \in \mathcal{F}_p$, we have

$$\psi_\kappa(\mathbf{q}) := \int_\kappa \mathbf{q}\cdot n\, p_k\, d\sigma$$

for all $p_k \in P^k(\kappa)$.

(WD2). For each $\tau \in \mathcal{T}$, we have

$$\psi_\tau(\mathbf{q}) := \int_\tau \mathbf{q}\cdot p_{k-1}\, dx$$

for all $p_{k-1} \in P^{k-1}(\tau)^3$.

By Chung and Engquist [12], any function $\mathbf{q}$ in the local $H(\text{div};\Omega)$-conforming finite element space W_h is uniquely determined by the degrees of freedom (WD1)-(WD2).

In the space W_h, we define the following norms

$$\|\mathbf{p}\|^2_{X'} = \int_\Omega |\mathbf{p}|^2\, dx + \sum_{\kappa\in\mathcal{F}_p} h_\kappa \int_\kappa (\mathbf{p}\cdot n)^2\, d\sigma, \tag{3.6}$$

$$\|\mathbf{p}\|^2_{Z'} = \int_\Omega (\nabla\cdot\mathbf{p})^2\, dx + \sum_{\kappa\in\mathcal{F}_u^0} h_\kappa^{-1} \int_\kappa [\mathbf{p}\cdot n]^2\, d\sigma \tag{3.7}$$

where we remark that the integral of $\nabla\cdot\mathbf{p}$ in (3.7) is defined element by element. Here we recall that, by definition, $\mathbf{p}\in W_h$ has continuous normal component on each face in $\kappa \in \mathcal{F}_p$. We say $\|\mathbf{p}\|_{X'}$ is the discrete L^2-norm of $\mathbf{p}$ and $\|\mathbf{p}\|_{Z'}$ is the discrete $H(\text{div};\Omega)$-norm of $\mathbf{p}$. In the above definition, the jump $[\mathbf{p}\cdot n]$ is defined in the following way. Let $\kappa \subset \mathcal{F}_u^0$. Then there are exactly two tetrahedra τ_1 and τ_2 such that κ is a common face of them. Let ν_i be the node of τ_i that does not lie on κ. Then we have $\kappa \in \partial\mathcal{S}(\nu_i)$ for $i = 1, 2$. Let m_i be the outward unit normal vector of $\partial\mathcal{S}(\nu_i)$. We define

$$\delta_\kappa^{(i)} = \begin{cases} 1 & \text{if } m_i = n \text{ on } \kappa \\ -1 & \text{if } m_i = -n \text{ on } \kappa \end{cases}$$

where n is the unit normal vector of the face κ. Then the jump $[\mathbf{p}\cdot n]$ on the face κ is defined as

$$[\mathbf{p}\cdot n] = \delta_\kappa^{(1)}\mathbf{p}_1\cdot n + \delta_\kappa^{(2)}\mathbf{p}_2\cdot n,$$

where $\mathbf{p}_i = \mathbf{p}|_{\tau_i}$.

We define

$$\begin{aligned} B_h(\mathbf{p}_h, v) &= \int_\Omega \mathbf{p}_h\cdot\nabla v\,dx - \sum_{\kappa\in\mathcal{F}_p}\int_\kappa \mathbf{p}_h\cdot n\,[v]\,d\sigma, && (3.8)\\ B_h^*(u_h,\mathbf{q}) &= -\int_\Omega u_h\,\nabla\cdot\mathbf{q}\,dx + \sum_{\kappa\in\mathcal{F}_u^0}\int_\kappa u_h\,[\mathbf{q}\cdot n]\,d\sigma, && (3.9)\\ F_h(v) &= \int_\Omega fv\,dx. && (3.10)\end{aligned}$$

By Chung and Engquist [12], we have $B_h(v,\mathbf{q}) = B_h^*(\mathbf{q},v)$ for all $v\in U_h$ and $\mathbf{q}\in W_h$. Moreover, the following inf-sup condition holds:

$$K\|v\|_Z \le \sup_{\mathbf{q}\in W_h}\frac{B_h^*(v,\mathbf{q})}{\|\mathbf{q}\|_{X'}} \tag{3.11}$$

for all $v\in U_h$. Furthermore, there exist interpolation operators $\mathcal{I}$ and $\mathcal{J}$ such that $\|u-\mathcal{I}u\|\le Ch^{k+1}|u|_{H^{k+1}(\Omega)}$, $\|u-\mathcal{I}u\|_Z \le Ch^k|u|_{H^{k+1}(\Omega)}$ and $\|\mathbf{p}-\mathcal{J}\mathbf{p}\|\le Ch^{k+1}|\mathbf{p}|^d_{H^{k+1}(\Omega)}$ for smooth functions u and $\mathbf{p}$.

Our new staggered DG method is then defined as: find $(\mathbf{p}_h,\mathbf{w}_h,u_h)\in W_h\times W_h\times U_h$ such that

$$\begin{aligned} \int_\Omega \mathbf{p}_h\cdot\mathbf{q}\,dx &= B_h^*(u_h,\mathbf{q}) - \frac{1}{2}\int_\Omega \mathbf{w}_h\cdot\mathbf{q}\,dx, && (3.12)\\ \int_\Omega \mathbf{w}_h\cdot\mathbf{q}\,dx &= \int_\Omega u_h\mathbf{b}_h\cdot\mathbf{q}\,dx, && (3.13)\\ \int_\Omega \frac{\partial u_h}{\partial t}v\,dx &= -B_h(\mathbf{p}_h,v) - \frac{1}{2}\int_\Omega \mathbf{b}_h\cdot\mathbf{p}_h\,v - \frac{1}{4}\int_\Omega \mathbf{b}_h\cdot\mathbf{w}_h\,v\,dx + F_h(v) && (3.14)\end{aligned}$$

for all test functions $\mathbf{q}\in W_h$ and $v\in U_h$. The derivation of (3.12)-(3.14) follows a similar technique as in Chung and Engquist [12]. We emphasis here that in (3.14), we use $\mathbf{w}_h$ instead of $\mathbf{b}\,u_h$. This is one of the key steps for the conservation of structures. Furthermore, the given vector field $\mathbf{b}$ is approximated by $\mathbf{b}_h$ in the space W_h, and it is defined by

$$B_h(\mathbf{b}-\mathbf{b}_h, v) = 0, \quad \forall v\in U_h.$$

The existence of such approximation is proved in [12]. Since $\nabla \cdot \mathbf{b} = 0$ and $\mathbf{b}$ has continuous normal component on each face κ,

$$B_h(\mathbf{b}_h, v) = B_h(\mathbf{b}, v) = B_h^*(v, \mathbf{b}) = 0. \tag{3.15}$$

For given u_h, we first find $\mathbf{p}_h$ by (3.12) and $\mathbf{w}_h$ by (3.13), then find u_h for the next time step by using (3.14) and some suitable time-stepping numerical scheme. For example, if the Crank Nicolson method is used for time-stepping, the resulting fully discrete scheme is

$$\begin{aligned}
&\int_\Omega (\mathbf{p}_h^n + \mathbf{p}_h^{n+1}) \cdot \mathbf{q}\, dx = B_h^*(u_h^n + u_h^{n+1}, \mathbf{q}) - \frac{1}{2}\int_\Omega (\mathbf{w}_h^{n+\frac{1}{2},n} + \mathbf{w}_h^{n+\frac{1}{2},n+1}) \cdot \mathbf{q}\, dx, \\
&\int_\Omega \mathbf{w}_h^{n+\frac{1}{2},n} \cdot \mathbf{q}\, dx = \int_\Omega \mathbf{b}_h^{n+\frac{1}{2}} u_h^n \cdot \mathbf{q}\, dx \\
&\int_\Omega \mathbf{w}_h^{n+\frac{1}{2},n+1} \cdot \mathbf{q}\, dx = \int_\Omega \mathbf{b}_h^{n+\frac{1}{2}} u_h^{n+1} \cdot \mathbf{q}\, dx \\
&\int_\Omega (\frac{u_h^{n+1} - u_h^n}{\triangle t})\, v\, dx + B_h(\frac{\mathbf{p}_h^{n+1} + \mathbf{p}_h^n}{2}, v) + \frac{1}{2}\int_\Omega \mathbf{b}_h^{n+\frac{1}{2}} \cdot (\frac{\mathbf{p}_h^{n+1} + \mathbf{p}_h^n}{2})\, v\, dx \\
&+ \frac{1}{4}\int_\Omega \mathbf{b}_h^{n+\frac{1}{2}} \cdot (\mathbf{w}_h^{n+\frac{1}{2},n} + \mathbf{w}_h^{n+\frac{1}{2},n+1})\, v\, dx = \int_\Omega f^{n+\frac{1}{2}} v\, dx.
\end{aligned}$$

The approximation properties of these schemes will be studied in detail in Section 3.4 and 3.5.

3.3 Preservation of physical structures

In this section, we will prove that the numerical solution of the new staggered DG scheme (3.12)-(3.14) preserves the properties (1.7)-(1.3) in some discrete sense.

Let Ω' be a subdomain formed by the union of connected tetrahedra $\mathcal{S}(\nu)$ and let Ω'' be a subdomain formed by the union of $\mathcal{R}(\kappa)$ for those faces κ that lie on the tetrahedra in Ω'. Notice that $\Omega' \subset \Omega''$. Then we have the following theorem.

Theorem 3.3.1 *The relation (1.7) is preserved in a discrete sense, namely,*

$$\int_{\Omega''} \frac{\partial u_h}{\partial t}\, dx = \sum_{\kappa \in \partial\Omega''} \int_\kappa (\boldsymbol{p}_h - \frac{1}{2} u_h \boldsymbol{b}_h) \cdot m\, d\sigma + \int_{\Omega''} f\, dx + \epsilon_1 \tag{3.16}$$

where m is the unit outward normal for $\partial\Omega''$ and the remainder

$$\epsilon_1 = -\frac{1}{2}\int_{\Omega'' \setminus \Omega'} (\boldsymbol{p}_h + \frac{1}{2}\boldsymbol{w}_h - \nabla u_h) \cdot \boldsymbol{b}_h\, dx.$$

Proof. We define test functions $v \in U_h$ and $\mathbf{q} \in W_h$ by

$$v = \begin{cases} 1 & x \in \Omega'' \\ 0 & \text{otherwise} \end{cases}, \qquad \mathbf{q} = \begin{cases} \mathbf{b}_h & x \in \Omega' \\ \mathbf{0} & \text{otherwise.} \end{cases}$$

Then using these test functions in (3.14) and (3.12) respectively, we have

$$\int_{\Omega'} \mathbf{p}_h \cdot \mathbf{b}_h \, dx = B_h^*(u_h, \mathbf{q}) - \frac{1}{2}\int_{\Omega'} \mathbf{w}_h \cdot \mathbf{b}_h \, dx, \tag{3.17}$$

$$\int_{\Omega''} \frac{\partial u_h}{\partial t} \, dx = -B_h(\mathbf{p}_h, v) - \frac{1}{2}\int_{\Omega''} \mathbf{b}_h \cdot \mathbf{p}_h - \frac{1}{4}\int_{\Omega''} \mathbf{b}_h \cdot \mathbf{w}_h \, dx + \int_{\Omega''} f \, dx. \tag{3.18}$$

By the definitions of B_h and v, as well as the fact that $[v] = 0$ on all internal faces of Ω'', we have

$$B_h(\mathbf{p}_h, v) = -\sum_{\kappa \in \partial\Omega''} \int_\kappa \mathbf{p}_h \cdot n \, [v] \, d\sigma = -\sum_{\kappa \in \partial\Omega''} \int_\kappa \mathbf{p}_h \cdot m \, d\sigma$$

where m is the unit outward normal for $\partial\Omega''$. By (3.17), the equation (3.18) becomes

$$\begin{aligned} \int_{\Omega''} \frac{\partial u_h}{\partial t} \, dx = &\sum_{\kappa \in \partial\Omega''} \int_\kappa \mathbf{p}_h \cdot m \, d\sigma - \frac{1}{2} B_h^*(u_h, \mathbf{q}) \\ &+ \int_{\Omega''} f \, dx - \frac{1}{2}\int_{\Omega''\backslash\Omega'} (\mathbf{p}_h + \frac{1}{2}\mathbf{w}_h) \cdot \mathbf{b}_h \, dx. \end{aligned} \tag{3.19}$$

By the definitions of B_h^* and $\mathbf{q}$ as well as the relation (3.15), we have

$$B_h^*(u_h, \mathbf{q}) = -\int_{\Omega''\backslash\Omega'} u_h \nabla \cdot \mathbf{b}_h \, dx + \sum_{\kappa \in \mathcal{F}_u^0 \cap \partial\Omega'} \int_\kappa u_h \, \mathbf{b}_h \cdot n \, d\sigma.$$

Take one triangle $\tau \in \Omega''\backslash\Omega'$ with face $\kappa_0 \in \partial\Omega'$ and faces κ_i, $(i = 1, 2, 3)$, in $\partial\Omega''$, then by the Green's identity,

$$\int_\tau \nabla u_h \cdot \mathbf{b}_h \, dx + \int_\tau u_h \, \nabla \cdot \mathbf{b}_h \, dx = \int_{\partial\tau} u_h \mathbf{b}_h \cdot n \, d\sigma.$$

Thus, we have

$$-\int_\tau u_h \, \nabla \cdot \mathbf{b}_h \, dx + \int_{\kappa_0} u_h \mathbf{b}_h \cdot n \, d\sigma = -\sum_{i=1}^{3} \int_{\kappa_i} u_h \mathbf{b}_h \cdot n \, d\sigma + \int_\tau \nabla u_h \cdot \mathbf{b}_h \, dx.$$

Then (3.19) becomes

$$\begin{aligned} \int_{\Omega''} \frac{\partial u_h}{\partial t} \, dx = &\sum_{\kappa \in \partial\Omega''} \int_\kappa (\mathbf{p}_h - \frac{1}{2} u_h \mathbf{b}_h) \cdot m \, d\sigma \\ &+ \int_{\Omega''} f \, dx - \frac{1}{2}\int_{\Omega''\backslash\Omega'} (\mathbf{p}_h + \frac{1}{2}\mathbf{w}_h - \nabla u_h) \cdot \mathbf{b}_h \, dx \end{aligned}$$

which proves (3.16).

□

From Theorem 3.3.1, we see that the numerical solution u_h satisfies a discrete analog (3.16) of the continuous counterpart (1.7). We emphasize that the term $\mathbf{p}_h - \frac{1}{2}u_h\mathbf{b}$ can be seen as a discrete analog of the continuous quantity $\nabla u - u\mathbf{b}$. Moreover, the term $\mathbf{p}_h + \frac{1}{2}\mathbf{w}_h$ can be seen as a discrete analog of ∇u. Thus, by the result of the next section, the remainder term ϵ_1, which involves the integral of the difference of $\mathbf{p}_h + \frac{1}{2}\mathbf{w}_h$ and ∇u_h, converges to zero.

In the next theorem, we prove that the numerical solution u_h also satisfies a discrete analog of (1.8) and (1.3).

Theorem 3.3.2 *The relations (1.8) and (1.3) are preserved in a discrete sense. For the whole domain Ω, we have*

$$\frac{1}{2}\frac{d}{dt}\int_\Omega |u_h|^2\,dx + \int_\Omega |\boldsymbol{p}_h + \frac{1}{2}\,\boldsymbol{w}_h|^2\,dx = \int_\Omega f u_h\,dx \tag{3.20}$$

while for any subdomain $\Omega'' \subset \Omega$, we have

$$\frac{1}{2}\frac{d}{dt}\int_{\Omega''} |u_h|^2\,dx + \int_{\Omega''} |\boldsymbol{p}_h + \frac{1}{2}\,\boldsymbol{w}_h|^2\,dx - \int_{\partial\Omega''} u_h\,\boldsymbol{p}_h\cdot m\,d\sigma = \int_{\Omega''} f u_h\,dx + \epsilon_2 \tag{3.21}$$

where m is the unit outward normal on $\partial\Omega''$ and

$$\epsilon_2 = -\int_{\Omega''\setminus\Omega'} \boldsymbol{p}_h\cdot(\boldsymbol{p}_h + \frac{1}{2}\boldsymbol{w}_h - \nabla u_h)\,dx.$$

Proof. Taking $\mathbf{q} = \mathbf{p}_h$ and $v = u_h$ in (3.12) and (3.14) respectively, we have

$$\int_\Omega \mathbf{p}_h\cdot\mathbf{p}_h\,dx = B_h^*(u_h,\mathbf{p}_h) - \frac{1}{2}\int_\Omega \mathbf{w}_h\cdot\mathbf{p}_h\,dx, \tag{3.22}$$

$$\int_\Omega \frac{\partial u_h}{\partial t}u_h\,dx = -B_h(\mathbf{p}_h,u_h) - \frac{1}{2}\int_\Omega \mathbf{b}_h\cdot\mathbf{p}_h\,u_h - \frac{1}{4}\int_\Omega \mathbf{b}_h\cdot\mathbf{w}_h\,u_h\,dx + \int_\Omega f u_h\,dx. \tag{3.23}$$

Using (3.13), equation (3.23) becomes

$$\int_\Omega \frac{\partial u_h}{\partial t}u_h\,dx = -B_h(\mathbf{p}_h,u_h) - \frac{1}{2}\int_\Omega \mathbf{w}_h\cdot\mathbf{p}_h - \frac{1}{4}\int_\Omega \mathbf{w}_h\cdot\mathbf{w}_h\,dx + \int_\Omega f u_h\,dx. \tag{3.24}$$

Adding (3.22) and (3.24),

$$\frac{1}{2}\frac{d}{dt}\int_\Omega |u_h|^2\,dx + \int_\Omega |\mathbf{p}_h + \frac{1}{2}\,\mathbf{w}_h|^2\,dx = \int_\Omega f u_h\,dx$$

which proves (3.20).

To prove (3.21), we define the test functions $v \in U_h$ and $\mathbf{q} \in W_h$ by

$$v = \begin{cases} u_h & x \in \Omega'' \\ 0 & \text{otherwise} \end{cases}, \qquad \mathbf{q} = \begin{cases} \mathbf{p}_h & x \in \Omega' \\ \mathbf{0} & \text{otherwise} \end{cases}.$$

Then, using the above test functions in (3.14) and (3.12) respectively, we have

$$\int_{\Omega'} \mathbf{p}_h \cdot \mathbf{p}_h \, dx = B_h^*(u_h, \mathbf{q}) - \frac{1}{2} \int_{\Omega'} \mathbf{w}_h \cdot \mathbf{p}_h \, dx, \tag{3.25}$$

$$\int_{\Omega''} \frac{\partial u_h}{\partial t} u_h \, dx = -B_h(\mathbf{p}_h, v) - \frac{1}{2} \int_{\Omega''} \mathbf{b}_h \cdot \mathbf{p}_h \, u_h - \frac{1}{4} \int_{\Omega''} \mathbf{b}_h \cdot \mathbf{w}_h \, u_h \, dx + \int_{\Omega''} f u_h \, dx. \tag{3.26}$$

In (3.13), we take the test function $\mathbf{q} = \mathbf{p}_h$ in Ω' and $\mathbf{q} = \mathbf{0}$ elsewhere, we see that

$$\int_{\Omega'} u_h \mathbf{b}_h \cdot \mathbf{p}_h \, dx = \int_{\Omega'} \mathbf{p}_h \cdot \mathbf{w}_h \, dx.$$

Similarly, in (3.13), we take the test function $\mathbf{q} = \mathbf{w}_h$ in Ω' and $\mathbf{q} = \mathbf{0}$ elsewhere, we obtain

$$\int_{\Omega'} u_h \mathbf{b}_h \cdot \mathbf{w}_h \, dx = \int_{\Omega'} \mathbf{w}_h \cdot \mathbf{w}_h \, dx.$$

Moreover, by the definition of B_h, we have

$$B_h(\mathbf{p}_h, v) = \int_{\Omega''} \mathbf{p}_h \cdot \nabla u_h \, dx - \sum_{\kappa \in \mathcal{F}_p \cap \Omega'} \int_\kappa \mathbf{p}_h \cdot n \, [u_h] \, d\sigma - \sum_{\kappa \in \partial\Omega''} \int_\kappa u_h \, \mathbf{p}_h \cdot n \, d\sigma$$

By the definition of B_h^*, we have

$$B_h^*(u_h, \mathbf{q}) = B_h(\mathbf{q}, u_h) = \int_{\Omega'} \mathbf{p}_h \cdot \nabla u_h \, dx - \sum_{\kappa \in \mathcal{F}_p \cap \Omega'} \int_\kappa \mathbf{p}_h \cdot n \, [u_h] \, d\sigma.$$

Adding (3.25) and (3.26),

$$\begin{aligned} &\frac{1}{2} \frac{d}{dt} \int_{\Omega''} |u_h|^2 \, dx + \int_{\Omega''} |\mathbf{p}_h + \frac{1}{2} \mathbf{w}_h|^2 \, dx - \int_{\partial\Omega''} u_h \, \mathbf{p}_h \cdot n \, d\sigma \\ &= \int_{\Omega''} f u_h \, dx - \int_{\Omega'' \setminus \Omega'} \mathbf{p}_h \cdot (\mathbf{p}_h + \frac{1}{2} \mathbf{w}_h - \nabla u_h) \, dx \end{aligned}$$

which shows (3.21).

□

3.4 Stability and convergence

In this section, we will prove the stability and convergence of our new staggered DG method for both the static and time-dependent convection-diffusion equations. For the time-dependent problem, we will consider the semi-discrete case in this section. The corresponding fully discrete method will be analyzed in the next section. In the following, $\|\cdot\|$ denotes the standard L^2 norm defined on Ω.

3.4.1 Static problem

In this part of the paper, we will analyze the static version of the convection-diffusion equation (1.6). Our new staggered DG method can be written as: find $(u_h, \mathbf{p}_h) \in U_h \times W_h$ such that

$$\int_\Omega \mathbf{p}_h \cdot \mathbf{q}\, dx = B_h^*(u_h, \mathbf{q}) - \frac{1}{2}\int_\Omega \mathbf{w}_h \cdot \mathbf{q}\, dx, \tag{3.27}$$

$$\int_\Omega \mathbf{w}_h \cdot \mathbf{q}\, dx = \int_\Omega u_h \mathbf{b}_h \cdot \mathbf{q}\, dx, \tag{3.28}$$

$$B_h(\mathbf{p}_h, v) + \frac{1}{2}\int_\Omega \mathbf{b}_h \cdot \mathbf{p}_h\, v + \frac{1}{4}\int_\Omega \mathbf{b}_h \cdot \mathbf{w}_h\, v\, dx = \int_\Omega fv\, dx \tag{3.29}$$

for all test functions $(v, \mathbf{q}) \in U_h \times W_h$. We assume that the corresponding functions $u, \mathbf{p}$ and $\mathbf{w}$ satisfy the following system

$$\int_\Omega \mathbf{p} \cdot \mathbf{q}\, dx = B_h^*(u, \mathbf{q}) - \frac{1}{2}\int_\Omega \mathbf{w} \cdot \mathbf{q}\, dx, \tag{3.30}$$

$$B_h(\mathbf{p}, v) + \frac{1}{2}\int_\Omega \mathbf{b} \cdot \mathbf{p}\, v + \frac{1}{4}\int_\Omega \mathbf{b} \cdot \mathbf{w}\, v\, dx = \int_\Omega fv\, dx \tag{3.31}$$

for all test functions $(v, \mathbf{q}) \in U_h \times W_h$, and $\mathbf{w} = \mathbf{b}\, u$. The following theorem gives stability and optimal error estimates for the method (3.27)-(3.29).

Theorem 3.4.1 *Let $(u_h, \boldsymbol{p}_h) \in U_h \times W_h$ be the solution of (3.27)-(3.29). Then the following stability holds:*

$$\|u_h\|_Z \le K\|f\|. \tag{3.32}$$

Moreover, we have the following optimal error bounds

$$\|\mathcal{I}u - u_h\|_Z \le Ch^{k+1}, \quad \|u - u_h\| \le Ch^{k+1}, \quad \text{and} \quad \|u - u_h\|_Z \le Ch^k. \tag{3.33}$$

Proof. By (3.27), we have

$$\int_\Omega (\mathbf{p}_h + \frac{1}{2}\mathbf{w}_h) \cdot \mathbf{q}\, dx = B_h^*(u_h, \mathbf{q}).$$

Thus, by the inf-sup condition (3.11) for the operator B_h^*,

$$\begin{aligned}\|\mathbf{p}_h + \frac{1}{2}\mathbf{w}_h\| &= \sup_{\mathbf{q}\in W_h} \frac{\int_\Omega (\mathbf{p}_h + \frac{1}{2}\mathbf{w}_h) \cdot \mathbf{q}\, dx}{\|\mathbf{q}\|} \\ &\geq \sup_{\mathbf{q}\in W_h} \frac{B_h^*(u_h, \mathbf{q})}{\|\mathbf{q}\|_{X'}} \\ &\geq K\|u_h\|_Z.\end{aligned}$$

Moreover, by taking the test functions $v = u_h$ and $\mathbf{q} = \mathbf{p}_h$ in (3.27)-(3.29) and following the proof of (3.20), we get

$$\|\mathbf{p}_h + \frac{1}{2}\mathbf{w}_h\|^2 = \int_\Omega f\, u_h\, dx.$$

Therefore,

$$\|u_h\|_Z^2 \leq K\|\mathbf{p}_h + \frac{1}{2}\mathbf{w}_h\|^2 = K\int_\Omega f u_h\, dx \leq K\|f\|\|u_h\| \leq K\|f\|\|u_h\|_Z$$

where we use the inequality $\|u_h\| \leq K\|u_h\|_Z$. Thus, (3.32) is proved.

Now we will prove the error bound (3.33). Subtracting (3.30) from (3.27), we have

$$\int_\Omega (\mathbf{p} - \mathbf{p}_h) \cdot \mathbf{q}\, dx = B_h^*(u - u_h, \mathbf{q}) - \frac{1}{2}\int_\Omega (\mathbf{w} - \mathbf{w}_h) \cdot \mathbf{q}\, dx. \tag{3.34}$$

Similarly, subtracting (3.31) from (3.29), we have

$$\begin{aligned} &B_h(\mathbf{p} - \mathbf{p}_h, v) + \frac{1}{2}\int_\Omega \mathbf{b}_h \cdot (\mathbf{p} - \mathbf{p}_h)\, v\, dx + \frac{1}{4}\int_\Omega \mathbf{b}_h \cdot (\mathbf{w} - \mathbf{w}_h) v\, dx \\ &= -\frac{1}{2}\int_\Omega (\mathbf{b} - \mathbf{b}_h) \cdot \mathbf{p}\, v\, dx - \frac{1}{4}\int_\Omega (\mathbf{b} - \mathbf{b}_h) \cdot \mathbf{w}\, v\, dx. \end{aligned} \tag{3.35}$$

Taking $\mathbf{q} = \mathcal{J}\mathbf{p} - \mathbf{p}_h$ in (3.34), we have

$$\int_\Omega (\mathbf{p} - \mathbf{p}_h) \cdot (\mathcal{J}\mathbf{p} - \mathbf{p}_h)\, dx = B_h^*(u - u_h, \mathcal{J}\mathbf{p} - \mathbf{p}_h) - \frac{1}{2}\int_\Omega (\mathbf{w} - \mathbf{w}_h) \cdot (\mathcal{J}\mathbf{p} - \mathbf{p}_h)\, dx.$$

Similarly, taking $v = \mathcal{I}u - u_h$ in (3.35), we have

$$\begin{aligned} &B_h(\mathbf{p} - \mathbf{p}_h, \mathcal{I}u - u_h) \\ &+ \frac{1}{2}\int_\Omega \mathbf{b}_h \cdot (\mathbf{p} - \mathbf{p}_h)\, (\mathcal{I}u - u_h)\, dx + \frac{1}{4}\int_\Omega \mathbf{b}_h \cdot (\mathbf{w} - \mathbf{w}_h)(\mathcal{I}u - u_h)\, dx \\ &= -\frac{1}{2}\int_\Omega (\mathbf{b} - \mathbf{b}_h) \cdot \mathbf{p}\, (\mathcal{I}u - u_h)\, dx - \frac{1}{4}\int_\Omega (\mathbf{b} - \mathbf{b}_h) \cdot \mathbf{w}\, (\mathcal{I}u - u_h)\, dx. \end{aligned}$$

Using the facts that $B_h^*(u-\mathcal{I}u,\mathbf{q})=0$ for all $\mathbf{q}\in W_h$ and $B_h(\mathbf{p}-\mathcal{J}\mathbf{p},v)=0$ for all $v\in U_h$ (see [12]) as well as adding the above two equations, we have

$$\begin{aligned}&\int_\Omega(\mathbf{p}-\mathbf{p}_h)\cdot(\mathcal{J}\mathbf{p}-\mathbf{p}_h)\,dx+\frac{1}{2}\int_\Omega(\mathbf{w}-\mathbf{w}_h)\cdot(\mathcal{J}\mathbf{p}-\mathbf{p}_h)\,dx\\&+\frac{1}{2}\int_\Omega\mathbf{b}_h\cdot(\mathbf{p}-\mathbf{p}_h)\,(\mathcal{I}u-u_h)\,dx+\frac{1}{4}\int_\Omega\mathbf{b}_h\cdot(\mathbf{w}-\mathbf{w}_h)(\mathcal{I}u-u_h)\,dx\\=&-\frac{1}{2}\int_\Omega(\mathbf{b}-\mathbf{b}_h)\cdot\mathbf{p}\,(\mathcal{I}u-u_h)\,dx-\frac{1}{4}\int_\Omega(\mathbf{b}-\mathbf{b}_h)\cdot\mathbf{w}\,(\mathcal{I}u-u_h)\,dx.\end{aligned}$$

Let $\widehat{\mathbf{w}}=\Pi_h(\mathbf{b}_h\mathcal{I}u)$ be the L^2 projection of $\mathbf{b}_h\mathcal{I}u$, that is, $\widehat{\mathbf{w}}\in W_h$ is defined via the relation $\int_\Omega(\widehat{\mathbf{w}}-\mathbf{b}_h\mathcal{I}u)\cdot\mathbf{q}\,dx=0$ for all $\mathbf{q}\in W_h$. Then

$$\begin{aligned}&\int_\Omega(\mathbf{p}-\mathbf{p}_h)\cdot(\mathcal{J}\mathbf{p}-\mathbf{p}_h)\,dx+\frac{1}{2}\int_\Omega(\mathbf{w}-\mathbf{w}_h)\cdot(\mathcal{J}\mathbf{p}-\mathbf{p}_h)\,dx\\&+\frac{1}{2}\int_\Omega(\mathbf{p}-\mathbf{p}_h)\cdot(\widehat{\mathbf{w}}-\mathbf{w}_h)\,dx+\frac{1}{4}\int_\Omega(\mathbf{w}-\mathbf{w}_h)\cdot(\widehat{\mathbf{w}}-\mathbf{w}_h)\,dx\\=&\frac{1}{2}\int_\Omega(\mathbf{p}-\mathbf{p}_h)\cdot\eta\,dx+\frac{1}{4}\int_\Omega(\mathbf{w}-\mathbf{w}_h)\cdot\eta\,dx\\&-\frac{1}{2}\int_\Omega(\mathbf{b}-\mathbf{b}_h)\cdot\mathbf{p}\,(\mathcal{I}u-u_h)\,dx-\frac{1}{4}\int_\Omega(\mathbf{b}-\mathbf{b}_h)\cdot\mathbf{w}\,(\mathcal{I}u-u_h)\,dx.\end{aligned}$$

where

$$\eta=(\widehat{\mathbf{w}}-\mathbf{w}_h)-(\mathbf{b}_h\mathcal{I}u-\mathbf{b}_hu_h).$$

Simplifying, we have

$$\begin{aligned}&\int_\Omega\Big((\mathbf{p}-\mathbf{p}_h)+\frac{1}{2}(\mathbf{w}-\mathbf{w}_h)\Big)\cdot\Big((\mathcal{J}\mathbf{p}-\mathbf{p}_h)+\frac{1}{2}(\widehat{\mathbf{w}}-\mathbf{w}_h)\Big)\,dx\\=&\frac{1}{2}\int_\Omega(\mathbf{p}-\mathbf{p}_h)\cdot\eta\,dx+\frac{1}{4}\int_\Omega(\mathbf{w}-\mathbf{w}_h)\cdot\eta\,dx\\&-\frac{1}{2}\int_\Omega(\mathbf{b}-\mathbf{b}_h)\cdot\mathbf{p}\,(\mathcal{I}u-u_h)\,dx-\frac{1}{4}\int_\Omega(\mathbf{b}-\mathbf{b}_h)\cdot\mathbf{w}\,(\mathcal{I}u-u_h)\,dx.\end{aligned}$$

Then,

$$\begin{aligned}&\int_\Omega\Big((\mathcal{J}\mathbf{p}-\mathbf{p}_h)+\frac{1}{2}(\widehat{\mathbf{w}}-\mathbf{w}_h)\Big)\cdot\Big((\mathcal{J}\mathbf{p}-\mathbf{p}_h)+\frac{1}{2}(\widehat{\mathbf{w}}-\mathbf{w}_h)\Big)\,dx\\=&\int_\Omega\Big((\mathcal{J}\mathbf{p}-\mathbf{p})+\frac{1}{2}(\widehat{\mathbf{w}}-\mathbf{w})\Big)\cdot\Big((\mathcal{J}\mathbf{p}-\mathbf{p}_h)+\frac{1}{2}(\widehat{\mathbf{w}}-\mathbf{w}_h)\Big)\,dx\\&+\frac{1}{2}\int_\Omega(\mathbf{p}-\mathbf{p}_h)\cdot\eta\,dx+\frac{1}{4}\int_\Omega(\mathbf{w}-\mathbf{w}_h)\cdot\eta\,dx\\&-\frac{1}{2}\int_\Omega(\mathbf{b}-\mathbf{b}_h)\cdot\mathbf{p}\,(\mathcal{I}u-u_h)\,dx-\frac{1}{4}\int_\Omega(\mathbf{b}-\mathbf{b}_h)\cdot\mathbf{w}\,(\mathcal{I}u-u_h)\,dx.\end{aligned}$$

By (3.28) and the definition of $\widehat{\mathbf{w}}$, we have $\int_\Omega \eta \cdot \mathbf{q}\, dx = 0$ for all $\mathbf{q} \in W_h$, and consequently,

$$\begin{aligned}\frac{1}{2}\int_\Omega (\mathbf{p}-\mathbf{p}_h)\cdot\eta\, dx + \frac{1}{4}\int_\Omega (\mathbf{w}-\mathbf{w}_h)\cdot\eta\, dx &= \frac{1}{2}\int_\Omega (\mathbf{p}+\frac{1}{2}\mathbf{w})\cdot\eta\, dx \\ &= \frac{1}{2}\int_\Omega \nabla u\cdot\eta\, dx \\ &= \frac{1}{2}\int_\Omega (\nabla u - \mathcal{J}\nabla u)\cdot\eta\, dx\end{aligned}$$

where $\mathcal{J}\nabla u$ is the projection of the vector ∇u onto W_h. So,

$$\begin{aligned}&\int_\Omega \Big((\mathcal{J}\mathbf{p}-\mathbf{p}_h)+\frac{1}{2}(\widehat{\mathbf{w}}-\mathbf{w}_h)\Big)\cdot\Big((\mathcal{J}\mathbf{p}-\mathbf{p}_h)+\frac{1}{2}(\widehat{\mathbf{w}}-\mathbf{w}_h)\Big)\, dx \\ &= \int_\Omega \Big((\mathcal{J}\mathbf{p}-\mathbf{p})+\frac{1}{2}(\widehat{\mathbf{w}}-\mathbf{w})\Big)\cdot\Big((\mathcal{J}\mathbf{p}-\mathbf{p}_h)+\frac{1}{2}(\widehat{\mathbf{w}}-\mathbf{w}_h)\Big)\, dx \\ &\quad + \frac{1}{2}\int_\Omega (\nabla u-\mathcal{J}\nabla u)\cdot\eta\, dx - \frac{1}{2}\int_\Omega (\mathbf{b}-\mathbf{b}_h)\cdot\mathbf{p}\,(\mathcal{I}u-u_h)\, dx \\ &\quad - \frac{1}{4}\int_\Omega (\mathbf{b}-\mathbf{b}_h)\cdot\mathbf{w}\,(\mathcal{I}u-u_h)\, dx.\end{aligned} \tag{3.36}$$

Using (3.34),

$$\int_\Omega (\mathbf{p}-\mathbf{p}_h)\cdot\mathbf{q}\, dx + \frac{1}{2}\int_\Omega (\mathbf{w}-\mathbf{w}_h)\cdot\mathbf{q}\, dx = B_h^*(u-u_h,\mathbf{q}).$$

Therefore,

$$\begin{aligned}&\int_\Omega \Big((\mathbf{p}-\mathcal{J}\mathbf{p})+\frac{1}{2}(\mathbf{w}-\widehat{\mathbf{w}})\Big)\cdot\mathbf{q}\, dx + \int_\Omega \Big((\mathcal{J}\mathbf{p}-\mathbf{p}_h)+\frac{1}{2}(\widehat{\mathbf{w}}-\mathbf{w}_h)\Big)\cdot\mathbf{q}\, dx \\ &= B_h^*(\mathcal{I}u-u_h,\mathbf{q})\end{aligned}$$

where we use $B_h^*(u-\mathcal{I}u,\mathbf{q})=0$. Thus, by the inf-sup condition (3.11),

$$K\|\mathcal{I}u-u_h\|_Z \le \|\Big((\mathcal{J}\mathbf{p}-\mathbf{p}_h)+\frac{1}{2}(\widehat{\mathbf{w}}-\mathbf{w}_h)\Big)\| + \|\Big((\mathbf{p}-\mathcal{J}\mathbf{p})+\frac{1}{2}(\mathbf{w}-\widehat{\mathbf{w}})\Big)\|. \tag{3.37}$$

Note that

$$\int_\Omega \eta\cdot\eta\, dx = \int_\Omega \eta\cdot\Big\{(\widehat{\mathbf{w}}-\mathbf{w}_h)-(\mathbf{b}_h\mathcal{I}u-\mathbf{b}_h u_h)\Big\}\, dx = -\int_\Omega \eta\cdot(\mathbf{b}_h\mathcal{I}u-\mathbf{b}_h u_h)\, dx$$

and consequently

$$\|\eta\| \le \Big(\max_{x\in\Omega}|\mathbf{b}_h|\Big)\,\|\mathcal{I}u-u_h\|.$$

By the discrete Poincaré inequality, i.e. $\|\mathcal{I}u-u_h\| \le C\|\mathcal{I}u-u_h\|_Z$, we have

$$\|\eta\| \le C\{\|\Big((\mathcal{J}\mathbf{p}-\mathbf{p}_h)+\frac{1}{2}(\widehat{\mathbf{w}}-\mathbf{w}_h)\Big)\| + \|\Big((\mathbf{p}-\mathcal{J}\mathbf{p})+\frac{1}{2}(\mathbf{w}-\widehat{\mathbf{w}})\Big)\|\}.$$

Hence, by (3.36) and the Young's inequality, we get

$$\begin{aligned}&\|\Big((\mathcal{J}\mathbf{p}-\mathbf{p}_h)+\frac{1}{2}(\widehat{\mathbf{w}}-\mathbf{w}_h)\Big)\|\\ &\leq C\{\|\Big((\mathbf{p}-\mathcal{J}\mathbf{p})+\frac{1}{2}(\mathbf{w}-\widehat{\mathbf{w}})\Big)\|+\|\nabla u-\mathcal{J}\nabla u\|+\|\mathbf{b}-\mathbf{b}_h\|\}.\end{aligned}$$

Hence, by (3.37),

$$\|\mathcal{I}u-u_h\|_Z\leq C\{\|\Big((\mathbf{p}-\mathcal{J}\mathbf{p})+\frac{1}{2}(\mathbf{w}-\widehat{\mathbf{w}})\Big)\|+\|\nabla u-\mathcal{J}\nabla u\|+\|\mathbf{b}-\mathbf{b}_h\|\}.$$

Notice that, since $\mathbf{w}=\mathbf{b}u$,

$$\mathbf{w}-\widehat{\mathbf{w}}=\mathbf{w}-\Pi_h(\mathbf{w})+\Pi_h(\mathbf{b}u)-\Pi_h(\mathbf{b}_hu)+\Pi_h(\mathbf{b}_hu)-\Pi_h(\mathbf{b}_h\mathcal{I}u).$$

Therefore,

$$\begin{aligned}\|\mathbf{w}-\widehat{\mathbf{w}}\|&\leq\|\mathbf{w}-\Pi_h(\mathbf{w})\|+\|\Pi_h(\mathbf{b}u)-\Pi_h(\mathbf{b}_hu)\|+\|\Pi_h(\mathbf{b}_hu)-\Pi_h(\mathbf{b}_h\mathcal{I}u)\|\\ &\leq\|\mathbf{w}-\mathcal{J}\mathbf{w}\|+\|u(\mathbf{b}-\mathbf{b}_h)\|+\|\mathbf{b}_h(u-\mathcal{I}u)\|\end{aligned}$$

By using the interpolation error estimates for the operators $\mathcal{I}$ and $\mathcal{J}$, we obtain the first inequality in (3.33). The second inequality is obtained by using the discrete Poincare inequality $\|\mathcal{I}u-u_h\|\leq K\|\mathcal{I}u-u_h\|_Z$ and the interpolation error estimate for $\mathcal{I}$. Finally, the third inequality in (3.33) is proved by the error estimate of the operator $\mathcal{I}$ with respect to the Z-norm.

□

3.4.2 Time-dependent problem

In the time-dependent problem, We consider

$$\frac{\partial u}{\partial t}-\Delta u+\nabla\cdot(\mathbf{b}u)=f.$$

The corresponding numerical method is

$$\int_\Omega\mathbf{p}_h\cdot\mathbf{q}\,dx=B_h^*(u_h,\mathbf{q})-\frac{1}{2}\int_\Omega\mathbf{w}_h\cdot\mathbf{q}\,dx, \tag{3.38}$$

$$\int_\Omega\mathbf{w}_h\cdot\mathbf{q}\,dx=\int_\Omega u_h\mathbf{b}_h\cdot\mathbf{q}\,dx, \tag{3.39}$$

$$\int_\Omega\frac{\partial u_h}{\partial t}v\,dx+B_h(\mathbf{p}_h,v)+\frac{1}{2}\int_\Omega\mathbf{b}_h\cdot\mathbf{p}_h\,v\,dx+\frac{1}{4}\int_\Omega\mathbf{b}_h\cdot\mathbf{w}_h\,v\,dx=\int_\Omega fv\,dx. \tag{3.40}$$

for all $(v,\mathbf{q})\in U_h\times W_h$. The next theorem examines the stability and convergence of numerical method (3.38)-(3.40).

Theorem 3.4.2 *Let $(u_h, \boldsymbol{p}_h) \in U_h \times W_h$ be the solution of (3.38)-(3.40). Then the following stability holds:*

$$\max_{0\le t\le T} \|u_h(\cdot,t)\| + \Big(\int_0^T \|u_h\|_Z^2 \, d\tau\Big)^{\frac{1}{2}} \le C\Big(\|u_h(\cdot,0)\| + \int_0^T \|f\| \, d\tau\Big). \tag{3.41}$$

Moreover, we have the following optimal error bounds

$$\max_{0\le t\le T} \|(\mathcal{I}u - u_h)(\cdot,t)\| \le \|(\mathcal{I}u - u_h)(\cdot,0)\| + Ch^{k+1}. \tag{3.42}$$

Proof. As in the static case, we have

$$\|u_h\|_Z \le K\|\mathbf{p}_h + \frac{1}{2}\mathbf{w}_h\|.$$

Hence, by taking $\mathbf{q} = \mathbf{p}_h$ in (3.38), $v = u_h$ in (3.40) and summing up the two equations, we have

$$\begin{aligned} & \frac{1}{2}\frac{d}{dt}\|u_h\|^2 + \|u_h\|_Z^2 \\ \le\ & C\Big(\frac{1}{2}\frac{d}{dt}\|u_h\|^2 + \|\mathbf{p}_h + \frac{1}{2}\mathbf{w}_h\|^2\Big) \\ =\ & C\int_\Omega f u_h \, dx \le C\|f\|\|u_h\|. \end{aligned}$$

Integrating in time from 0 to $t \le T$ and using Young's inequality, we have

$$\begin{aligned} & \|u_h(\cdot,t)\|^2 + \int_0^t \|u_h\|_Z^2 \, d\tau \\ \le\ & C\Big(\|u_h(\cdot,0)\|^2 + \max_{0\le t\le T}\|u_h(\cdot,t)\| \int_0^T \|f\| \, d\tau\Big) \\ \le\ & C\Big(\|u_h(\cdot,0)\|^2 + \frac{1}{2C}\Big(\max_{0\le t\le T}\|u_h(\cdot,t)\|\Big)^2 + \frac{C}{2}\Big(\int_0^T \|f\| \, d\tau\Big)^2\Big). \end{aligned}$$

As this is true for all $0 \le t \le T$, we have

$$\max_{0\le t\le T} \|u_h(\cdot,t)\| + \Big(\int_0^T \|u_h\|_Z^2 \, d\tau\Big)^{\frac{1}{2}} \le C\Big(\|u_h(\cdot,0)\| + \int_0^T \|f\| \, d\tau\Big).$$

This gives the stability (3.41).

Next, we derive the error estimates (3.42). Note that we have

$$\begin{aligned} & \int_\Omega (\mathbf{p} - \mathbf{p}_h)\cdot\mathbf{q} \, dx = B_h^*(u - u_h, \mathbf{q}) - \frac{1}{2}\int_\Omega (\mathbf{w} - \mathbf{w}_h)\cdot\mathbf{q} \, dx, \\ & \int_\Omega \frac{\partial(u - u_h)}{\partial t} v \, dx + B_h(\mathbf{p} - \mathbf{p}_h, v) \\ & + \frac{1}{2}\int_\Omega \mathbf{b}_h\cdot(\mathbf{p} - \mathbf{p}_h)\, v \, dx + \frac{1}{4}\int_\Omega \mathbf{b}_h\cdot(\mathbf{w} - \mathbf{w}_h) v \, dx \\ = & -\frac{1}{2}\int_\Omega (\mathbf{b} - \mathbf{b}_h)\cdot\mathbf{p}\, v \, dx - \frac{1}{4}\int_\Omega (\mathbf{b} - \mathbf{b}_h)\cdot\mathbf{w} v \, dx. \end{aligned}$$

Again, define $\widehat{\mathbf{w}}$ to be the L^2 projections of $\mathbf{b}_h\mathcal{I}u$ onto $\mathcal{W}_h$. Following the same steps as in Theorem 3.4.1, we have

$$\begin{aligned}
&\int_\Omega \frac{\partial(\mathcal{I}u-u_h)}{\partial t}(\mathcal{I}u-u_h)\,dx + \int_\Omega \Big((\mathcal{J}\mathbf{p}-\mathbf{p}_h)+\frac{1}{2}(\widehat{\mathbf{w}}-\mathbf{w}_h)\Big)\cdot\Big((\mathcal{J}\mathbf{p}-\mathbf{p}_h)+\frac{1}{2}(\widehat{\mathbf{w}}-\mathbf{w}_h)\Big)\,dx\\
=&\int_\Omega \frac{\partial(\mathcal{I}u-u)}{\partial t}(\mathcal{I}u-u_h) + \int_\Omega \Big((\mathcal{J}\mathbf{p}-\mathbf{p})+\frac{1}{2}(\widehat{\mathbf{w}}-\mathbf{w})\Big)\cdot\Big((\mathcal{J}\mathbf{p}-\mathbf{p}_h)+\frac{1}{2}(\widehat{\mathbf{w}}-\mathbf{w}_h)\Big)\,dx\\
&+\frac{1}{2}\int_\Omega(\mathbf{p}-\mathbf{p}_h)\cdot\eta\,dx+\frac{1}{4}\int_\Omega(\mathbf{w}-\mathbf{w}_h)\cdot\eta\,dx\\
&-\frac{1}{2}\int_\Omega(\mathbf{b}-\mathbf{b}_h)\cdot\mathbf{p}\,(\mathcal{I}u-u_h)\,dx-\frac{1}{4}\int_\Omega(\mathbf{b}-\mathbf{b}_h)\cdot\mathbf{w}\,(\mathcal{I}u-u_h)\,dx\\
=&\int_\Omega \frac{\partial(\mathcal{I}u-u)}{\partial t}(\mathcal{I}u-u_h) + \int_\Omega \Big((\mathcal{J}\mathbf{p}-\mathbf{p})+\frac{1}{2}(\widehat{\mathbf{w}}-\mathbf{w})\Big)\cdot\Big((\mathcal{J}\mathbf{p}-\mathbf{p}_h)+\frac{1}{2}(\widehat{\mathbf{w}}-\mathbf{w}_h)\Big)\,dx\\
&+\frac{1}{2}\int_\Omega(\nabla u-\mathcal{J}\nabla u)\cdot\eta\,dx-\frac{1}{2}\int_\Omega(\mathbf{b}-\mathbf{b}_h)\cdot\mathbf{p}\,(\mathcal{I}u-u_h)\,dx\\
&-\frac{1}{4}\int_\Omega(\mathbf{b}-\mathbf{b}_h)\cdot\mathbf{w}\,(\mathcal{I}u-u_h)\,dx..
\end{aligned}$$

where η is set to be same as the one in the proof of Theorem 3.4.1 and therefore the following estimate still hold:

$$\|\eta\| \le \Big(\max_{x\in\Omega}|\mathbf{b}_h|\Big)\,\|\mathcal{I}u-u_h\|.$$

Integrating in time from 0 to $t \le T$ and using Young's inequality, we have

$$\begin{aligned}
&\|(\mathcal{I}u-u_h)(\cdot,t)\|^2+\int_0^t\|(\mathcal{J}\mathbf{p}-\mathbf{p}_h)+\frac{1}{2}(\widehat{\mathbf{w}}-\mathbf{w}_h)\|^2\,d\tau\\
\le\;& C\Big(\|(\mathcal{I}u-u_h)(\cdot,0)\|^2+\max_{0\le t\le T}\|(\mathcal{I}u-u_h)(\cdot,t)\|\int_0^T\|\frac{\partial(\mathcal{I}u-u)}{\partial t}\|\,d\tau\\
&+\int_0^T\|(\mathcal{J}\mathbf{p}-\mathbf{p}_h)+\frac{1}{2}(\widehat{\mathbf{w}}-\mathbf{w}_h)\|\|(\mathbf{p}-\mathcal{J}\mathbf{p})+\frac{1}{2}(\mathbf{w}-\widehat{\mathbf{w}})\|\,d\tau\\
&+\max_{0\le t\le T}\|(\mathcal{I}u-u_h)(\cdot,t)\|\int_0^T\|\nabla u-\mathcal{J}\nabla u\|\,d\tau\\
&+\max_{0\le t\le T}\|(\mathcal{I}u-u_h)(\cdot,t)\|\int_0^T\|\mathbf{b}-\mathbf{b}_h\|\,d\tau\Big)\\
\le\;& C\Big(\|(\mathcal{I}u-u_h)(\cdot,0)\|^2+\frac{1}{4C}\Big(\max_{0\le t\le T}\|(\mathcal{I}u-u_h)(\cdot,t)\|\Big)^2+C\Big(\int_0^T\|\frac{\partial(\mathcal{I}u-u)}{\partial t}\|\,d\tau\Big)^2\\
&+\frac{1}{2}\int_0^T\|(\mathcal{J}\mathbf{p}-\mathbf{p}_h)+\frac{1}{2}(\widehat{\mathbf{w}}-\mathbf{w}_h)\|^2+\|(\mathbf{p}-\mathcal{J}\mathbf{p})+\frac{1}{2}(\mathbf{w}-\widehat{\mathbf{w}})\|^2\,d\tau\\
&+\frac{1}{4C}\Big(\max_{0\le t\le T}\|(\mathcal{I}u-u_h)(\cdot,t)\|\Big)^2+C\Big(\int_0^T\|\nabla u-\mathcal{J}\nabla u\|\,d\tau\Big)^2\\
&+\frac{1}{4C}\Big(\max_{0\le t\le T}\|(\mathcal{I}u-u_h)(\cdot,t)\|\Big)^2+C\Big(\int_0^T\|\mathbf{b}-\mathbf{b}_h\|\,d\tau\Big)^2\Big).
\end{aligned}$$

As this is true for all $0 \le t \le T$, we have

$$\begin{aligned}
&\max_{0\le t\le T} \|(\mathcal{I}u - u_h)(\cdot,t)\| \\
\le\ & C\Big(\|(\mathcal{I}u - u_h)(\cdot,0)\| + \int_0^T \|\frac{\partial(\mathcal{I}u - u)}{\partial t}\|\, d\tau \\
&+\Big(\int_0^T \|\mathbf{p} - \mathcal{J}\mathbf{p}\|^2\, d\tau\Big)^{\frac{1}{2}} + \Big(\int_0^T \|\mathbf{w} - \widehat{\mathbf{w}}\|^2\, d\tau\Big)^{\frac{1}{2}} + \int_0^T \|\nabla u - \mathcal{J}\nabla u\|\, d\tau \\
&\int_0^T \|\mathbf{b} - \mathbf{b}_h\|\, d\tau\Big).
\end{aligned}$$

By using the interpolation error estimates for the operator $\mathcal{I}$ and $\mathcal{J}$, we have

$$\begin{aligned}
&\max_{0\le t\le T} \|(\mathcal{I}u - u_h)(\cdot,t)\| \\
\le\ & C_1\|(\mathcal{I}u - u_h)(\cdot,0)\| + C_2 h^{k+1}\Big(\int_0^T |u_t(\cdot,\tau)|_{H^{k+1}(\Omega)}\, d\tau \\
&+\Big(\int_0^T |\mathbf{p}(\cdot,\tau)|^2_{H^{k+1}(\Omega)}\, d\tau\Big)^{\frac{1}{2}} + \Big(\int_0^T |\mathbf{w}(\cdot,\tau)|^2_{H^{k+1}(\Omega)}\, d\tau\Big)^{\frac{1}{2}} \\
&+\Big(\int_0^T |u(\cdot,\tau)|^2_{H^{k+1}(\Omega)}\, d\tau\Big)^{\frac{1}{2}} + \Big(\int_0^T |\mathbf{b}(\cdot,\tau)|^2_{H^{k+1}(\Omega)}\, d\tau\Big)^{\frac{1}{2}} \\
&+\int_0^T |\nabla u(\cdot,\tau)|_{H^{k+1}(\Omega)}\, d\tau + \int_0^T |\mathbf{b}(\cdot,\tau)|_{H^{k+1}(\Omega)}\, d\tau\Big).
\end{aligned}$$

So the error estimate (3.42) is proved.

□

3.5 Fully discrete scheme

We further discretize (3.40) using the Crank-Nicolson scheme for time stepping. Let T be the final time, $\triangle t$ be the time step size and denote $N_T = \frac{T}{\triangle t}$ the number of time steps and $t_n = n(\triangle t)$. We let also u_h^n and $\mathbf{p}_h^n$ be the numerical approximation of $u(t_n)$ and $\mathbf{p}(t_n)$ respectively. Then the resulting fully discrete numerical scheme for (1.5) is as follows: For $n = 0, 1, \dots, N_T - 1$,

$$\begin{aligned}
&\int_\Omega (\mathbf{p}_h^n + \mathbf{p}_h^{n+1}) \cdot \mathbf{q}\; dx = B_h^*(u_h^n + u_h^{n+1}, \mathbf{q}) - \frac{1}{2}\int_\Omega (\mathbf{w}_h^{n+\frac{1}{2},n} + \mathbf{w}_h^{n+\frac{1}{2},n+1}) \cdot \mathbf{q}\; dx,\\
&\int_\Omega \mathbf{w}_h^{n+\frac{1}{2},n} \cdot \mathbf{q}\; dx = \int_\Omega \mathbf{b}_h^{n+\frac{1}{2}} u_h^n \cdot \mathbf{q}\; dx\\
&\int_\Omega \mathbf{w}_h^{n+\frac{1}{2},n} \cdot \mathbf{q}\; dx = \int_\Omega \mathbf{b}_h^{n+\frac{1}{2}} u_h^n + 1 \cdot \mathbf{q}\; dx\\
&\int_\Omega (\frac{u_h^{n+1} - u_h^n}{\triangle t})\; v\; dx + B_h(\frac{\mathbf{p}_h^{n+1} + \mathbf{p}_h^n}{2}, v) + \frac{1}{2}\int_\Omega \mathbf{b}_h^{n+\frac{1}{2}} \cdot (\frac{\mathbf{p}_h^{n+1} + \mathbf{p}_h^n}{2})\; v\; dx\\
&+ \frac{1}{4}\int_\Omega \mathbf{b}_h^{n+\frac{1}{2}} \cdot (\mathbf{w}_h^{n+\frac{1}{2},n} + \mathbf{w}_h^{n+\frac{1}{2},n+1})\; v\; dx = \int_\Omega f^{n+\frac{1}{2}} v\; dx,
\end{aligned} \tag{3.43}$$

for all $(v, \mathbf{q}) \in U_h \times W_h$, where $\mathbf{b}_h^{n+\frac{1}{2}} = \mathcal{J}\mathbf{b}(t_{n+\frac{1}{2}})$ and $f^{n+\frac{1}{2}} = f(t_{n+\frac{1}{2}})$.

Now we analyze the stability and convergence of the scheme.

Theorem 3.5.1 *Let $(u_h, \boldsymbol{p}_h) \in U_h \times W_h$ be the solution of (3.38)-(3.40). Then the following stability holds:*

$$\|u_h^{n+1}\| \le \|u_h^0\| + \triangle t \sum_{k=0}^{n} \|f^{k+\frac{1}{2}}\|. \tag{3.44}$$

Moreover, we have the following optimal error bounds

$$\max_{0 \le n \le N_t} \|e_h(u)^n\| \;\;\le\;\; \|e_h(u)^0\| + C(h^{k+1} + \triangle t^2). \tag{3.45}$$

Proof. We first take $\mathbf{q} = \frac{\mathbf{p}_h^n + \mathbf{p}_h^{n+1}}{2}$ in the first equation of (3.43) and get

$$\begin{aligned}
&\int_\Omega (\mathbf{p}_h^n + \mathbf{p}_h^{n+1}) \cdot (\frac{\mathbf{p}_h^n + \mathbf{p}_h^{n+1}}{2})\; dx =\\
&B_h^*(u_h^n + u_h^{n+1}, \frac{\mathbf{p}_h^n + \mathbf{p}_h^{n+1}}{2}) - \frac{1}{2}\int_\Omega (\mathbf{w}_h^{n+\frac{1}{2},n} + \mathbf{w}_h^{n+\frac{1}{2},n+1}) \cdot (\frac{\mathbf{p}_h^n + \mathbf{p}_h^{n+1}}{2})\; dx.
\end{aligned} \tag{3.46}$$

Next, take $v = u_h^n + u_h^{n+1}$ in the last equation of (3.43), we get

$$\begin{aligned}
&\int_\Omega \frac{(u_h^{n+1})^2 - (u_h^n)^2}{\triangle t}\; dx + \frac{1}{4}\int_\Omega (\frac{\mathbf{w}_h^{n+\frac{1}{2},n} + \mathbf{w}_h^{n+\frac{1}{2},n+1}}{2}) \cdot (\mathbf{w}_h^{n+\frac{1}{2},n} + \mathbf{w}_h^{n+\frac{1}{2},n+1})\; dx\\
&+ B_h(\frac{\mathbf{p}_h^{n+1} + \mathbf{p}_h^n}{2}, u_h^n + u_h^{n+1}) + \frac{1}{2}\int_\Omega (\frac{\mathbf{p}_h^{n+1} + \mathbf{p}_h^n}{2}) \cdot (\mathbf{w}_h^{n+\frac{1}{2},n} + \mathbf{w}_h^{n+\frac{1}{2},n+1})\; dx\\
&= \int_\Omega f^{n+\frac{1}{2}} (u_h^n + u_h^{n+1})\; dx.
\end{aligned} \tag{3.47}$$

Summing up (3.46) and (3.47) we have

$$\begin{aligned}
&\frac{1}{\triangle t}(\|u_h^{n+1}\|^2 - \|u_h^n\|^2) + \frac{1}{2}\|(\mathbf{p}_h^{n+1} + \mathbf{p}_h^n) + (\frac{\mathbf{w}_h^{n+\frac{1}{2},n} + \mathbf{w}_h^{n+\frac{1}{2},n+1}}{2})\|^2 \\
= &\int_\Omega f^{n+\frac{1}{2}}(u_h^n + u_h^{n+1}).
\end{aligned}$$

Hence, by Cauchy-Schwarz and triangle inequalities, we get

$$\frac{1}{\triangle t}(\|u_h^{n+1}\|^2 - \|u_h^n\|^2) \leq \int_\Omega f^{n+\frac{1}{2}}(u_h^n + u_h^{n+1}) \leq \|f^{n+\frac{1}{2}}\|\big(\|u_h^n\| + \|u_h^{n+1}\|\big).$$

Therefore, if $\|u_h^n\| + \|u_h^{n+1}\| \neq 0$, we have

$$\|u_h^{n+1}\| \leq \|u_h^n\| + \triangle t\|f^{n+\frac{1}{2}}\| \leq \|u_h^0\| + \triangle t\sum_{k=0}^{n}\|f^{k+\frac{1}{2}}\|.$$

So the scheme is unconditionally stable and (3.44) is proved. Next, we will analyze the convergence of the scheme. In order to lucidly convey the results, we adopt the following notations:

$$\begin{aligned}
&e_h(u)^n = u_h^n - \mathcal{I}u(\cdot,t_n), \quad e(u)^n = u(\cdot,t_n) - \mathcal{I}u(\cdot,t_n), \\
&e_h(\mathbf{p})^n = \mathbf{p}_h^n - \mathcal{J}\mathbf{p}(\cdot,t_n), \quad e(\mathbf{p})^n = \mathbf{p}(\cdot,t_n) - \mathcal{J}\mathbf{p}(\cdot,t_n), \\
&e_h(\mathbf{w})^{n+\frac{1}{2},n} = \mathbf{w}_h^{n+\frac{1}{2},n} - \widehat{\mathbf{w}}^{n+\frac{1}{2},n}, \quad e(\mathbf{w})^{n+\frac{1}{2},n} = \mathbf{w}^{n+\frac{1}{2},n} - \widehat{\mathbf{w}}^{n+\frac{1}{2},n},
\end{aligned}$$

where $\widehat{\mathbf{w}}^{n+\frac{1}{2},n}$ is the L^2 projection of $\mathbf{b}_h^{n+\frac{1}{2}}\mathcal{I}u(\cdot,t_n)$ onto the space U_h and $\mathbf{w}^{n+\frac{1}{2},n} = \mathbf{b}_h^{n+\frac{1}{2}}u(\cdot,t_n)$. We define $e_h(\mathbf{w})^{n+\frac{1}{2},n+1}$ and $e(\mathbf{w})^{n+\frac{1}{2},n+1}$ similarly. Note that from the first equation of (3.43), we have

$$\begin{aligned}
&\int_\Omega(e_h(\mathbf{p})^n + e_h(\mathbf{p})^{n+1})\cdot\mathbf{q}\,dx = B_h^*(e_h(u)^n + e_h(u)^{n+1},\mathbf{q}) \\
&-\frac{1}{2}\int_\Omega(e_h(\mathbf{w})^{n+\frac{1}{2},n} + e_h(\mathbf{w})^{n+\frac{1}{2},n+1})\cdot\mathbf{q}\,dx + \int_\Omega(e(\mathbf{p})^n + e(\mathbf{p})^{n+1})\cdot\mathbf{q}\,dx \\
&-B_h^*(e(u)^n + e(u)^{n+1},\mathbf{q}) + \frac{1}{2}\int_\Omega(e(\mathbf{w})^{n+\frac{1}{2},n} + e(\mathbf{w})^{n+\frac{1}{2},n+1})\cdot\mathbf{q}\,dx \\
&+\frac{1}{2}\int_\Omega(u(\cdot,t_n) + u(\cdot,t_{n+1}))(\mathbf{b}^{n+\frac{1}{2}} - \mathbf{b}_h^{n+\frac{1}{2}})\cdot\mathbf{q}\,dx + R_1^{n+\frac{1}{2}}(\mathbf{q}),
\end{aligned}$$

where

$$\begin{aligned}
R_1^{n+\frac{1}{2}}(\mathbf{q}) \quad = \quad & -\int_\Omega(\mathbf{p}(\cdot,t_n) + \mathbf{p}(\cdot,t_{n+1}))\cdot\mathbf{q}\,dx + B_h^*(u(\cdot,t_n) + u(\cdot,t_{n+1}),\mathbf{q}) \\
&-\frac{1}{2}\int_\Omega(u(\cdot,t_n) + u(\cdot,t_{n+1}))\mathbf{b}^{n+\frac{1}{2}}\cdot\mathbf{q}\,dx.
\end{aligned}$$

By the definition of $\mathcal{I}u$, $B_h^*(e(u)^n + e(u)^{n+1}, \mathbf{q}) = 0$. Hence,

$$
\begin{aligned}
&\int_\Omega (e_h(\mathbf{p})^n + e_h(\mathbf{p})^{n+1}) \cdot \mathbf{q}\, dx \\
= \quad & -\frac{1}{2}\int_\Omega (e_h(\mathbf{w})^{n+\frac{1}{2},n} + e_h(\mathbf{w})^{n+\frac{1}{2},n+1}) \cdot \mathbf{q}\, dx + \int_\Omega (e(\mathbf{p})^n + e(\mathbf{p})^{n+1}) \cdot \mathbf{q}\, dx \\
& - B_h^*(e(u)^n + e(u)^{n+1}, \mathbf{q}) + \frac{1}{2}\int_\Omega (e(\mathbf{w})^{n+\frac{1}{2},n} + e(\mathbf{w})^{n+\frac{1}{2},n+1}) \cdot \mathbf{q}\, dx \\
& + \frac{1}{2}\int_\Omega (u(\cdot,t_n) + u(\cdot,t_{n+1}))(\mathbf{b}^{n+\frac{1}{2}} - \mathbf{b}_h^{n+\frac{1}{2}}) \cdot \mathbf{q}\, dx + R_1^{n+\frac{1}{2}}(\mathbf{q}),,
\end{aligned} \tag{3.48}
$$

On the other hand, from the last equation of (3.43), we have

$$
\begin{aligned}
&\int_\Omega \Big(\frac{e_h(u)^{n+1} - e_h(u)^n}{\triangle t}\Big) v\, dx + \frac{1}{2}\int_\Omega \mathbf{b}_h^{n+\frac{1}{2}} \cdot \Big(\frac{e_h(\mathbf{p})^n + e_h(\mathbf{p})^{n+1}}{2}\Big) v\, dx \\
& + B_h\Big(\frac{e_h(\mathbf{p})^n + e_h(\mathbf{p})^{n+1}}{2}, v\Big) + \frac{1}{4}\int_\Omega \mathbf{b}_h^{n+\frac{1}{2}} \cdot \Big(\frac{e_h(\mathbf{w})^{n+\frac{1}{2},n} + e_h(\mathbf{w})^{n+\frac{1}{2},n+1}}{2}\Big) v\, dx \\
= \quad & \int_\Omega \Big(\frac{e(u)^{n+1} - e(u)^n}{\triangle t}\Big) v\, dx + \frac{1}{2}\int_\Omega \mathbf{b}_h^{n+\frac{1}{2}} \cdot \Big(\frac{e(\mathbf{p})^n + e(\mathbf{p})^{n+1}}{2}\Big) v\, dx \\
& + B_h\Big(\frac{e(\mathbf{p})^n + e(\mathbf{p})^{n+1}}{2}, v\Big) + \frac{1}{4}\int_\Omega \mathbf{b}_h^{n+\frac{1}{2}} \cdot \Big(\frac{(e(\mathbf{w})^{n+\frac{1}{2},n} + e(\mathbf{w})^{n+\frac{1}{2},n+1})}{2}\Big) v\, dx \\
& + \frac{1}{4}\int_\Omega (\mathbf{p}(\cdot,t_n) + \mathbf{p}(\cdot,t_{n+1}))(\mathbf{b}^{n+\frac{1}{2}} - \mathbf{b}_h^{n+\frac{1}{2}}) \cdot v\, dx \\
& + \frac{1}{8}\int_\Omega (\mathbf{w}^{n+\frac{1}{2},n} + \mathbf{w}^{n+\frac{1}{2},n+1})(\mathbf{b}^{n+\frac{1}{2}} - \mathbf{b}_h^{n+\frac{1}{2}}) \cdot v\, dx + R_2^{n+\frac{1}{2}}(v),
\end{aligned}
$$

where

$$
\begin{aligned}
R_2^{n+\frac{1}{2}}(v) = & \int_\Omega f^{n+\frac{1}{2}} v\, dx - \int_\Omega \Big(\frac{u(\cdot,t_{n+1}) - u(\cdot,t_n)}{\triangle t}\Big) v\, dx - B_h\Big(\frac{\mathbf{p}(\cdot,t_n) + \mathbf{p}(\cdot,t_{n+1})}{2}, v\Big) \\
& - \frac{1}{2}\int_\Omega \mathbf{b}^{n+\frac{1}{2}} \cdot \Big(\frac{\mathbf{p}(\cdot,t_n) + \mathbf{p}(\cdot,t_{n+1})}{2}\Big) v\, dx - \frac{1}{4}\int_\Omega \mathbf{b}^{n+\frac{1}{2}} \cdot \mathbf{b}^{n+\frac{1}{2}} \Big(\frac{u(\cdot,t_n) + u(\cdot,t_{n+1})}{2}\Big) v\, dx
\end{aligned}
$$

By the definition of $\mathcal{J}\mathbf{p}$, $B_h(\frac{e_h(\mathbf{p})^n + e_h(\mathbf{p})^{n+1}}{2}, v) = 0$. Hence,

$$
\begin{aligned}
&\int_\Omega \Big(\frac{e_h(u)^{n+1} - e_h(u)^n}{\triangle t}\Big) v\, dx + \frac{1}{2}\int_\Omega \mathbf{b}_h^{n+\frac{1}{2}} \cdot \Big(\frac{e_h(\mathbf{p})^n + e_h(\mathbf{p})^{n+1}}{2}\Big) v\, dx \\
& + \frac{1}{4}\int_\Omega \mathbf{b}_h^{n+\frac{1}{2}} \cdot \Big(\frac{e_h(\mathbf{w})^{n+\frac{1}{2},n} + e_h(\mathbf{w})^{n+\frac{1}{2},n+1}}{2}\Big) v\, dx \\
= \quad & \int_\Omega \Big(\frac{e(u)^{n+1} - e(u)^n}{\triangle t}\Big) v\, dx + \frac{1}{2}\int_\Omega \mathbf{b}_h^{n+\frac{1}{2}} \cdot \Big(\frac{e(\mathbf{p})^n + e(\mathbf{p})^{n+1}}{2}\Big) v\, dx \\
& + B_h\Big(\frac{e(\mathbf{p})^n + e(\mathbf{p})^{n+1}}{2}, v\Big) + \frac{1}{4}\int_\Omega \mathbf{b}_h^{n+\frac{1}{2}} \cdot \Big(\frac{(e(\mathbf{w})^{n+\frac{1}{2},n} + e(\mathbf{w})^{n+\frac{1}{2},n+1})}{2}\Big) v\, dx \\
& + \frac{1}{4}\int_\Omega (\mathbf{p}(\cdot,t_n) + \mathbf{p}(\cdot,t_{n+1}))(\mathbf{b}^{n+\frac{1}{2}} - \mathbf{b}_h^{n+\frac{1}{2}}) \cdot v\, dx \\
& + \frac{1}{8}\int_\Omega (\mathbf{w}^{n+\frac{1}{2},n} + \mathbf{w}^{n+\frac{1}{2},n+1})(\mathbf{b}^{n+\frac{1}{2}} - \mathbf{b}_h^{n+\frac{1}{2}}) \cdot v\, dx + R_2^{n+\frac{1}{2}}(v),.
\end{aligned} \tag{3.49}
$$

We first give estimate for $\|R_1^{n+\frac{1}{2}}\|$ and $\|R_2^{n+\frac{1}{2}}\|$. Notice that since u, $\mathbf{p}$ satisfy the continuous problem, we have

$$\int_\Omega \mathbf{p}(\cdot,t_{n+\frac{1}{2}})\cdot\mathbf{q}\,dx - B_h^*(u(\cdot,t_{n+\frac{1}{2}}),\mathbf{q}) + \frac{1}{2}\int_\Omega (u(\cdot,t_{n+\frac{1}{2}})\mathbf{b}^{n+\frac{1}{2}}\cdot\mathbf{q}\,dx = 0.$$

Thus,

$$\begin{aligned} R_1^{n+\frac{1}{2}}(\mathbf{q}) &= \int_\Omega (2\mathbf{p}(\cdot,t_{n+\frac{1}{2}}) - (\mathbf{p}(\cdot,t_n)+\mathbf{p}(\cdot,t_{n+1})))\cdot\mathbf{q}\,dx \\ &\quad + B_h^*(u(\cdot,t_n)+u(\cdot,t_{n+1})-2u(\cdot,t_{n+\frac{1}{2}}),\mathbf{q}) \\ &\quad + \frac{1}{2}\int_\Omega (2u(\cdot,t_{n+\frac{1}{2}}) - (u(\cdot,t_n)+u(\cdot,t_{n+1})))\mathbf{b}^{n+\frac{1}{2}}\cdot\mathbf{q}\,dx \\ &\le \|\mathbf{p}(\cdot,t_n)+\mathbf{p}(\cdot,t_{n+1})-2\mathbf{p}(\cdot,t_{n+\frac{1}{2}})\|\|\mathbf{q}\| \\ &\quad + C\|u(\cdot,t_n)+u(\cdot,t_{n+1})-2u(\cdot,t_{n+\frac{1}{2}})\|_Z\|\mathbf{q}\|_{X'} \\ &\quad + \frac{1}{2}\|\mathbf{b}\|_\infty\|u(\cdot,t_n)+u(\cdot,t_{n+1})-2u(\cdot,t_{n+\frac{1}{2}})\|\|\mathbf{q}\|. \end{aligned}$$

Similarly,

$$\begin{aligned} \int_\Omega f^{n+\frac{1}{2}}v\,dx &= \int_\Omega \frac{\partial u}{\partial t}(\cdot,t_{n+\frac{1}{2}})\,v\,dx + B_h(\mathbf{p}(\cdot,t_{n+\frac{1}{2}}),v) \\ &\quad + \frac{1}{2}\int_\Omega \mathbf{b}^{n+\frac{1}{2}}\cdot\mathbf{p}(\cdot,t_{n+\frac{1}{2}})\,v\,dx + \frac{1}{4}\int_\Omega \mathbf{b}^{n+\frac{1}{2}}\cdot\mathbf{b}^{n+\frac{1}{2}}u(\cdot,t_{n+\frac{1}{2}})\,v\,dx \end{aligned}$$

Thus,

$$\begin{aligned} R_2^{n+\frac{1}{2}}(v) &\le C\Big(\|\frac{\partial u}{\partial t}(\cdot,t_{n+\frac{1}{2}}) - \frac{u(\cdot,t_{n+1})-u(\cdot,t_n)}{\triangle t}\|\|v\| \\ &\quad + \|\mathbf{p}(\cdot,t_{n+\frac{1}{2}}) - \frac{\mathbf{p}(\cdot,t_n)+\mathbf{p}(\cdot,t_{n+1})}{2}\|_{Z'}\|v\|_X \\ &\quad + \|\mathbf{b}\|_\infty\|\mathbf{p}(\cdot,t_{n+\frac{1}{2}}) - \frac{\mathbf{p}(\cdot,t_n)+\mathbf{p}(\cdot,t_{n+1})}{2}\|\|v\| \\ &\quad + \|\mathbf{b}\|_\infty^2\|u(\cdot,t_{n+\frac{1}{2}}) - \frac{u(\cdot,t_n)+u(\cdot,t_{n+1})}{2}\|\|v\|\Big). \end{aligned}$$

Using Taylor's expansion, and the norm equivalence, we obtain

$$\begin{aligned} \|R_1^{n+\frac{1}{2}}\| \le& C\triangle t^2\Big(\|\mathbf{p}_{tt}(\cdot,\zeta_{n+\frac{1}{2}}) + \mathbf{p}_{tt}(\cdot,\zeta'_{n+\frac{1}{2}})\| + \|u_{tt}(\cdot,\xi_{n+\frac{1}{2}}) + u_{tt}(\cdot,\xi'_{n+\frac{1}{2}})\|_Z \\ &+ \|u_{tt}(\cdot,\xi_{n+\frac{1}{2}}) + u_{tt}(\cdot,\xi'_{n+\frac{1}{2}})\|\Big), \end{aligned} \tag{3.50}$$

and

$$\begin{aligned} \|R_2^{n+\frac{1}{2}}\| \le& C\triangle t^2\Big(\|u_{ttt}(\cdot,\eta_{n+\frac{1}{2}}) + u_{ttt}(\cdot,\eta'_{n+\frac{1}{2}})\| + \|\mathbf{p}_{tt}(\cdot,\zeta_{n+\frac{1}{2}}) + \mathbf{p}_{tt}(\cdot,\zeta'_{n+\frac{1}{2}})\|_{Z'} \\ &+ \|\mathbf{p}_{tt}(\cdot,\zeta_{n+\frac{1}{2}}) + \mathbf{p}_{tt}(\cdot,\zeta'_{n+\frac{1}{2}})\| + \|u_{tt}(\cdot,\xi_{n+\frac{1}{2}}) + u_{tt}(\cdot,\xi'_{n+\frac{1}{2}})\|\Big). \end{aligned} \tag{3.51}$$

We will make use of these two estimates later. Now we take $\mathbf{q} = \dfrac{e_h(\mathbf{p})^n + e_h(\mathbf{p})^{n+1}}{2}$ in (3.48), $v = e_h(u)^n + e_h(u)^{n+1}$ in (3.49) and adding the two equations, we get

$$
\begin{aligned}
&\frac{1}{\triangle t}(\|e_h(u)^{n+1}\|^2 - \|e_h(u)^n\|^2) + \frac{1}{2}\|(e_h(\mathbf{p})^n + e_h(\mathbf{p})^{n+1}) + \frac{1}{2}(e_h(\mathbf{w})^{n+\frac{1}{2},n} + e_h(\mathbf{w})^{n+\frac{1}{2},n+1})\|^2 \\
&= \int_\Omega (\frac{e(u)^{n+1} - e(u)^n}{\triangle t})\,(e_h(u)^n + e_h(u)^{n+1})\,dx \\
&+ \int_\Omega (e(\mathbf{p})^n + e(\mathbf{p})^{n+1})(\frac{e_h(\mathbf{p})^n + e_h(\mathbf{p})^{n+1}}{2})\,dx \\
&+ \frac{1}{2}\int_\Omega \mathbf{b}_h^{n+\frac{1}{2}}(e(u)^n + e(u)^{n+1})(\frac{e_h(\mathbf{p})^n + e_h(\mathbf{p})^{n+1}}{2})\,dx \\
&+ \frac{1}{2}\int_\Omega \mathbf{b}_h^{n+\frac{1}{2}}(\frac{e(\mathbf{p})^n + e(\mathbf{p})^{n+1}}{2})\,(e_h(u)^n + e_h(u)^{n+1})\,dx \\
&+ \frac{1}{4}\int_\Omega \mathbf{b}_h^{n+\frac{1}{2}}(\frac{(e(\mathbf{w})^{n+\frac{1}{2},n} + e(\mathbf{w})^{n+\frac{1}{2},n+1})}{2})\,v\,dx \\
&+ \frac{1}{4}\int_\Omega (u(\cdot,t_n) + u(\cdot,t_{n+1}))(\mathbf{b}^{n+\frac{1}{2}} - \mathbf{b}_h^{n+\frac{1}{2}})\mathbf{q}\,dx \\
&+ \frac{1}{4}\int_\Omega (\mathbf{p}(\cdot,t_n) + \mathbf{p}(\cdot,t_{n+1}))(\mathbf{b}^{n+\frac{1}{2}} - \mathbf{b}_h^{n+\frac{1}{2}})v\,dx \\
&+ \frac{1}{8}\int_\Omega (\mathbf{w}^{n+\frac{1}{2},n} + \mathbf{w}^{n+\frac{1}{2},n+1})(\mathbf{b}^{n+\frac{1}{2}} - \mathbf{b}_h^{n+\frac{1}{2}})v\,dx \\
&+ R_1^{n+\frac{1}{2}}(\frac{e_h(\mathbf{p})^n + e_h(\mathbf{p})^{n+1}}{2}) + R_2^{n+\frac{1}{2}}(e_h(u)^n + e_h(u)^{n+1}),
\end{aligned}
$$

where we have used the fact that $B_h(v, \mathbf{q}) = B_h^*(\mathbf{q}, v)$.

Using Cauchy-Schwarz and Young's inequalities, with suitable scaling, we arrive

$$
\begin{aligned}
\frac{1}{\triangle t}\|e_h(u)^{n+1}\|^2 \leq& \frac{1}{\triangle t}\|e_h(u)^n\|^2 + \frac{1}{\triangle t}\|e(u)^{n+1} - e(u)^n\|\|e_h(u)^n + e_h(u)^{n+1}\| \\
&+ C\Big(\|e(\mathbf{p})^n + e(\mathbf{p})^{n+1}\|^2 + \|e(u)^n + e(u)^{n+1}\|^2 \\
&+ \|\mathbf{b}^{n+\frac{1}{2}} - \mathbf{b}_h^{n+\frac{1}{2}}\|^2 + \|R_1^{n+\frac{1}{2}}\|^2 + \|R_2^{n+\frac{1}{2}}\|\|e_h(u)^n + e_h(u)^{n+1}\|\Big).
\end{aligned}
\tag{3.52}
$$

Note that

$$
\begin{aligned}
\|e(u)^{n+1} - e(u)^n\| &= \|\int_{t_n}^{t_{n+1}} \frac{\partial(u - \mathcal{I}u)}{\partial t}(\cdot,t)\,dt\| \\
&\leq \int_{t_n}^{t_{n+1}} \|\frac{\partial(u - \mathcal{I}u)}{\partial t}(\cdot,t)\|\,dt.
\end{aligned}
$$

Hence,

$$\begin{aligned}
\|e_h(u)^{n+1}\|^2 &= \|e_h(u)^n\|^2 + \int_{t_n}^{t_{n+1}} \|\frac{\partial(u-\mathcal{I}u)}{\partial t}(\cdot,t)\|\,dt\|e_h(u)^n + e_h(u)^{n+1}\| \\
&\quad + C\triangle t\Big(\|e(\mathbf{p})^n + e(\mathbf{p})^{n+1}\|^2 + \|(e(u)^n + e(u)^{n+1})\|^2 \\
&\quad + \|\mathbf{b}^{n+\frac{1}{2}} - \mathbf{b}_h^{n+\frac{1}{2}}\|^2 + \|R_1^{n+\frac{1}{2}}\|^2 + \|R_2^{n+\frac{1}{2}}\|\|e_h(u)^n + e_h(u)^{n+1}\|\Big) \\
&\le \|e_h(u)^0\|^2 + \max_{0\le n\le N_t}\|e_h(u)^n\| \int_0^T \|\frac{\partial(u-\mathcal{I}u)}{\partial t}(\cdot,t)\|\,dt \\
&\quad + C\triangle t\Big(\sum_{n=0}^{N_t}\|e(\mathbf{p})^n\|^2 + \sum_{n=0}^{N_t}\|e(u)^n\|^2 + \sum_{n=0}^{N_t-1}\|\mathbf{b}^{n+\frac{1}{2}} - \mathbf{b}_h^{n+\frac{1}{2}}\|^2 \\
&\quad + \sum_{n=0}^{N_t-1}\|R_1^{n+\frac{1}{2}}\|^2 + \max_{0\le n\le N_t}\|e_h(u)^n\|\sum_{n=0}^{N_t-1}\|R_2^{n+\frac{1}{2}}\|\Big).
\end{aligned}$$

As this is true for all $0 \le n \le N_t$, using Young's inequality, we get

$$\begin{aligned}
\max_{0\le n\le N_t}\|e_h(u)^n\| &\le \|e_h(u)^0\| + \int_0^T \|\frac{\partial(u-\mathcal{I}u)}{\partial t}(\cdot,t)\|\,dt + C\sqrt{\triangle t}\Big(\sum_{n=0}^{N_t}\|e(\mathbf{p})^n\| \\
&\quad + \sum_{n=0}^{N_t}\|e(u)^n\| + \sum_{n=0}^{N_t-1}\|\mathbf{b}^{n+\frac{1}{2}} - \mathbf{b}_h^{n+\frac{1}{2}}\| + \sum_{n=0}^{N_t-1}\|R_1^{n+\frac{1}{2}}\| \\
&\quad + \sqrt{\triangle t}\sum_{n=0}^{N_t-1}\|R_2^{n+\frac{1}{2}}\|\Big).
\end{aligned}$$

Using the interpolation error estimates for the operators $\mathcal{I}$ and $\mathcal{J}$, together with (3.50) and (3.51), the error bound (3.45) follows.

3.6 Numerical examples

In this section, numerical tests illustrating the convergence of the new staggered DG method are presented. Both the static problem and the time dependent problem are considered. Our results show that the new method has the expected rate of convergence. In all examples below, the domain Ω is taken as $[0,1]^d$, $d = 2, 3$.

3.6.1 The static problem

Now we will present numerical results to verify the convergence rate of the new staggered DG method (3.27)-(3.29) for the approximation of the static problem (3.30)-(3.31). We will consider the two-dimensional case, that is, $d = 2$, and three choices of $\mathbf{b}$ defined as follows:

$$\mathbf{b}_1(x,y) = \begin{pmatrix} 1 \\ 1 \end{pmatrix} \quad , \quad \mathbf{b}_2(x,y) = \begin{pmatrix} x+y+1 \\ x-y+1 \end{pmatrix} \quad , \quad \mathbf{b}_3(x,y) = \begin{pmatrix} \cos(\pi y) \\ \cos(\pi x) \end{pmatrix} .$$

For the convergence test, we take the exact solution as

$$u(x,y) = \sin(\pi x)\sin(2\pi y)e^x$$

and take the source term f accordingly. We will consider both the piecewise constant and piecewise linear cases, that is, $k = 0, 1$. The numerical results for $\mathbf{b}_1, \mathbf{b}_2, \mathbf{b}_3$ are shown respectively in Figures 3.2-3.4 where the logarithm of the errors are plotted against the logarithm of the mesh sizes. For each figure, both the L^2 and the H^1 errors are shown. All of these results show that we obtain the expected rate of convergence.

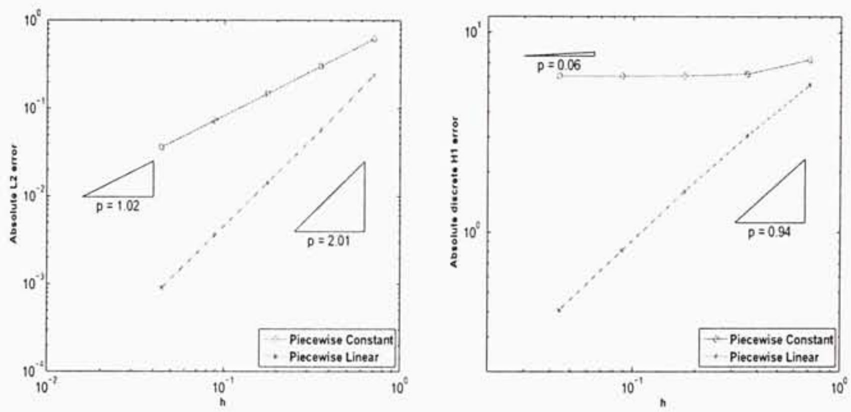

Figure 3.2: Log-log plots for $\mathbf{b} = \mathbf{b}_1$. Left: L^2 error. Right: H^1 error.

3.6.2 Time dependent problem

Next, we will present the convergence test for the time dependent problem (1.5). We will consider both the two-dimensional and three-dimensional cases. For the two-dimensional case, we take

$$\mathbf{b}(x,y,t) = \begin{pmatrix} y - 0.3 - t \\ -x + 0.5 + t \end{pmatrix},$$

and the exact solution

$$u(x,y,t) = e^{-(2t+\frac{1}{3}t^3)}\sin(x - (y - 0.3 - t)t)\sin(y + (x - 0.5 - t)t).$$

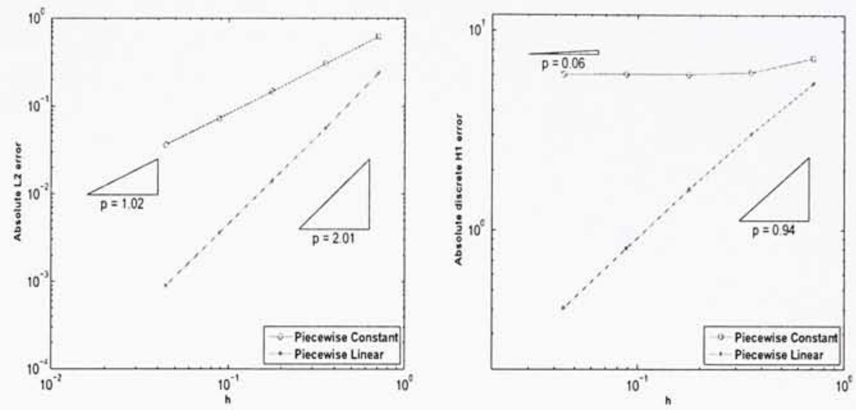

Figure 3.3: Log-log plots for $\mathbf{b} = \mathbf{b_2}$. Left: L^2 error. Right: H^1 error.

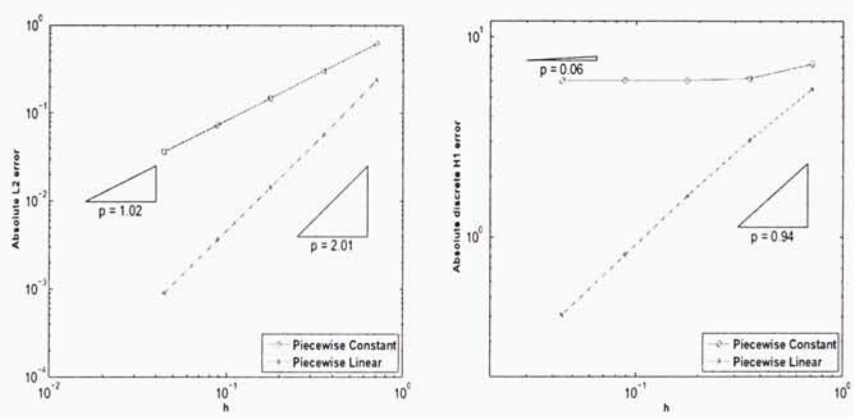

Figure 3.4: Log-log plots for $\mathbf{b} = \mathbf{b_3}$. Left: L^2 error. Right: H^1 error.

The source term f is taken accordingly. The log-log plots of errors are shown in Figure 3.5 for the piecewise linear case, that is, $k = 1$. For the three-dimensional case, we take

$$\mathbf{b}(x, y, z, t) = \begin{pmatrix} y - 0.3 - t \\ (x - 0.6 - t) - (x - 0.5 - t) \\ -(y - 0.4 - t) \end{pmatrix},$$

and the exact solution

$$u(x, y, z, t) = e^{b_1 x + b_2 y + b_3 z - t}.$$

The source term f is taken accordingly. The log-log plots of errors are shown in Figure 3.6 for the piecewise linear case, that is, $k = 1$.

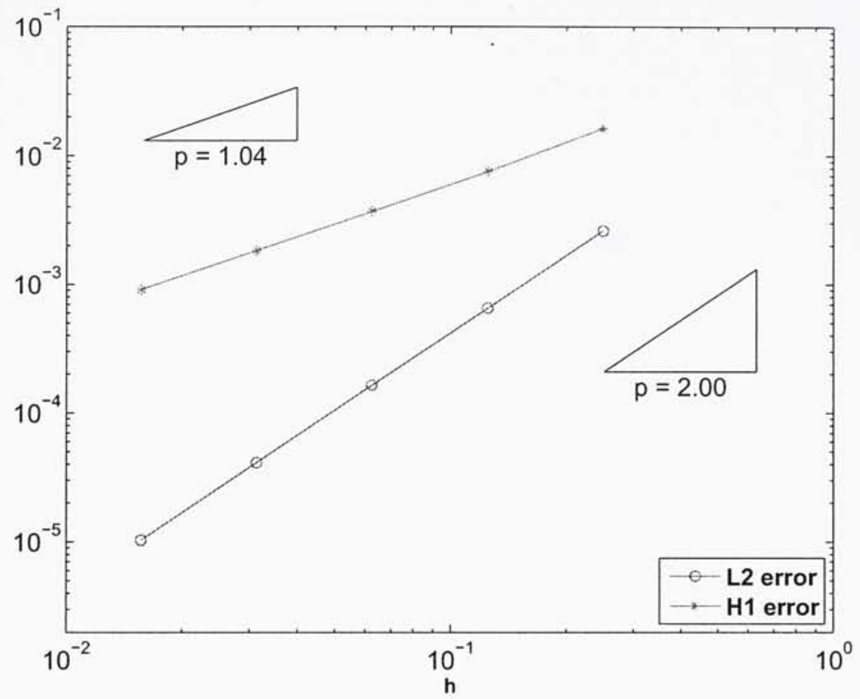

Figure 3.5: Log-log plots for the errors of the 2D time dependent case in L^2 and H^1 norms.

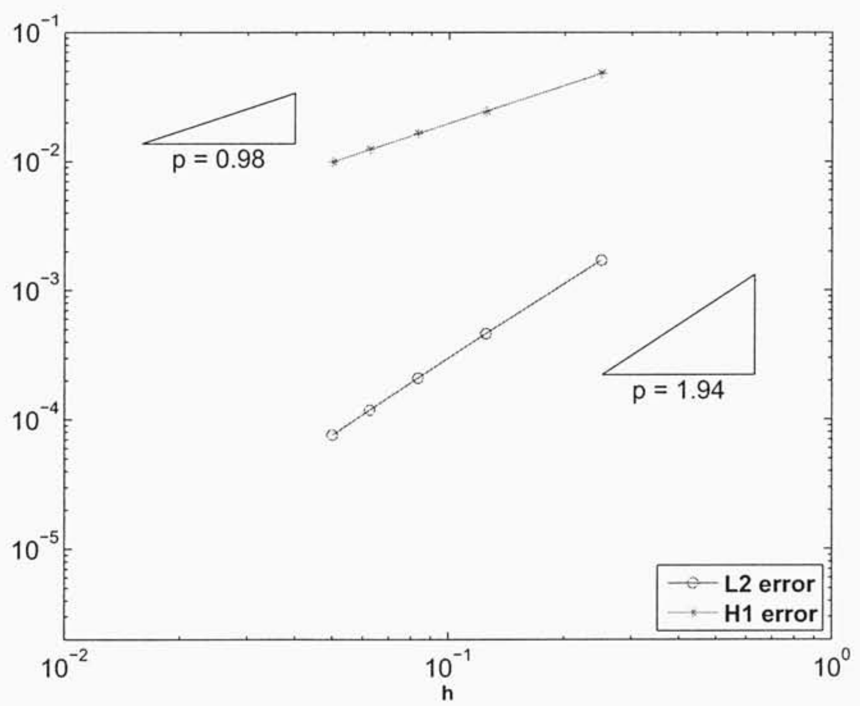

Figure 3.6: Log-log plots for the errors of the 3D time dependent case in L^2 and H^1 norms.

3.7 Concluding Remark

In this chapter, a new staggered DG method for the convection-diffusion equation is presented. The new method has the distinctive advantage that some physical laws arising from the equation are automatically preserved. Moreover, stability and optimal error estimates are proved. Numerical results are shown to verify the order of convergence.

Bibliography

[1] D.N. ARNOLD, F. BREZZI, B. COCKBURN, L.D. MARINI, *Discontinuous Galerkin methods for elliptic problems*, In Discontinuous Galerkin Methods B. Cockburn, G.E. Karniadakis and C.-W. Shu Eds, Lecture Notes in Computational Science and Engineering, 11, Springer, (2000), 89-101

[2] D.N. ARNOLD, F. BREZZI, B. COCKBURN, L.D. MARINI, *Unified analysis of discontinuous Galerkin methods for elliptic problems*, SIAM J. Num. Anal, 39 (2002), 1749-1779.

[3] S. C. BRENNER, F. LI AND L.-Y. SUNG, *A locally divergence-free interior penalty method for two-dimensional curl-curl problems*, SIAM J. Numer. Anal., 46 (2008), 1190-1211.

[4] F. BREZZI, L. D. MARINI, AND E. SÜLI, *Discontinuous Galerkin methods for first-order hyperbolic problems*, Math. Models Methods Appl. Sci., 14(2004), 1893-1903.

[5] A. BUFFA, P. HOUSTON AND I. PERUGIA, *Discontinuous Galerkin computation of the Maxwell eigenvalues on simplicial meshes*, J. Comput. Appl. Math., 204 (2007), 317-333.

[6] A. BUFFA AND I. PERUGIA, *Discontinuous Galerkin approximation of the Maxwell eigenproblem*, SIAM J. Numer. Anal., 44 (2006), 2198-2226.

[7] T. S. CHUNG AND J. ZOU, *A finite volume method for Maxwell's equations with discontinuous physical coefficients*, Int. J. Appl. Math., 7, (2001), 201-224.

[8] E. T. CHUNG, Q. DU AND J. ZOU, *Convergence analysis on a finite volume method for Maxwell's equations in non-homogeneous media*, SIAM J. Numer. Anal., 41, (2003), 37-63.

[9] E. T. CHUNG AND B. ENGQUIST, *Convergence analysis of fully discrete finite volume methods for Maxwell's equations in nonhomogeneous media*, SIAM J. Numer. Anal., 43, (2005), 303-317.

[10] E. T. CHUNG AND P. CIARLET, JR., *Scalar transmission problems between dielectrics and metamaterials: T-coercivity for the discontinuous Galerkin approach*, Submitted.

[11] E. T. CHUNG AND B. ENGQUIST, *Optimal discontinuous galerkin methods for wave propagation*, SIAM J. Numer. Anal., 44 (2006), 2131-2158.

[12] E. T. CHUNG AND B. ENGQUIST, *Optimal discontinuous galerkin methods for the acoustic wave equation in higher dimensions*, SIAM J. Numer. Anal., 47 (2009), 3820-3848.

[13] M. COSTABEL, *A coercive bilinear form for Maxwell's equations*, J. Math. Anal. Appl. 157, (1991), 527-541.

[14] M. COSTABEL AND M.DAUGE *Singularities of electromagnetic fields in polyhedral domains*, Arch. Ration. Mech. Anal. 151, (2000), 221-276.

[15] M. DAUGE, *Computatons for Maxwell equations for the approximation of highly singular solution.*
http://perso.univ-rennes1.fr/monique.dauge/benchmax.html.

[16] V. GIRAULT, P. A. RAVIART, *Finite element methods for Navier-Stokes equations: theory and algorithms*, Springer, Berlin, (1986).

[17] C. J. GITTELSON, R. HIPTMAIR AND I. PERUGIA, *Plane wave discontinuous Galerkin methods: analysis of the h-version*, M2AN Math. Model. Numer. Anal., 2 (2009), 297-331.

[18] M. GROTE, A. SCHNEEBELI AND D. SCHÖTZAU, *Interior penalty discontinuous Galerkin methods for Maxwell's equations: Optimal L^2 norm error estimates*, IMA J. Numer. Anal., 28 (2008), 440-468.

[19] J. S. HESTHAVEN AND T. WARBURTON *High order nodal discontinuous Galerkin method for the Maxwell eigenvalue problem*, Royal Soc. London Ser A, (2004), 493-524.

[20] R. HIPTMAIR, *Finite elements in computational electromagnetics*, Acta Numerica, 11 (2002), 237-339.

[21] P. HOUSTON, I. PERUGIA AND D. SCHÖTZAU, *Mixed discontinuous Galerkin approximation of the Maxwell operator*, SIAM J. Numer. Anal., 42, (2004) 434–459.

[22] P. HOUSTON, I. PERUGIA, A. SCHNEEBELI AND D. SCHÖTZAU, *Interior penalty method for the indefinite time-harmonic Maxwell equations*, Numer. Math., 100, (2005a), 485-518.

[23] P. HOUSTON, I. PERUGIA, A. SCHNEEBELI AND D. SCHÖTZAU, *Mixed discontinuous Galerkin approximation of the Maxwell operator: the indefinite case*, M2AN Math. Model. Numer. Anal., 39 (2005b), 727-753.

[24] P. MONK, *Finite element methods for Maxwell's equations*, Oxford University Press, New York, (2003).

[25] R. NICOLAIDES AND X. WU, *Covolume solutions to three-dimensional div-curl equations*, SIAM J. Numer. Anal., 34 (1997), 2195-2203.

[26] I. PERUGIA, D. SCHÖTZAU AND P. MONK *Stabilized interior penalty methods for the time-harmonic Maxwell equations*, Comput. Methods Appl. Mech. Eng., 191, (2002), 4675–4697.

[27] I. PERUGIA AND D. SCHÖTZAU, *The hp-local discontinuous Galerkin method for low-frequency time-harmonic Maxwell equations*, Math. Comp., 72 (2003), 1179-1214.

[28] K. S. YEE, *Numerical solution of initial boundary value problems involving Maxwell's equations in isotropic media*, IEEE Trans. Antennas Propagat., 14 (1966), 302-307.